PHONON–MEDIATED ELECTRON–ELECTRON INTERACTION IN CONFINED MEDIA: LOW–DIMENSIONAL BIPOLARONS

A THESIS

SUBMITTED TO THE DEPARTMENT OF PHYSICS

AND THE INSTITUTE OF ENGINEERING AND SCIENCE

OF BİLKENT UNIVERSITY

IN PARTIAL FULFILLMENT OF THE REQUIREMENTS

FOR THE DEGREE OF

DOCTOR OF PHILOSOPHY

By

R. Tuğrul Senger

September 2000

I certify that I have read this thesis and that in my opinion it is fully adequate, in scope and in quality, as a dissertation for the degree of Doctor of Philosophy.

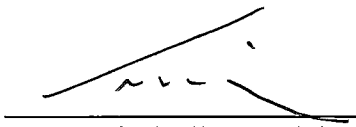

Prof. Atilla Erçelebi (Supervisor)

I certify that I have read this thesis and that in my opinion it is fully adequate, in scope and in quality, as a dissertation for the degree of Doctor of Philosophy.

Prof. Tacettin Altanhan

I certify that I have read this thesis and that in my opinion it is fully adequate, in scope and in quality, as a dissertation for the degree of Doctor of Philosophy.

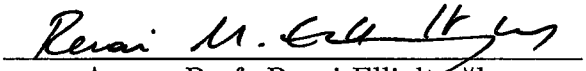

Assoc. Prof. Recai Ellialtıoğlu

I certify that I have read this thesis and that in my opinion it is fully adequate, in scope and in quality, as a dissertation for the degree of Doctor of Philosophy.

Prof. Metin Gürses

I certify that I have read this thesis and that in my opinion it is fully adequate, in scope and in quality, as a dissertation for the degree of Doctor of Philosophy.

Prof. Bilal Tanatar

Approved for the Institute of Engineering and Science:

Prof. Mehmet Baray
Director of Institute of Engineering and Science

Abstract

PHONON–MEDIATED ELECTRON–ELECTRON
INTERACTION IN CONFINED MEDIA:
LOW–DIMENSIONAL BIPOLARONS

R. Tuğrul Senger
Doctor of Philosophy in Physics
Supervisor: Prof. Atilla Erçelebi
September 2000

We study the criterion for the formation of confined large bipolarons and their stability. In order to deal with this specific subject of polaron theory, it is required to adopt some particular approximation methods, because the polaronic systems do not admit exact analytic solutions in general. Those approximation techniques, which are applied to the low-dimensional one-polaron problems, are presented to some extend to form a working basis for our main theme; bipolarons.

As the model of confined bipolaron, the electrons are treated as bounded within an external potential while being coupled to one another via the Fröhlich interaction Hamiltonian. Within the framework of the bulk-phonon approximation, the model that we use consists of a pair of electrons immersed in a reservoir of bulk LO phonons and confined within an anisotropic parabolic potential box, the barrier slopes of which can be tuned arbitrarily from zero to infinity. Thus, encompassing the bulk and all low-dimensional geometric configurations of general interest, we obtain an explicit tracking of the critical values of material parameters for the bipolarons to exist in confined media.

First, in the limit of strong electron-phonon coupling, we present a unified insight into the stability criterion by applying the Landau-Pekar strong coupling approximation. This crude approximation provides us the condition on the ratio of dielectric constants ($\eta = \epsilon_\infty/\epsilon_0$) for large values of electron-phonon coupling constant α. For more reliable results, we consider the path-integral formulation of the problem adopting the Feynman-polaron model to derive variational results over a wide range of the Coulomb interaction and phonon coupling strengths. It is shown that the critical values of α and η exhibit some non-trivial features as the effective dimensionality is varied, and the path integral results conform to that of strong coupling approximation in the limit of large α.

Keywords:

Electron-phonon interaction, optical polaron, bipolaron, stability, Fröhlich Hamiltonian, low dimensional structures, quantum wire, quantum dot, path integral.

Özet

SINIRLANDIRILMIŞ ORTAMLARDA FONON YOLLU ELEKTRON ELEKTRON ETKİLEŞMESİ: DÜŞÜK BOYUTLU ÇİFTPOLARONLAR

R. Tuğrul Senger
Fizik Doktora
Tez Yöneticisi: Prof. Atilla Erçelebi
Eylül 2000

Sınırlandırılmış büyük çiftpolaronların oluşum kıstası ve kararlılığı çalışıldı. Polaron kuramının bu özgül konusunu ele alırken, bazı yaklaşım yöntemlerini kullanmak gerekir, çünkü genelde polaron sistemlerinin kesin analitik çözümleri yoktur. Bu yaklaşım teknikleri, düşük boyutta, tek-polaron problemlerine uygulanarak, asıl konumuz olan çiftpolaronlar için bir çalışma zemini oluşturmak üzere sunuldu.

Sınırlandırılmış çiftpolaronu modellemek üzere, birbiriyle Fröhlich Hamiltoniyeni aracılığıyla etkileşen elektronlar bir dış potansiyel içine hapsedilmiş olarak alındı. Fononların ise üç boyutlu olduklarının varsayıldığı modelimizde, boylamsal optik (LO) fonon denizine daldırılmış bir çift elektron, şiddeti ayarlanabilen eşyönsüz parabolik bir potansiyel kutusunun içine konuldu. Böylece, olası tüm düşük boyutlu geometrileri içerecek şekilde, sınırlandırılmış ortamlarda, malzeme parametrelerinin çiftpolaronların oluşumuna izin veren eşik değerleri hesaplandı.

İlk olarak, güçlü elektron-fonon etkileşmesi limitinde, Landau-Pekar güçlü

bağlaşım yaklaşımı kullanılarak çiftpolaronların kararlılık kıstasına geometrik anlamda birleştirici bir bakış açısı sunuldu. Bu kaba yaklaşım bize elektron-fonon bağlaşım sabiti α'nın büyük değerleri için, dielektrik sabitlerin oranının ($\eta = \epsilon_\infty/\epsilon_0$) sağlaması gereken koşulları verdi. Daha genel ve güvenilir sonuçlar için ise, Feynman polaron modeli kullanılarak yol integrali yöntemi probleme uygulandı. Bu yöntemle, Coulomb etkileşme ve fonon bağlaşım sabitlerinin geniş değer aralığında sonuçlar elde edildi. Etkin boyutluluk değiştirildiğinde α ve η'nın eşik değerlerinin ilginç değişimler gösterdiği, ve kendi limitinde, güçlü bağlaşım yaklaşımı sonuçlarının yol integrali yöntemi sonuçlarıyla uyumlu olduğu görüldü.

Anahtar sözcükler:

Elektron-fonon etkileşmesi, optik polaron, çiftpolaron, kararlılık, Fröhlich Hamiltoniyeni, düşük boyutlu yapılar, kuvantum kuyusu, kuvantum teli, yol integralleri.

Acknowledgement

It is my pleasure to express deep gratitude to my supervisor, Prof. Atilla Erçelebi, for his guidance and support throughout my graduate study, and the development of the present study in particular.

I would like to thank all the members of the Department of Physics, for their moral and technical support, in every case that I needed some.

The Ph.D. scholarship offered by TÜBİTAK - Münir Birsel Vakfı is acknowledged.

Finally, it is my pleasure to thank to my wife, Süheyla, with whom everything is more meaningful.

Contents

Abstract i

Özet iii

Acknowledgement v

Contents vi

List of Figures viii

List of Tables ix

1 INTRODUCTION 1

1.1 Fröhlich Hamiltonian 7

2 APPROXIMATION METHODS 14

2.1 Perturbation Theory 18

2.2 Strong Coupling Theory 24

2.2.1 Displaced Oscillator Transformation 25

2.2.2 Confined Polaron In The Strong-Coupling Limit 27

2.3 Intermediate Coupling Theory 28

2.3.1 LLP Transformation 28

2.4 Perturbative Variational Approach 30

2.5 Feynman Path-Integral Theory 37

2.5.1 Basic Concepts 37

2.5.2 Elimination of the Phonon Field 39
2.5.3 A Variational Principle 40
2.5.4 Application: Confined Polaron 42
2.6 Weak– and Strong–Coupling Domains 56

3 BIPOLARON **60**
3.1 Introduction 60
3.2 Strong Coupling Theory 62
3.2.1 Results 66
3.3 Path Integral Treatment 74
3.3.1 Bipolaron Model 74
3.3.2 The Trial Model and its Diagonalization 75
3.3.3 Path-Integral Averages 79
3.3.4 Integer-dimensional-space limits 82
3.3.5 One-polaron limit 83
3.3.6 Q2D Slab Confinement 84
3.3.7 Q1D Wire Confinement 93

4 CONCLUSIONS **100**

List of Figures

2.1 Perturbation theory results for quasi-2-dimensional polaron 23
2.2 Sketch of displaced oscillator potential. 26
2.3 2D and 3D polaron energy and mass 35
2.4 Illustration of Jensen's inequality. 41
2.5 The model of confined polaron. 46
2.6 Polaron properties in three- and two-dimensions. 51
2.7 Comparison of different confinement geometries. 54
2.8 The scaling of polaron properties, in Q2D confinement. 55
2.9 The extended domain of validity of strong coupling theory in highly confined systems. 57
2.10 Domain of validity of perturbation and adiabatic strong coupling theories 58
3.1 How to determine η_c ? 68
3.2 Critical η for different confinement types. 70
3.3 Bipolaron phase-diagram, strong coupling approximation 73
3.4 Q2D bipolaron phase diagram 86
3.5 Critical α for Q2D bipolaron 88
3.6 The critical ratio η_c for Q2D bipolaron 90
3.7 Binding energy and variational parameters of the bipolaron state . 91
3.8 Energy and variational parameters 93
3.9 Phase diagram for Q1D bipolaron 95
3.10 The critical ratio η_c for Q1D bipolaron 96
3.11 The critical coupling constant α_c for Q1D bipolaron 98

List of Tables

2.1 Coupling constants and LO-phonon frequencies of some common materials 15
2.2 Leading order terms of perturbation and strong coupling theories for the polaron properties 16
2.3 Scaling factors for polaron properties from 3D to 2D 17
2.4 Comparison of polaron binding energies in different confinement geometries 24
3.1 The polaron and bipolaron ground state energies 69

Chapter 1

INTRODUCTION

The history of polaron goes back to the early 1930's. Since then, the polaron problem remained as a popular subject of solid state and condensed matter physics, and there still occurs a considerable amount of work in the literature, devoted to the study of polarons and related problems. The motivation of this continuing interest in the subject includes several aspects. Admitting no exact solution, the polaron represents a simple but nontrivial example of a particle coupled to a quantum field, presenting a challenging formal mathematical structure. Many approximation methods of quantum field theory and quantum statistics have been applied to tackle polaronic properties, making the polaron a testing ground for those techniques. Besides, the direct relevance of the subject to the electronic structure of ionic or polar-semiconductor materials requires investigation of electron-phonon interaction effects for detailed understanding of properties of those materials. In the last two decades, with the theoretical prediction and subsequent fabrication of semiconductor based quantum-well confined systems, the field is enriched with the polarons of lower dimensionality. The progress in the fabrication techniques, such as molecular beam epitaxy and lithographic methods, made it possible to obtain low dimensional microstructures, namely quantum–wells, –wires and –dots, where the charge carriers are confined in one or more spatial directions. Consequently, there occurred a renewed interest in the study of polarons within the context of reduced dimensionality.

The concept of polaron is based on the motion of an electron in an ionic or polar semiconductor crystal. The long range Coulomb interaction of the electron with the ions of the crystal produces a polarization field around it due to the displacements of ions from their equilibrium positions. Alternatively stating, the electron couples to the phonon modes of the crystal, resulting in a cloud of phonons surrounding and accompanying it, as it moves. The system of electron plus the concomitant phonon cloud (or the lattice deformation) is called the polaron. The interaction with phonons modifies the electron properties, lowering the self energy and increasing the inertia of it by an amount depending on the strength of the coupling. The localized electron can move through the action of temperature or zero–point motion. In the former case the polaron moves by thermally activated hopping. In the latter, for $kT < \hbar\omega/2$, the motion is coherent and the polaron behaves like a heavy particle with an increased effective mass and with a mean free path determined by the phonon and impurity scattering.

The first conceptual approach to polaron problem was by Landau[1] in 1933. If an electron is placed into the conduction band of an ionic crystal there would be a force $e^2/\epsilon_0 r^2$ on an other electron at a distance r from it. But if the ions did not move the force would be $e^2/\epsilon_\infty r^2$, where ϵ_0 and ϵ_∞ are the static and high-frequency dielectric constants respectively. Thus the electron is acted upon by a potential

$$-\frac{e^2(\epsilon_\infty^{-1} - \epsilon_0^{-1})}{r}$$

which is Coulombic, and localized states must exist. In other words, "the electron is trapped by digging its own hole". In 1937, introducing the concept of polarization field, Fröhlich[2] gave a quantitative treatment of electron scattering in ionic crystals. After some early semiclassical works[3–5] on the subject, in which the lattice properties were incorporated into a classical macroscopic polarization, the formulation of the problem in the framework of quantum field theory was first given by Fröhlich, Pelzer and Zienau[6] in 1950, by proposing a microscopic model Hamiltonian, which now bears the name of Fröhlich.

At this point we should distinguish between the "large" and "small" polaron terms which exist in the literature. For ionic crystals the polaronic binding energy

can be written as

$$E_p \sim \frac{e^2(\epsilon_\infty^{-1} - \epsilon_0^{-1})}{r_p}$$

where r_p is the radius of the volume within the wavefunction trapped by the lattice deformation (polaron radius). This can be greater than or comparable to the lattice constant a. For large r_p, it is possible that the wavefunction attains a small phase shift at each hop if $E_p \ll \hbar^2/ma^2$, where m is the rigid band mass. The polaron is then called "large" and can be described as a free particle moving in an elastic continuum. Large polarons exist if the bare electron band is sufficiently narrow. The most sophisticated treatment of the large polaron is due to Feynman,[7] following that given by Pekar[8] and Fröhlich.[9]

The "small" polaron problem requires a different treatment and is generally described by the Holstein model. It assumes a short–range electron–phonon interaction and explicitly includes the lattice periodicity.[10,11] Recently, a detailed review of small polaron and bipolaron formation, and its relevance to high-T_c superconductivity have been given by Alexandrov and Mott.[12] In the present work we will focus solely on "large" polarons and bipolarons which are characterized by the Fröhlich Hamiltonian.

Bipolaron

Bipolaron is a generalization of the polaron concept to the case of two particles. Normally two conduction electrons would repel each other because of their repulsive Coulomb interaction, but in polar materials there is an additional interaction between electrons mediated by virtual phonons which is attractive. If this phonon mediated attractive interaction can overcome the mutual Coulomb repulsion then the electrons can form a bipolaronic bound state. It was first conjectured by Vinetskii and Gitterman,[13] and subsequently by many other scientists, that bipolarons can be realized in selective materials where a pair of electrons can form a composite bound state. As one of the pioneering works in this area we should mention the paper by Bishop and Overhauser[14] where they explore the phonon-mediated interaction between two electrons and show that for

ionic crystals, the effective electron-electron potential may lead to an attractive deep potential well with a minimum occurring for particle separations as small as a few tens of Angstrom units.

The bipolaron studies have been of general interest both for academic reasons and for its importance in semiconductor technology. In 1975 Anderson,[15] advocated the bipolaron concept in negative U centers to study the electronic properties of the amorphous semiconductor. Lakkis *et al.*[16] extended the idea of Anderson to propose intersite bipolarons to explain the mechanism of two successive metal-insulator transitions in titanium oxide. But perhaps the greatest impetus to the renewed interest in the bipolaron came from its possible connection with the high T_c superconductivity, where singlet bipolarons, such as bosons in Bose condensation, have been conjectured as a possible mechanism for high T_c superconductivity.[12,17–19] However, all these important developments do not help to resolve the question of the first-principles existence of bipolarons in a solid. This probably sparked the recent state of interest in the study of the stability of the bipolarons. The existence of *small* bipolarons in polar materials has been supported both theoretically[20] and experimentally,[16] but for the Fröhlich (or *large*) bipolarons, the debate seems to be still open. Our present concern will be to investigate formation criteria of *large* singlet optical bipolarons in low dimensional systems.

Among the numerous amount of papers published within the context of two-polaron systems, we cite a few examples[21–35] which are relevant to the long-range Fröhlich interaction with the optical phonons. The fundamental conclusion led by these studies is that the domain of stability of bipolarons is determined critically by the upper and lower bounds for the repulsive Coulomb and the attractive electron-phonon coupling strengths, respectively, and that a bipolaron phase can exist only at strong phonon coupling. In parallel with the study of optical bipolarons, there has also appeared some alternative attention[36,37] devoted to the investigation of the two polaron complex where the electrons are assumed to couple to the longitudinal acoustic phonons through the deformation potential interaction. The acoustic phonon interaction have been proposed as an additional

mechanism to help stabilizing the bipolaron. In our present study however, we shall disregard any pertinence to acoustic phonon coupling and give all emphasis to the optical bipolaron problem.

Of particular relevance to the content of the present work are the recent solutions of this problem in strict two dimensions (2D) [23–25,28,29] where it has been found that bipolaron formation should be easier in a space of low dimensions. In this report we would like to extend the bipolaron problem into a more general context and present a comprehensive review of the two-polaron system in a confined medium through a description interpolating between integer-dimensional-space limits. We adopt an oversimplified model of a pair of electrons immersed in a reservoir of bulk LO phonons and confined within a deformable three dimensional box of parabolic boundary, given in usual polaron units ($m^* = \hbar = \omega_{\rm LO} = 1$) by

$$V_{\rm conf}(\varrho, z) = \frac{1}{2}(\Omega_1^2 \varrho^2 + \Omega_2^2 z^2)$$

in which the dimensionless frequencies Ω_1 and Ω_2 serve for the measures of the degree of confinement of the electrons in the respective lateral (ϱ) and $\pm z$ directions. Setting $\Omega_1 = 0$ and varying Ω_2 from zero to infinity, one can trace the variational upper estimate for the bipolaron energy and the corresponding stability criterion interpolating between the three and two dimensional space limits. On the other hand, deleting the confining potential along the z-axis ($\Omega_2 = 0$) and fixing Ω_1 at non-zero finite values, the theory reflects the Q1D-description in a free standing QWW-like tubular structure.

The above choice for the confining potential is appealing in the sense that the static depletion fields achieved in microstructures such as quantum wires and dots which are laterally confined by Schottky gates exhibit nearly parabolic potentials. Besides this, the usage of quadratic potential profiles greatly facilitates the calculations and leads to rather concise and tractable analytic expressions. We have thus refrained ourselves from treating potentials of other forms which possibly would lead to complicated and even prohibitively difficult expressions and numerical complications and yet yield qualitative features similar to those

for parabolic potential shapes. Indeed, calculations pertaining to the cyclotron study of polarons confined to an interface indicate that the phonon-coupling - induced shift in the resonant energy is sensitive dominantly to the strength of the confining potential rather than its shape.[38] Moreover, due to the absence of an abrupt variation in the medium structure and properties, the parabolic confining potential allows one to disregard any pertinence to the interface phonon modes.[39]

A complementary remark regarding the particular parabolic form of the potential used here is that it also finds its relevance in the study of bipolarons under external magnetic fields, where a field for a 3D-bipolaron conforms it effectively to a Q1D-bipolaron and a field applied normally to a Q2D-system makes it effectively zero dimensional. Specifically, under the symmetric gauge for the magnetic vector potential, one readily achieves the cyclotron frequency (measured in units of ω_{LO}) to undertake the role of the confining parameter Ω_1.

Throughout this thesis, we will apply the *bulk phonon approximation.* We will give most emphasis to the generic low dimensional aspect of the dynamical behavior of the electron(s) confined in an external potential, and leave out all the other effects; thus our concern will primarily be to give a view of the bulk phonon effects stripped from all other perturbing quantities. Apart from omitting the contributions that may come from all other kinds of phonon modes, we will also ignore any screening effects and further complications such as those due to the nonparabolicity corrections to the electron band or the loss of validity of both the effective-mass approximation and the Fröhlich continuum Hamiltonian in very small microstructures.

The rest of this thesis is organized as follows. In the next section of this chapter, the Fröhlich Hamiltonian will be derived starting from the basic principles. In chapter 2 we will review some perturbative and variational approximating techniques for handling the Fröhlich Hamiltonian within the context of single polaron properties in low dimensions. The ultimate goal of the thesis, i.e. investigation of stability criteria of confined large-bipolarons will be presented in the 3rd chapter. Finally a short summary together with relevant discussions and conclusions will form the last chapter.

1.1 Fröhlich Hamiltonian

In this section, we shall drive the Hamiltonian describing the system composed of a single electron, confined in an external potential, and interacting with the LO-branch of bulk phonon modes of the crystal. Although the label *Fröhlich Hamiltonian* is used for all class of more complicated systems involving electron-phonon interactions, with such considerations as polaron gas, confined phonon modes, etc., we shall restrict ourselves within the scope of the present work. For a more detailed derivation one may consult to the original paper by Fröhlich *et al.*,[6] and some relevant books.[40,41]

To represent the motion of the electron and of the lattice vibrations in the simplest possible form, we shall consider that, the electron lies close to the lower edge of the band, where the related Bloch functions have small $\vec{k}$-vector values, so that the corresponding wavelengths are large compared to the lattice constant. Then, it is appropriate, to ignore the detailed lattice structure and to treat the lattice as a dielectric continuum, and also, to apply the effective mass approximation for the electron. As a further approximation we shall take the LO-phonon modes to be dispersionless; $\omega(\vec{Q}) = \omega_{\mathrm{LO}}$.

In view of these simplifying considerations, the total polaron Hamiltonian can be stated as composed of three parts,

$$H = H_{\mathrm{e}} + H_{\mathrm{ph}} + H_{\mathrm{e-ph}}, \tag{1.1}$$

where the subscripts 'e', 'ph' and 'e-ph' stand for 'electron', 'phonon', 'electron-phonon interaction' respectively.

The first term in the above, is simply

$$H_{\mathrm{e}} = \frac{p^2}{2m^\star} + V_{\mathrm{conf}}(\vec{r}; \{\Omega_i\}) \tag{1.2}$$

where $\vec{r}$ and $\vec{p}$ are electron position and momentum operators, $m^\star$ is the effective band mass of electron and V_{conf} defines the external potential through which the electron is confined. The set of parameters $\{\Omega_i\}$ characterizing the potential, will generally be taken as tunable, by means of which we shall obtain several low dimensional confinement geometries.

For the remaining two terms in Eq.(1.1), we will first consider the energy of the polarization oscillations induced by the electron, and the electron-polarization field interaction energy within the framework of classical electrodynamics. Afterwards, the form of the Hamiltonian in the language of quantum field theory will be obtained through the quantization of the polarization field.

As a model of the polarization $\vec{P}(\vec{r})$ of the medium, consider individual dipoles $\vec{d}_n = e_n^\star \vec{q}_n$, located at the sites of the lattice. The dipoles oscillate with the characteristic frequency $\omega_{\rm LO}$, the frequency of optical lattice vibrations, and they correspond to oscillating masses m_n, with effective charges $e_n^\star$, in the normal coordinates $\vec{q}_n(t)$. With the assumption that the dipoles are not coupled, the total energy is stated as,

$$\frac{1}{2}\sum_n m_n \left(\dot{\vec{q}}^2 + \omega_{\rm LO}^2 \vec{q}^2\right). \tag{1.3}$$

Switching from the individual dipoles to a dielectric continuum is achieved through the following substitutions;

$$e_n^\star \vec{q}_n \;\rightarrow\; \vec{P}(\vec{r}) \qquad m_n \;\rightarrow\; \varrho(\vec{r}) d^3 r \tag{1.4}$$

where $\varrho(\vec{r})$ is the mass density. If we further let $\varrho(\vec{r})/e^\star(\vec{r}) = \gamma$ to be a constant, the total energy of the polarization field gets the form;

$$\frac{1}{2}\gamma \int d^3 r \left(\dot{\vec{P}}^2(\vec{r}) + \omega_{\rm LO}^2 \vec{P}^2(\vec{r})\right). \tag{1.5}$$

Therefore, introducing the momentum variable $\vec{\Pi} = \dot{\vec{P}}/\gamma$, canonically conjugate to $\vec{P}$, one can express the polarization Hamiltonian H_P as,

$$H_P = \int d^3 r \left(\frac{1}{2\gamma}\vec{\Pi}^2 + \frac{\gamma\omega_{\rm LO}^2}{2}\vec{P}^2\right). \tag{1.6}$$

In the above, the undetermined γ is to be found from the phenomenological theory.

Let us, therefore, consider the interaction energy between the electron and the polarization oscillations. From electrostatics, we know that the interaction energy

density between an electric charge e at point $\vec{r}$ and a continuously distributed dipole density $\vec{P}(\vec{r}')$ is given by,

$$-e\vec{\nabla}_r\left(\frac{1}{|\vec{r}-\vec{r}'|}\right)\cdot\vec{P}(\vec{r}')d^3r'. \tag{1.7}$$

Integration with respect to $\vec{r}'$, gives the interaction Hamiltonian H_I,

$$H_I = -e\int d^3r'\vec{\nabla}_r\left(\frac{1}{|\vec{r}-\vec{r}'|}\right)\cdot\vec{P}(\vec{r}')\ . \tag{1.8}$$

To determine the free constant γ, for the time being, let us consider the electron to be stationary and investigate the equations of motion for the polarization vibrations under the influence of the electron. With the Hamiltonian $H = H_P + H_I$, the Hamilton's equations of motion,

$$\dot{P}_i = \frac{\delta H}{\delta \Pi_i} \qquad \dot{\Pi}_i = -\frac{\delta H}{\delta P_i} \qquad i = x, y, z \tag{1.9}$$

lead us to the following equation;

$$\gamma\left(\ddot{\vec{P}}(\vec{r}') + \omega_{\rm LO}^2\vec{P}(\vec{r}')\right) = -e\vec{\nabla}_r\left(\frac{1}{|\vec{r}-\vec{r}'|}\right). \tag{1.10}$$

Notice that the right-hand side of the equation represents simply the dielectric displacement $\vec{D}(\vec{r}')$ due to the electron. In the static case, i.e. $\ddot{\vec{P}}(\vec{r}') = 0$, we have,

$$\gamma\omega_{\rm LO}^2\vec{P}(\vec{r}') = \vec{D}(\vec{r}')\ . \tag{1.11}$$

Using the relation between the field strength and the dielectric displacement,

$$\vec{D} = \vec{E} + 4\pi\vec{P}_{\rm tot} = \epsilon_0\vec{E}\ , \tag{1.12}$$

one can write,

$$4\pi\vec{P}_{\rm tot} = \left(1 - \frac{1}{\epsilon_0}\right)\vec{D}. \tag{1.13}$$

Here, $\vec{P}_{\rm tot} = \Delta\vec{P} + \vec{P}$ is the total polarization, which consists of two parts; one from the polarization of the electrons in the ionic shells, $\Delta\vec{P}$, and the other from the ionic displacements, $\vec{P}$. With an applied static field, both contributions develop fully, so that ϵ_0 is the static dielectric constant.

Since the effect of the polarization due to the electrons of ionic shells has already been accounted in the effective mass approximation for the electron, we are only interested in the contribution coming from the polarization of the lattice itself. To isolate this contribution, let us think of the external electron as having been suddenly created in the lattice. Only the electrons are able to keep up with this sudden switch-on of the field, because the ions are much more inertial than the electrons. Consequently, we obtain a formula relating $\Delta\vec{P}$ to $\vec{D}$, similar to Eq.(1.13), but where now ϵ_0 is replaced by the high frequency dielectric constant ϵ_∞;

$$4\pi\Delta\vec{P} = \left(1 - \frac{1}{\epsilon_\infty}\right)\vec{D}. \tag{1.14}$$

Therefore, for the part of the polarization due to the lattice vibrations, we obtain,

$$4\pi\vec{P} = \left(\frac{1}{\epsilon_\infty} - \frac{1}{\epsilon_0}\right)\vec{D} = \frac{1}{\bar{\epsilon}}\vec{D}. \tag{1.15}$$

Comparing the Eqs.(1.11) and (1,15), the value of γ is obtained as

$$\gamma = \frac{4\pi\bar{\epsilon}}{\omega_{\rm LO}^2} \quad . \tag{1.16}$$

Having found γ, we can proceed with the quantization of the polarization field, as a consequence of which $H_P \rightarrow H_{\rm ph}$ and $H_I \rightarrow H_{\rm e-ph}$. However, before that, let us express the interaction part of the Hamiltonian in Eq.(1.8), in a more convenient form. Using the relation

$$\begin{aligned} \vec{\nabla}_r\left(\frac{1}{|\vec{r}-\vec{r}'|}\right)\cdot\vec{P}(\vec{r}') &= -\vec{\nabla}_{r'}\left(\frac{1}{|\vec{r}-\vec{r}'|}\right)\cdot\vec{P}(\vec{r}') \\ &= -\vec{\nabla}_{r'}\cdot\left(\frac{\vec{P}(\vec{r}')}{|\vec{r}-\vec{r}'|}\right) + \left(\frac{1}{|\vec{r}-\vec{r}'|}\right)\vec{\nabla}_{r'}\cdot\vec{P}(\vec{r}') \end{aligned} \tag{1.17}$$

the contribution coming from the first term after the substitution in Eq.(1.8), becomes zero due to the boundary conditions, and H_I reduces to,

$$H_I = -\int d^3r' \frac{e}{|\vec{r}-\vec{r}'|}\vec{\nabla}_{r'}\cdot\vec{P}(\vec{r}') \; . \tag{1.18}$$

An important remark pertaining to this form of the interaction Hamiltonian is that the plane wave expansion of the term $\vec{\nabla}_{r'}\cdot\vec{P}(\vec{r}')$ contains only longitudinal

waves. We are, therefore, confirmed in restricting our considerations only to the longitudinal lattice vibrations, from the beginning.

To quantize the polarization field, the conjugate variables $\vec{P}$ and $\vec{\Pi}$ are to be considered as operators obeying the commutation relation,

$$[\Pi_i, P_j] = -i\hbar\delta_{ij} \qquad i,j = x,y,z \ . \tag{1.19}$$

The phonon annihilation and creation operators are defined as,

$$\begin{aligned} \vec{A}(\vec{r}) &= \sqrt{\frac{\gamma\omega_{\mathrm{LO}}}{2\hbar}}\vec{P}(\vec{r}) + i\frac{1}{\sqrt{2\gamma\hbar\omega_{\mathrm{LO}}}}\vec{\Pi}(\vec{r}) \\ \vec{A}^{\dagger}(\vec{r}) &= \sqrt{\frac{\gamma\omega_{\mathrm{LO}}}{2\hbar}}\vec{P}(\vec{r}) - i\frac{1}{\sqrt{2\gamma\hbar\omega_{\mathrm{LO}}}}\vec{\Pi}(\vec{r}) \end{aligned} \tag{1.20}$$

with

$$\left[A_i(\vec{r}), A_j^{\dagger}(\vec{r}')\right] = \delta_{ij}\ \delta(\vec{r}-\vec{r}') \ . \tag{1.21}$$

Expanding the operators in plane waves;

$$\begin{aligned} \vec{A}(\vec{r}) &= \frac{1}{\sqrt{V}}\sum_Q \frac{\vec{Q}}{Q}\, a_Q\, e^{i\vec{Q}\cdot\vec{r}} \\ \vec{A}^{\dagger}(\vec{r}) &= \frac{1}{\sqrt{V}}\sum_Q \frac{\vec{Q}}{Q}\, a_Q^{\dagger}\, e^{-i\vec{Q}\cdot\vec{r}} \end{aligned} \tag{1.22}$$

where V is the normalization volume, and $\vec{Q}$ is the phonon wave vector, the commutation relation (1.21) implies for the new operators,

$$\left[a_i, a_j^{\dagger}\right] = \delta_{ij} \qquad \text{and} \qquad [a_i, a_j] = \left[a_i^{\dagger}, a_j^{\dagger}\right] = 0 \ . \tag{1.23}$$

Inverting the set of equations (1.20) and substituting $\vec{A}(\vec{r})$ and $\vec{A}^{\dagger}(\vec{r})$ as given in Eq.(1.22), we have,

$$\begin{aligned} \vec{P}(\vec{r}) &= \sqrt{\frac{\hbar}{2\gamma\omega_{\mathrm{LO}}V}}\sum_Q \frac{\vec{Q}}{Q}\left(a_Q e^{i\vec{Q}\cdot\vec{r}} + a_Q^{\dagger}e^{-i\vec{Q}\cdot\vec{r}}\right) \\ \vec{\Pi}(\vec{r}) &= i\sqrt{\frac{\gamma\hbar\omega_{\mathrm{LO}}}{2V}}\sum_Q \frac{\vec{Q}}{Q}\left(a_Q^{\dagger}e^{-i\vec{Q}\cdot\vec{r}} - a_Q e^{i\vec{Q}\cdot\vec{r}}\right) \ . \end{aligned} \tag{1.24}$$

Inserting these expressions in equations (1.6) and (1.18), we obtain,

$$\begin{aligned} H_{\rm ph} &= \hbar\omega_{\rm LO}\sum_Q a_Q^\dagger a_Q \\ H_{\rm e-ph} &= \sum_Q \left(V_Q a_Q e^{i\vec{Q}\cdot\vec{r}} + V_Q^* a_Q^\dagger e^{-i\vec{Q}\cdot\vec{r}}\right) \end{aligned} \tag{1.25}$$

where $V_Q = -i4\pi\sqrt{e^2\hbar/2\gamma\omega_{\rm LO}V}(1/Q)$ is the interaction amplitude. With the value of γ as given in Eq.(1.16) substituted in, and choosing $\hbar\omega_{\rm LO}$ as a unit of energy, $u = (\hbar/2m^*\omega_{\rm LO})^{1/2}$ as a unit of length, i.e. making the following scaling transformations,

$$H \rightarrow \hbar\omega_{\rm LO}H \qquad \vec{r} \rightarrow u\,\vec{r} \qquad \vec{Q} \rightarrow \vec{Q}/u \qquad V \rightarrow u^3V \tag{1.26}$$

the dimensionless Fröhlich Hamiltonian, in its well established form, is written as

$$H = p^2 + V_{\rm conf}(\vec{r};\{\Omega_i\}) + \sum_Q a_Q^\dagger a_Q + \sum_Q V_Q\left(a_Q e^{i\vec{Q}\cdot\vec{r}} + a_Q^\dagger e^{-i\vec{Q}\cdot\vec{r}}\right) \tag{1.27}$$

where now,

$$V_Q = \sqrt{\frac{4\pi\alpha}{V}}\frac{1}{Q} \tag{1.28}$$

is taken as real for notational convenience, and in which,

$$\alpha = \frac{e^2}{2}\left(\frac{1}{\epsilon_\infty} - \frac{1}{\epsilon_0}\right)\sqrt{\frac{2m^*\omega_{\rm LO}}{\hbar}}\frac{1}{\hbar\omega_{\rm LO}} \tag{1.29}$$

is the dimensionless electron-phonon coupling constant.

The polaron calculations are performed generally in dimensionless units. It is convenient to choose $\hbar = \omega_{\rm LO} = 1$, to facilitate the notation. If further, $2m^* = 1$ is chosen, the form of the Hamiltonian in Eq.(1.27) remains the same, but if $m^* = 1$ is the choice, the scaling unit length becomes $u = 1/\sqrt{2}$, so that we have a factor of $1/2$ in front of p^2, also the interaction amplitude becomes modified as $V_Q = (2\sqrt{2}\alpha/V)^{1/2}(1/Q)$, where the numerical value of α remains the same for both cases.

The Hamiltonian derived in this section, will be the starting point for all the calculations to be presented in this work. Since the exact solution of the

Hamiltonian is not available, we will consider several approximation methods, common in the literature, for obtaining the ground state properties of the polaron, giving most emphasis to the bulk phonon effects on the low dimensionally confined electron.

In the next chapter we will briefly consider those approximation techniques for the solution of one-polaron problem, which will form a framework for the bipolaron problem to be handled in the following chapter.

Chapter 2

APPROXIMATION METHODS

In the Fröhlich Hamiltonian, when expressed in units of $\hbar\omega_{\mathrm{LO}}$, all the material dependent parameters are summed up into the dimensionless constant α. The numerical value of this electron-phonon interaction constant can be quite different for different types of the materials, ranging from ~ 0.01 up to ~ 10. It is large for highly polar materials such as alkali halides, whereas it is small for compound semiconductors. In Table 2.1 we list the values of α and the energy unit $\hbar\omega_{\mathrm{LO}}$ for several common materials, as calculated with the given data in a review article by Kartheuser.[42]

The interpretation of the polaron problem and its mathematical structure are relatively simple and well understood in the asymptotic limits of the interaction strength. One of the basic points of view is the case where the kinetic energy of the electron is much smaller than the energy of the phonon modes, and $\alpha \ll 1$. In this case the lattice deformation tends to follow the electron, as it moves through the crystal. A reasonable treatment to such a case is to take the electron-phonon interaction, $H_{\mathrm{e-ph}}$, as a perturbation[6,43–45] and to calculate the corrections to the energy eigenvalues brought about by the polaron effect.

Another approach which successfully gives a good description of the behavior of the electron and its concomitant lattice deformation at weak coupling has been developed by Lee, Low and Pines[46] (LLP). This theory is of variational nature and leads to essentially the same results as the perturbation theory in the leading order

Material	α	$\hbar\omega_{LO}$ (meV)
KCl	5.6	26.7
NaCl	5.5	33.6
AgBr	1.56	17.1
CdTe	0.40	20.8
InP	0.11	43.3
GaAs	0.07	36.8
InAs	0.05	30.2

Table 2.1: Coupling constants and LO-phonon frequencies of some common materials
Note that these experimental values correspond to liquid helium temperature and one may expect slightly larger values at 0K.

in α, but this approximation remains valid for a broader domain of the coupling constant, therefore, it is generally referred to as the intermediate coupling theory. They have introduced a canonical transformation which eliminates the electron coordinates from the Hamiltonian. The LLP approximation became particularly influential and it has been applied as an important tool in many subsequent publications.[47–52]

A contrasting point of view originates from the idea that for a strong enough electron-phonon interaction ($\alpha \gg 1$) the electron goes into a bound state with a highly localized wave function in the self-induced potential, which is built up by the field of correlated virtual phonons.[8] If the electron is really deeply bound, one expects the lattice deformation to react back and produce some structure in the electronic wave function, and the presence of the electron in turn determines and maintains the size and shape of the deformation. The point of view presented by these arguments is referred to as the strong coupling (adiabatic) theory. The method, basically consists of proposing a trial wave function for the electron with some parameters, and making use of the variational principle, to calculate the ground state polaron properties. There are many other works on the strong coupling theory,[53–63] in the literature. Since for the bulk, the strong coupling theory gives dependable results only at some unrealistic values of the coupling

		E_g	$m_p - 1$
$\alpha \ll 1$	2D	$-(\pi/2)\alpha$	$(\pi/8)\alpha$
	3D	$-\alpha$	$(1/6)\alpha$
$\alpha \gg 1$	2D	$-(\pi/8)\alpha^2$	$(\pi^2/16)\alpha^4$
	3D	$-(1/3\pi)\alpha^2$	$(16/81\pi^2)\alpha^4$

Table 2.2: Leading order terms of perturbation and strong coupling theories for the polaron properties
Polaron ground state energy, E_g, is in units of $\hbar\omega_{LO}$ and the polaron mass, m_p, is taken in units of electron band mass $m^\star$.

constant, ($\alpha > 10$), it can be considered as an academic theory, but however, as we will see, the confinement effects bring about the concept of pseudo-enhancement in the electron-phonon coupling, extending the domain of validity of this approach in low dimensional systems.

The results of the perturbation and strong coupling theories, up to the leading orders in α, for the ground state energy, and the effective mass of the polaron, are summarized in Table 2.2. We have provided the results of 2-dimensional (2D) polaron as well as those of the bulk (3D) polaron, to demonstrate the effect of confinement, on the polaron properties.

It is seen that the functional dependences of the ground state energy and phonon contribution to effective mass ($m_p - 1$), on α, are quite different at the two limiting regimes. Besides, the numerical coefficients get considerably larger with the reduction in the dimensionality (cf. Table 2.3). Peeters *et al.*[64] have derived an interesting scaling relation for (2D) polaron properties, taking (3D) case as a reference;

$$E_g^{(2D)}(\alpha) = \frac{2}{3} E_g^{(3D)}\left(\frac{3\pi}{4}\alpha\right) \quad \text{and} \quad m_p^{(2D)}(\alpha) = m_p^{(3D)}\left(\frac{3\pi}{4}\alpha\right). \tag{2.1}$$

Similar relations hold true for other physical quantities of interest, such as mean number of phonons, linear mobility and impedance function. The form of the relations in Eq.(2.1) immediately signals the mentioned pseudo-enhancement of the interaction strength in low dimensional systems.

	$E_g(3D \rightarrow 2D)$	$m_p - 1(3D \rightarrow 2D)$
$\alpha \ll 1$	1.57	2.36
$\alpha \gg 1$	3.70	30.82

Table 2.3: Scaling factors for polaron properties from 3D to 2D

For a more general view of the problem, not restricted to the limiting regimes, one requires more powerful methods or interpolating approximations. One of such methods, which can be named as a "perturbative variational approach", has been introduced by Devreese *et al.* in an application to bound polaron.[65] The procedure is an extension of the adiabatic approximation, in the sense that a strongly coupled polaron state combined with a first order perturbative extension is used as a variational trial state, by which it is possible to achieve a satisfying extrapolation towards the weak coupling regime. The method has been recently applied to 3D and 2D free polarons,[66] Q1D polarons,[67] to the problem of polaron in a magnetic field,[68] and bulk and 2D bipolarons[29] quite successfully.

The final approach to the polaron problem, to be mentioned here, is the Feynman path integral formalism. It is the most successful theory, in the sense that it provides superior upper bound for the ground state energy of the Fröhlich polaron at arbitrary electron-phonon coupling strength, compared to the other approximations. It has been first applied to bulk polaron by Feynman[7] in 1955, and became an indispensable tool for the study of the Fröhlich Hamiltonian. The pioneering work of Feynman, initiated the development of functional-integral methods in the polaron theory, which, with refined variational procedures, proved to be an extremely powerful tool, if not the most powerful. There are very elegant applications of functional-integral methods in the literature,[69–84] and the Feynman path integral formalism applied to the case of polaron in a general quadratic confinement,[85] will be presented in the relevant section.

2.1 Perturbation Theory

When the electron-phonon interaction constant α is small, as it is, in most of the semiconductor compounds, it is appropriate to consider the interaction term of the Fröhlich Hamiltonian as a perturbation. The unperturbed Hamiltonian then, describes a decoupled system of an electron and phonons. The effect of electron-phonon interaction leads to small corrections for the eigenstates and eigenenergies of the unperturbed Hamiltonian, in the form of a power series in α. To demonstrate the approach of the perturbation theory consider the following Hamiltonian, in which $H^{(1)}$ is small compared to the unperturbed part, $H^{(0)}$.

$$H = H^{(0)} + H^{(1)} \tag{2.2}$$

For the polaron problem we have,

$$H^{(0)} = H_{\rm e} + H_{\rm ph}\,, \qquad H^{(1)} = H_{\rm e-ph}\,. \tag{2.3}$$

The solution of the time-independent Schrödinger equation

$$H\,|\Psi_n\rangle = E_n\,|\Psi_n\rangle \tag{2.4}$$

can be expanded in a perturbation series of the form,

$$\begin{aligned} |\Psi_n\rangle &= |\Psi_n^{(0)}\rangle + |\Psi_n^{(1)}\rangle + |\Psi_n^{(2)}\rangle + \cdots \\ E_n &= E_n^{(0)} + E_n^{(1)} + E_n^{(2)} + \cdots \end{aligned} \tag{2.5}$$

where n stands for all the quantum numbers characterizing the system. Substituting these series in Eq.(2.4), one can consider the terms with the same order independently. The zeroth-order terms give simply the equation for the unperturbed Hamiltonian,

$$H^{(0)}\,|\Psi_n^{(0)}\rangle = E_n^{(0)}\,|\Psi_n^{(0)}\rangle\,, \tag{2.6}$$

which can be assumed to be solved exactly. The first order correction to the energies can be found to be the expectation value of $H^{(1)}$ in the unperturbed states,

$$E_n^{(1)} = \langle\,\Psi_n^{(0)}|\,H^{(1)}\,|\Psi_n^{(0)}\rangle\,. \tag{2.7}$$

For the polaron, as we will see, this first order correction becomes zero, so one should consider the next order for the energy,

$$E_n^{(2)} = \sum_m{}' \frac{|\langle \Psi_n^{(0)}| H^{(1)} |\Psi_m^{(0)}\rangle|^2}{E_n^{(0)} - E_m^{(0)}}. \tag{2.8}$$

Finally, for the eigenstates we have

$$|\Psi_n^{(1)}\rangle = \sum_m{}' \frac{|\Psi_m^{(0)}\rangle\langle \Psi_m^{(0)}| H^{(1)} |\Psi_n^{(0)}\rangle}{E_n^{(0)} - E_m^{(0)}}, \tag{2.9}$$

as the leading order term in the perturbation series.

Among the polaron papers, in which perturbation theory has been applied, we will consider the one by Yıldırım and Erçelebi[45] as an example. In that work, they have attempted to give a unifying picture for all confinement geometries of weakly coupled polaron. It is instructive to review the essential steps of the formulation given therein, since in Section 2.5 the same problem will be treated within the framework of path integral formalism and the correspondence between the two methodologies will be discussed.

The simple model adopted in that work, is capable of reflecting the ground state property of the confined polaron, where the degree of confinement can be chosen flexibly, through the usage of an anisotropic parabolic potential box. However, here we will consider the quasi-2 dimensional slab-like configuration for the confinement of the electron.

With the appropriate units ($2m^\star = \hbar = \omega_{\rm LO} = 1$), the Hamiltonian describing the confined electron coupled to LO-phonons is in the form as given in Eq.(1.27). As the confining potential,

$$V_{\rm conf} = \frac{1}{4}\Omega^2 z^2 \tag{2.10}$$

has been taken, where the dimensionless frequency Ω in units of $\omega_{\rm LO}$ is the measure of the degree of confinement in the z-direction. By varying Ω from zero to values much larger than unity, one can achieve a continuous transition from bulk to the strict 2-dimensional geometry.

The unperturbed states of the system is expressed in a product form of the electron and phonon parts,

$$|\Psi^{(0)}_{\vec{k},\nu,n_Q}\rangle = |\Phi_{\vec{k},\nu}(\vec{\varrho},z)\rangle\ |n_Q\rangle \tag{2.11}$$

where the electronic part satisfies the wave equation

$$H_e \left|\Phi_{\vec{k},\nu}(\vec{\varrho},z)\right\rangle = \epsilon_\nu(\vec{k}) \left|\Phi_{\vec{k},\nu}(\vec{\varrho},z)\right\rangle \qquad \nu = 0,1,2,... \tag{2.12}$$

The electronic wave function is composed of harmonic oscillator states for the z-direction, and since the electron is free in the transverse directions, a plane wave representation is utilized for its motion parallel to the x-y plane,

$$\left|\Phi_{\vec{k},\nu}(\vec{\varrho},z)\right\rangle = \frac{1}{\sqrt{2^\nu \nu!}} \left(\frac{\Omega}{2\pi}\right)^{1/4} H_\nu\left(\sqrt{\frac{\Omega}{2}}z\right) \exp(-\frac{1}{4}\Omega z^2)\ \phi_{\vec{k}}(\vec{\varrho}) \tag{2.13}$$

$$\phi_{\vec{k}}(\vec{\varrho}) \sim \exp(i\vec{k}\cdot\vec{\varrho}) \tag{2.14}$$

with H_ν denoting the Hermite polynomial of degree ν. The corresponding energy eigenvalues of Eq.(2.12) are then given by

$$\epsilon_\nu(\vec{k}) = (\nu + \frac{1}{2})\Omega + k^2\,. \tag{2.15}$$

The phonon state $|n_Q\rangle$ is the Fock number state, with the ground state (phonon vacuum), $|0\rangle$, characterized as;

$$a_Q \left|0\right\rangle = 0\ . \tag{2.16}$$

For the ground state of the polaron, the electron should also be taken in the lowest subband ($\nu = 0$).

The first non-vanishing contribution to the ground state energy comes from the second order term, as given in Eq.(2.8),

$$E_g^{(2)} = -\sum_Q \sum_{\vec{k}'} \sum_\nu \frac{\left|\left\langle \Psi^{(0)}_{\vec{k}',\nu,1_Q} \right| H_{e-ph} \left|\Psi^{(0)}_{\vec{k},0,0}\right\rangle\right|^2}{1 + \epsilon_\nu(\vec{k}') - \epsilon_0(\vec{k})}\ . \tag{2.17}$$

With the form (1.27) of the Fröhlich interaction, the above equation can be written alternatively as,

$$E_g^{(2)} = -\sum_Q V_Q^2 \sum_{\vec{k}'} \sum_\nu \frac{\left|\left\langle \phi_{\vec{k}'} \right| \exp(-i\vec{q}\cdot\vec{\varrho}) \left|\phi_{\vec{k}}\right\rangle\right|^2}{1 + \Omega\nu + k'^2 - k^2} \left|h_\nu(q_z)\right|^2 \tag{2.18}$$

where

$$h_\nu(q_z) = \frac{1}{\sqrt{2^\nu \nu!}} \left(\frac{\Omega}{2\pi}\right)^{1/2} \int_{-\infty}^{\infty} dz \exp(-iq_z z)\, H_\nu\left(\sqrt{\frac{\Omega}{2}} z\right) \exp(-\frac{1}{2}\Omega z^2) \quad (2.19)$$

$$= \frac{(-i)^\nu}{\sqrt{\nu!}} \left(\frac{q_z^2}{\Omega}\right)^{\nu/2} \exp\left(-\frac{q_z^2}{2\Omega}\right) .$$

Projecting out the $\vec{k}'$ summation one obtains

$$E_{\rm g}^{(2)} = -\sum_Q V_Q^2 \sum_\nu \frac{1}{\nu!} \frac{1}{1+\Omega\nu+q^2-2\vec{k}\cdot\vec{q}} \left(\frac{q_z^2}{\Omega}\right)^\nu \exp\left(-\frac{q_z^2}{\Omega}\right) . \quad (2.20)$$

It should be noted that, in the ground state, the electron is stationary ($\vec{k}=0$). However, to keep trace of the effective mass of the polaron, one can consider the electron to have a small momentum ($\vec{k} \simeq 0$), and expand the summand in Eq.(2.20) in a power series up to second order in $\vec{k}\cdot\vec{q}$,

$$E_{\rm g}^{(2)} = -\sum_Q V_Q^2 \exp\left(-\frac{q_z^2}{\Omega}\right) \sum_\nu \frac{1}{\nu!} \left(\frac{q_z^2}{\Omega}\right)^\nu \left(\frac{1}{1+\Omega\nu+q^2} + \frac{(2\vec{k}\cdot\vec{q})^2}{(1+\Omega\nu+q^2)^3}\right) . \quad (2.21)$$

Using the identity

$$\sum_{\nu=0}^{\infty} \frac{1}{\nu!} \frac{\beta^\nu}{(a+b\nu)^{n+1}} = \frac{1}{n!} \int_0^\infty d\eta\, \eta^n \exp(-a\eta + \beta e^{-b\eta}) \qquad n = 0,1,2,... \quad (2.22)$$

and defining

$$\sigma(\eta) = \frac{\Omega\eta}{1-e^{-\Omega\eta}} , \quad (2.23)$$

the ground state energy, $E_{\rm g} = \frac{1}{2}\Omega + k^2 + E_{\rm g}^{(2)}$, can be written as,

$$E_{\rm g} = \frac{1}{2}\Omega - \mathcal{E}_{\rm p} + k^2(1-\mu) \quad (2.24)$$

where

$$\mathcal{E}_{\rm p} = \sum_Q V_Q^2 \int_0^\infty d\eta\, e^{-\eta} \exp\left[-(q^2 + \frac{q_z^2}{\sigma(\eta)})\eta\right] \quad (2.25)$$

and

$$\mu = \sum_Q V_Q^2\, q^2 \int_0^\infty d\eta\, \eta^2\, e^{-\eta} \exp\left[-(q^2 + \frac{q_z^2}{\sigma(\eta)})\eta\right] . \quad (2.26)$$

In the above, $\mathcal{E}_{\rm p}$ is the polaron binding energy and μ is the polaronic contribution to the composite inertia of the electron together with the concomitant cloud of virtual phonons, i.e.

$$m_{\rm p} = (1-\mu)^{-1} \simeq 1+\mu \tag{2.27}$$

is the polaron effective mass in units of $m^\star$.

The evaluation of the integrals in Eq.(2.25) and (2.26) require numerical treatment for arbitrary values of Ω. For the two special cases, however, the analytic results are readily available. In the case of $\Omega = 0$, $\sigma(\eta) = 1$ and one obtains the results relevant to the bulk polaron. For the binding energy one has

$$\mathcal{E}_{\rm p}^{(3D)} = \sum_Q V_Q^2 \int_0^\infty d\eta\, e^{-\eta} \exp\left[-(q^2+q_z^2)\eta\right] = \sum_Q \frac{V_Q^2}{1+Q^2} = \alpha\ . \tag{2.28}$$

Similarly, Eq.(2.26) reduces to

$$\begin{aligned} \mu^{(3D)} &= \sum_Q V_Q^2 q^2 \int_0^\infty d\eta\, \eta^2 e^{-\eta} \exp\left[-(q^2+q_z^2)\eta\right] \\ &= \sum_Q V_Q^2 q^2 \frac{2}{(1+Q^2)^3} = \frac{\alpha}{6}\ . \end{aligned} \tag{2.29}$$

In the strict $2D$ limit ($\Omega \to \infty$), $\sigma(\eta)$ tends to infinity, and the corresponding integrals simplify to

$$\mathcal{E}_{\rm p}^{(2D)} = \sum_Q \frac{V_Q^2}{1+q^2} = \frac{\pi}{2}\alpha \tag{2.30}$$

and

$$\mu^{(2D)} = \sum_Q V_Q^2 q^2 \frac{2}{(1+q^2)^3} = \frac{\pi}{8}\alpha\ . \tag{2.31}$$

The binding energy and the phonon contribution to the effective mass as functions of the degree of confinement, are provided in Fig.2.1. With the increasing value of Ω, both $\mathcal{E}_{\rm p}$ and μ approach smoothly to their asymptotic two-dimensional values.

For a total overview interpolating between all possible extremes of the effective dimensionality one should revise the calculations with a more general confining potential,

$$V_{\rm conf} = \frac{1}{4}\Omega_1^2 \varrho^2 + \frac{1}{4}\Omega_2^2 z^2\ . \tag{2.32}$$

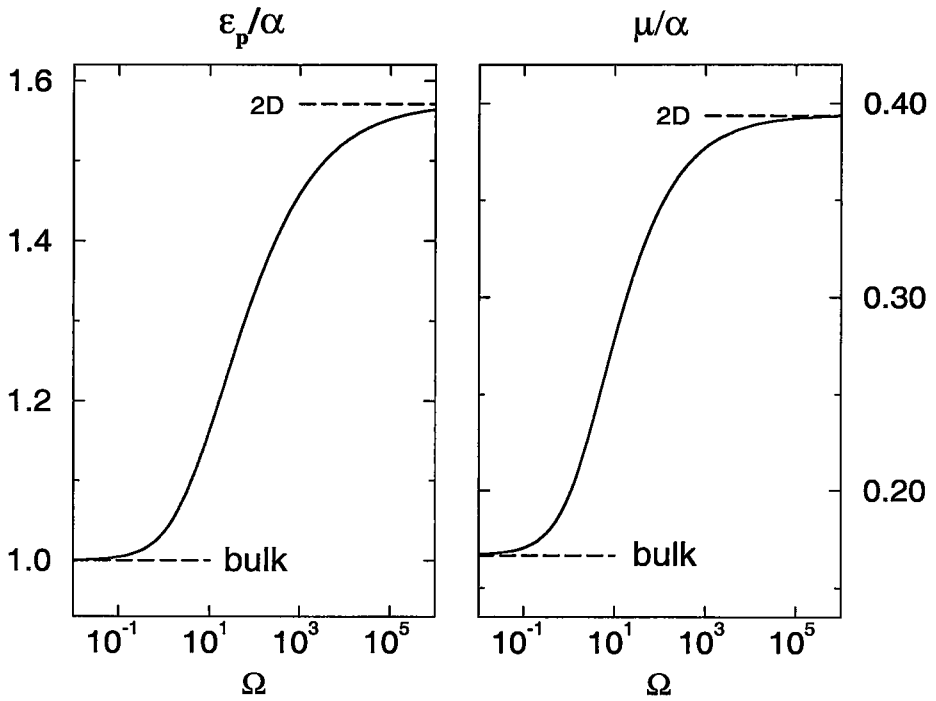

Figure 2.1: Perturbation theory results for quasi-2-dimensional polaron The binding energy $\mathcal{E}_{\rm p}$, and the phonon correction to the effective mass μ as functions of the degree of confinement Ω.

The binding energy thus obtained is given in the same form as in Eq.(2.25) where now it reads as

$$\mathcal{E}_{\rm p} = \sum_{Q} V_Q^2 \int_0^\infty d\eta\, e^{-\eta} \exp\left[-\left(\frac{q^2}{\sigma_1(\eta)} + \frac{q_z^2}{\sigma_2(\eta)}\right)\eta\right] \tag{2.33}$$

with

$$\sigma_i(\eta) = \frac{\Omega_i \eta}{1 - e^{-\Omega_i \eta}} \qquad i = 1, 2\ . \tag{2.34}$$

Projecting out the summations over the wave vector components one obtains,

$$\mathcal{E}_{\rm p} = \frac{\alpha}{\sqrt{\pi}} \int_0^\infty d\eta e^{-\eta} \sqrt{\frac{\sigma_2(\eta)}{\eta}} \frac{\arctan \gamma(\eta)}{\gamma(\eta)} \tag{2.35}$$

where

$$\gamma(\eta) = \left(\frac{\sigma_2(\eta)}{\sigma_1(\eta)} - 1\right)^{1/2}\ . \tag{2.36}$$

By varying the potential parameters Ω_i, one can trace out all possible extremes of the effective dimensionality. For a comparison of the different confinement

	$\mathcal{E}_p/\alpha$		
Ω_1 and/or Ω_2	slab ($\Omega_1 = 0$)	wire ($\Omega_2 = 0$)	box ($\Omega_1 = \Omega_2$)
10	1.16	1.44	2.02
100	1.33	2.23	5.72

Table 2.4: Comparison of polaron binding energies in different confinement geometries

geometries, consider the data given in Table 2.4. The binding gets deeper as the electron confinement is increased.

The domain of validity of perturbation theory is restricted to small values of α. In certain compound semiconductor structures, such as II-VI compounds, the relevant coupling constants cannot be regarded as sufficiently small ($\alpha \simeq 0.4$ for CdTe, for instance) for the perturbation approach to be totally dependable. Moreover, we have mentioned about the pseudo-enhancement in α, realized in confined systems, bringing about a strong coupling counterpart to the problem. Therefore, one requires alternative methods to deal with intermediate and strong coupling regimes, and yet more powerful interpolating theories to get a unifying picture over the complete range of α. Those theories will be the subject matter of the following sections.

2.2 Strong Coupling Theory

When the electron-phonon interaction is strong enough, due to the phonon field there induces a deep deformation potential surrounding the electron, and it appears to be trapped in this potential. With this consideration, the polaron, in strong coupling regime was studied by Pekar[8] (and others[53,54,47]) who hypothesized that in this limit the total ground state wave function could be taken as a product of an electronic function and a phonon part. The Pekar ansatz is based on the physically appealing notion that, at large coupling, the phonons cannot follow the rapidly moving electron (as they do at weak coupling) and so

resign themselves to interacting only with the mean electronic density (adiabatic condition).

Before discussing the details of these arguments, let us first consider the standard canonical transformation of strong coupling theory.

2.2.1 Displaced Oscillator Transformation

The Fröhlich polaron can be viewed as an assembly of harmonic oscillators interacting with the electron. Thus, considering one of those oscillators of the assembly, the wave equation describing the coupling of the oscillator to the electron is given by

$$H_Q \Psi_Q = \left(-\nabla^2_{X_Q} + \frac{1}{4} X_Q^2 - u_Q X_Q \right) \Psi_Q = \epsilon_Q \Psi_Q \tag{2.37}$$

where X_Q and ϵ_Q are the dimensionless coordinate and the energy of the oscillator with the wave vector $\vec{Q}$, and the parameter u_Q is the force term due to the interaction.

After completing to a square, the Eq.(2.37) takes the form

$$\left(-\nabla^2_{X_Q} + \frac{1}{4}(X_Q - 2u_Q)^2 - u_Q^2 \right) \Psi_Q = \epsilon_Q \Psi_Q \tag{2.38}$$

from which $2u_Q$ can be interpreted as the equilibrium coordinate. Assuming that all the phonon modes behave independently in the same way, the total Hamiltonian can be written in terms of the phonon creation and annihilation operators as,

$$H = \sum_Q \left[a_Q^\dagger a_Q - u_Q (a_Q^\dagger + a_Q) \right] . \tag{2.39}$$

The terms linear in $a_Q^\dagger$ and a_Q can easily be made to disappear by defining a set of new operators,

$$\tilde{a}_Q = a_Q - u_Q \qquad \tilde{a}_Q^\dagger = a_Q^\dagger - u_Q \tag{2.40}$$

which can be obtained through a canonical transformation of the previous ones,

$$\tilde{a}_Q = \mathbf{U}^{-1} a_Q \mathbf{U} \qquad \tilde{a}_Q^\dagger = \mathbf{U}^{-1} a_Q^\dagger \mathbf{U} \tag{2.41}$$

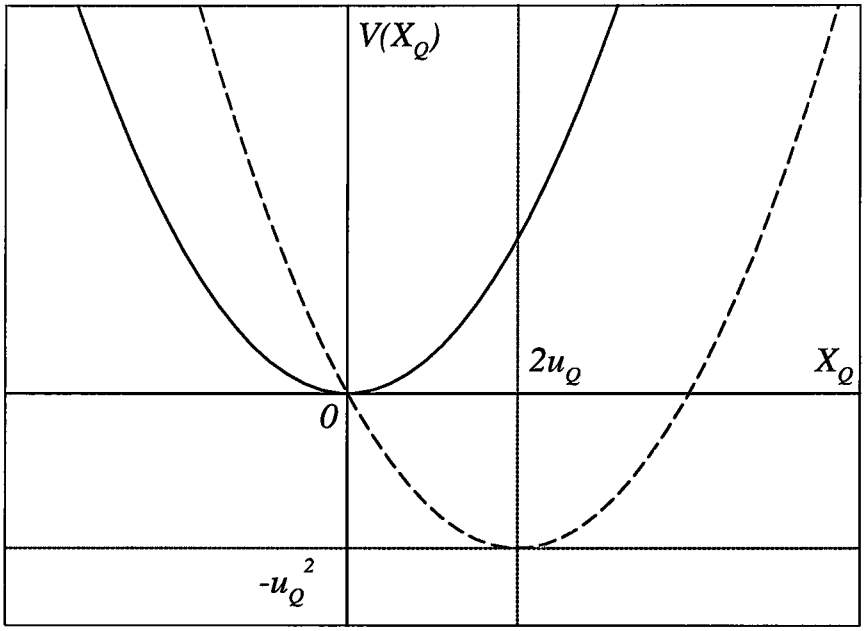

Figure 2.2: Sketch of displaced oscillator potential.
The solid and dashed curves represent undisplaced and displaced oscillators respectively.

where

$$\mathbf{U} = \exp \sum_{Q} u_Q (a_Q - a_Q^\dagger) \; . \tag{2.42}$$

Instead of transforming the phonon operators, one can equivalently consider the phonon ground state to be chosen as $\mathbf{U}|0\rangle$ rather than the bare phonon vacuum $|0\rangle$, where the origin is shifted over to the equilibrium coordinates (cf. Fig.2.2). This kind of representation is widely known as displaced oscillator transformation.

Clearly, the amount by which the origin is to be displaced depends on the interaction strength and further on the electronic charge density in a somewhat implicit manner. Therefore, the procedure of strong coupling theory will consist of proposing a variational wave function for the electron and through the minimization of the ground state energy, determining the variational parameters and the terms u_Q simultaneously. In the rest of this section, we will exemplify these arguments in the case of strongly coupled polaron in a parabolic confinement potential.

2.2.2 Confined Polaron In The Strong-Coupling Limit

The problem of the confined polaron in the limit of strong coupling has been studied previously.[61] Here we state the essential steps to calculate the ground state energy, since we will require the one-polaron results in the consideration of bipolaron formation criteria.

The confinement potential is taken as in Eq.(2.32). Using the variational principle, for the trial wave function we impose a product ansatz separable in the particle and phonon coordinates, i.e.,

$$\Psi = \phi(\varrho, z) \times \exp \sum_{Q} s_Q \, (a_Q - a_Q^{\dagger})|0\rangle \tag{2.43}$$

in which we use an oscillator particle-wavefunction

$$\phi(\varrho, z) = N \, \exp\left\{-\frac{1}{2}\kappa^2(\varrho^2 + \mu^2 z^2)\right\} . \tag{2.44}$$

Here, N is the normalization constant and κ, μ are variational parameters. μ accounts for the cylindrical anisotropy imposed by the external potential. The exponential operator acting on the phonon vacuum is the displaced oscillator transformation where s_Q is a variational parameter determined from the requirement: $\partial\langle\Psi|H|\Psi\rangle/\partial s_Q = 0$, to yield

$$\begin{aligned} s_Q &= V_Q \, \langle\phi|e^{\pm i\vec{Q}\cdot\vec{r}}|\phi\rangle \\ &= \exp\left(-\frac{1}{2\kappa^2\mu^2}(\mu^2 q^2 + q_z^2)\right) . \end{aligned} \tag{2.45}$$

Using (2.45) in (2.43), and projecting out the $\vec{Q}$-summations in $E_{\rm g} = \langle\Psi|H|\Psi\rangle$, we obtain the one-polaron ground state energy, given by

$$\begin{aligned} E_{\rm g} = \frac{1}{4}\kappa^2(2+\mu^2) \;&+\; \frac{1}{2\kappa^2}\left(\Omega_1^2 + \frac{\Omega_2^2}{2\mu^2}\right) \\ &-\; \frac{\alpha}{\sqrt{\pi}}\kappa\mu\frac{\arctan\sqrt{\mu^2-1}}{\sqrt{\mu^2-1}} . \end{aligned} \tag{2.46}$$

The energy expression above generates the well known bulk and 2D limits and displays the effect of external confinement on the polaron energy.[61] Choosing suitable domains of potential parameters, the single expression is capable of providing polaron ground state energy in all types of confinement geometries.

2.3 Intermediate Coupling Theory

In the last two sections, we have considered the two methods appropriate to the small and large values of the electron phonon interaction strength. However, in some cases of interest, the interaction constant has intermediate values, being so large that the perturbation theory breaks down, but on the other hand it is still small for the adiabatic approximation to be totally valid. The earliest attempt to deal with this intermediate coupling regime has been made by Lee, Low and Pines (LLP).[46] The method is based on a variational technique, which is equivalent to a simple canonical transformation. At weak coupling, LLP approximation reproduces the results of perturbation theory, and moreover, it has a considerable validity for intermediate values of the coupling constant up to $\alpha \sim 4$.

2.3.1 LLP Transformation

In quantum mechanics, the symmetry properties of the physical system lead to important conservation laws. In this regard, the conservation of linear momentum is a consequence of translational symmetry. For the polaron problem, the total momentum operator,

$$\vec{\mathsf{P}} = \vec{p} + \sum_{Q} \vec{Q} a_Q^\dagger a_Q \ , \tag{2.47}$$

of the system is a constant of motion and commutes with the Fröhlich Hamiltonian, which we restate here for the bulk polaron and in the usual dimensionless units (and $2m^\star = 1$),

$$H = p^2 + \sum_{Q} a_Q^\dagger a_Q + \sum_{Q} V_Q \left(a_Q e^{i\vec{Q}\cdot\vec{r}} + \mathrm{hc} \right) \ . \tag{2.48}$$

Therefore, it is possible to transform to a representation in which the electron coordinates are totally eliminated and in which the total momentum $\vec{\mathsf{P}}$ becomes a c-number. The required unitary transformation, introduced by Lee, Low and Pines,[46] is generated by,

$$\mathbf{U}_1 = \exp\left\{ i(\vec{\mathsf{P}} - \sum_{Q} \vec{Q} a_Q^\dagger a_Q) \cdot \vec{r} \right\} \ . \tag{2.49}$$

Since a unitary transformation preserves the eigenvalues of the Schrödinger equation, the basic polaron Hamiltonian can equivalently be taken as

$$\mathcal{H} = \mathbf{U}_1^{-1} H \mathbf{U}_1 \tag{2.50}$$

in this approximation.

The form of $\mathcal{H}$ is easily obtained by considering the transformation of the operators $\vec{p}$, a_Q, $a_Q^\dagger$ and $e^{i\vec{Q}\cdot\vec{r}}$. In the new representation one finds,

$$\mathbf{U}_1^{-1}\vec{p}\,\mathbf{U}_1 = \vec{\mathsf{P}} - \sum_Q \vec{Q} a_Q^\dagger a_Q + \vec{p} \tag{2.51}$$

and

$$\mathbf{U}_1^{-1} a_Q \mathbf{U}_1 = a_Q e^{-i\vec{Q}\cdot\vec{r}}\ ; \quad \mathbf{U}_1^{-1} a_Q^\dagger \mathbf{U}_1 = a_Q^\dagger e^{i\vec{Q}\cdot\vec{r}}\ , \tag{2.52}$$

while $e^{i\vec{Q}\cdot\vec{r}}$ is left invariant under this transformation. Setting $\vec{p} = 0$, the new Hamiltonian now gets the form,

$$\mathcal{H} = \left(\vec{\mathsf{P}} - \sum_Q \vec{Q} a_Q^\dagger a_Q\right)^2 + \sum_Q V_Q \left(a_Q + a_Q^\dagger\right)\ . \tag{2.53}$$

The problem is then reduced to the calculation of the ground state energy $E_{\mathrm{g}}(\mathsf{P})$ of this Hamiltonian, for a given momentum P. For the low-lying energy levels of the electron, $E_{\mathrm{g}}(\mathsf{P})$ can be represented by a power series expansion in P^2. Thus, up to first order in P^2, one can write $E_{\mathrm{g}}(\mathsf{P}) \simeq -\mathcal{E}_{\mathrm{p}} + \mathsf{P}^2/m_{\mathrm{p}}$, where $\mathcal{E}_{\mathrm{p}}$ is the polaronic binding energy and m_{p} is identified as the polaron mass (in units of $m^\star$).

The calculation of $E_{\mathrm{g}}(\mathsf{P})$ requires a variational procedure. It is the expectation value of the Hamiltonian $\mathcal{H}$ in the ground state Ψ_{g}, chosen in the form,

$$\Psi_{\mathrm{g}} = \mathbf{U}_2 |\,0\,\rangle, \tag{2.54}$$

where $|\,0\,\rangle$ is the phonon vacuum, and

$$\mathbf{U}_2 = \exp \sum_Q u_Q (a_Q - a_Q^\dagger) \tag{2.55}$$

is the generator of displaced oscillator transformation that we have introduced previously in the strong coupling theory. The parameters u_Q are to be determined variationally to minimize the ground state energy.

In their original work, using the outlined procedure, LLP have found the ground state polaronic binding energy in the leading order of α,

$$\mathcal{E}_{\rm p} = \alpha \ , \tag{2.56}$$

same as in second order perturbation theory, but the effective mass is obtained in the form

$$m_{\rm p} = 1 + \alpha/6 \tag{2.57}$$

regardless of the value of coupling constant. In contrast to that obtained by perturbation theory, $m_{\rm p} = 1/(1 - \alpha/6)$, this form of effective mass does not suffer from the unacceptable divergence at $\alpha \sim 6$. Therefore, it seems that LLP approximation expands the domain of validity of perturbation theory results up to intermediate values of α.

2.4 Perturbative Variational Approach

We have seen that for not too weak and pseudo-enhanced electron-phonon interaction the strong coupling polaron theory, though not capable of reflecting a totally dependable quantitative description, may serve so as to provide some qualitative insight into the study of polarons in confined media consisting of materials of somewhat strong polar crystals. On the other hand, a pure perturbation treatment may also be not perfectly appropriate except for too weak phonon coupling. We are therefore tempted to formulate the bulk- and 2D-polaron problem within the framework of a more convenient approach accounting for its weak and strong coupling counterparts simultaneously.[66] The formalism we follow in this section consists of the usage of a perturbative variational approach used previously by Devreese *et al.*[65] in their application to the bulk optical polaron bound to a Coulomb center. The procedure is structured on basing the starting ansatz on the standard displaced oscillator transformation of the Pekar strong

coupling theory[8] and then modify the adiabatic polaron state by a variationally determined perturbative extension serving for the theory to interpolate in the overall range of the coupling constant.

The variational approach that we adopt is based on utilizing the usual canonical transformation of the strong–coupling formalism and then extend the adiabatic polaron state by including an approximate first order perturbative correction by which it is possible to interrelate the strong and weak coupling counterparts of the coupled electron-phonon system. Regardless of the strength of the coupling constant the starting step in the foregoing theory is to assume a highly rapid charge density fluctuations for the electron to which the lattice responds by acquiring a relaxed deformation clothing the entire extent of the electron. The adiabatic polaron ground state thus formed is given through a product ansatz consisting of the electron and phonon parts, i.e.,

$$\Psi_{\mathrm{g}} = \Phi_{\mathrm{e}}(\vec{r}) \mid 0 \rangle \ , \tag{2.58}$$

together with the Hamiltonian subjected to the displaced oscillator transformation

$$H \rightarrow \tilde{H} = e^{-\mathbf{U}} H e^{\mathbf{U}} \tag{2.59}$$

where

$$\mathbf{U} = \sum_{Q} u_Q(\Phi_{\mathrm{e}})[a_Q - a_Q^{\dagger}] \ . \tag{2.60}$$

Here, $u_Q(\Phi_{\mathrm{e}})$ is the lattice variational parameter which will depend on $\vec{r}$, since it is via this parameter an interrelation establishes between the potential well set up by the lattice polarization and the electron which, in turn, becomes trapped in this well. It then follows that for each choice of Φ_{e} there is an optimal fit to u_Q and therefore the transformed Hamiltonian depends on Φ_{e} implicitly.

We set the electron wave function in the form

$$\Phi_{\mathrm{e}}(\vec{r}) = \phi(\vec{r}) \ e^{i\vec{\kappa}\cdot\vec{r}} \tag{2.61}$$

wherein the exponential factor (with $\vec{\kappa}$ to be determined variationally) sets the system in motion, thus enabling one to trace the polaron mass. The spatial

part, $\phi(\vec{r})$, is taken in the Gaussian form with variance σ, which is also treated as a variational parameter. In the above and the following all the vectors and operators should be considered as three (two) dimensional for the bulk (2D) polaron.

Under the transformation (2.59), the Hamiltonian conforms to

$$\begin{aligned}\tilde{H} = -\nabla^2 \;&+\; \sum_Q u_Q^2 - \sum_Q V_Q u_Q[\exp(i\vec{Q}\cdot\vec{r}) + \text{cc}] \\ &+\; \sum_Q a_Q^\dagger a_Q + \sum_Q \{[V_Q \exp(i\vec{Q}\cdot\vec{r}) - u_Q]a_Q + \text{hc}\} \; . \end{aligned} \tag{2.62}$$

Since the Hamiltonian is invariant under translations of the electron together with its concomitant lattice distortion, the total momentum

$$\vec{\mathsf{P}} = -i\vec{\nabla} + \sum_Q \vec{Q} a_Q^\dagger a_Q \tag{2.63}$$

must be conserved. The variation therefore requires an optimization of the polaron state $e^{\mathbf{U}}\Psi_{\mathrm{g}}$, which minimizes H subject to the constraint that $\vec{\mathsf{P}}$ is a constant of motion. Thus, minimizing the functional

$$\mathsf{F}(\sigma, \vec{v} \mid u_Q, \vec{\kappa}) \;\equiv\; \langle\, \Psi_{\mathrm{g}} \mid e^{-\mathbf{U}}(H - \vec{v}\cdot\vec{\mathsf{P}})e^{\mathbf{U}} \mid \Psi_{\mathrm{g}} \,\rangle \tag{2.64}$$

with respect to $\vec{\kappa}$ and u_Q yields

$$\vec{\kappa} = \frac{1}{2}\vec{v} \qquad \text{and} \qquad u_Q(\Phi_{\mathrm{e}}) = V_Q s_Q \rho_Q \tag{2.65}$$

where

$$s_Q \;=\; \langle\, \Phi_{\mathrm{e}} \mid \exp\{\pm i\vec{Q}\cdot\vec{r}\} \mid \Phi_{\mathrm{e}} \,\rangle \tag{2.66}$$

$$\rho_Q \;=\; (1 - \vec{v}\cdot\vec{Q})^{-1} \tag{2.67}$$

in which the Lagrange multiplier $\vec{v}$ is to be identified as the polaron velocity.[86] In equation (2.64) the symbol σ stands for the variational parameter(s) contained in $\Phi_{\mathrm{e}}(\vec{r})$.

In complete form, with the optimal fits for $\vec{\kappa}$ and u_Q substituted in, the Hamiltonian which we shall be referring hereafter is

$$\begin{aligned}\tilde{H} \;=\; -\nabla^2 \;+\; \sum_Q a_Q^\dagger a_Q + \sum_Q V_Q^2 s_Q^2 \rho_Q^2 \\ -\; \sum_Q V_Q^2 s_Q \rho_Q (e^{i\vec{Q}\cdot\vec{r}} + e^{-i\vec{Q}\cdot\vec{r}}) \;+\; \sum_Q V_Q (\eta_Q a_Q + \eta_Q^* a_Q^\dagger)\end{aligned} \tag{2.68}$$

where

$$\eta_Q = e^{i\vec{Q}\cdot\vec{r}} - s_Q \rho_Q \; . \tag{2.69}$$

Similarly, for the total momentum transformed accordingly, $\vec{\mathsf{P}} \rightarrow e^{-\mathsf{U}} \vec{\mathsf{P}} e^{\mathsf{U}}$, we have

$$\tilde{\vec{\mathsf{P}}} = -i\vec{\nabla} + \sum_Q \vec{Q} a_Q^\dagger a_Q + \sum_Q V_Q^2 \vec{Q} s_Q^2 \rho_Q^2 - \sum_Q V_Q \vec{Q} s_Q \rho_Q (a_Q + a_Q^\dagger) \; . \tag{2.70}$$

In what follows we shall consider the case of a stationary polaron, i.e. take $\langle \Psi_g \mid \tilde{\vec{\mathsf{P}}} \mid \Psi_g \rangle$ as zero, and thus regard $\vec{v}$ as a virtual velocity which we retain in our calculations to keep track of the effective mass of the coupled electron-phonon complex.

Regardless of the value of α, no matter how small it is, the procedure is still to continue with our considerations from Eq.(2.68), since with decreasing α the degree of localization of the electron becomes reduced in a significant manner; eventually s_Q tends to zero on the average, and thus $\tilde{H}$ converts back to its original form H stripped from the displaced oscillator transformation. In view of this reasoning one is led to include a first order correction to the trial state (2.61) with the last term in Eq.(2.68) treated as a perturbation. Since at present we limit ourselves to the case of a stationary polaron, we first would like to bring about an insight into the problem with ρ_Q in Eq.(2.68) set to unity, thereby obtain a means of characterizing the polaron (i.e., calculating the optimal Φ_e and hence the binding energy, for instance) for the case when $v = 0$. Thereafter we shall turn on the velocity to keep trace of the polaron mass under a virtual translation of the electron and the lattice distortion together.

In the perturbation treatment of the Fröhlich interaction, the first non-vanishing contribution to the ground-state energy comes from the term which

is of second order in the interaction amplitude. Correspondingly, the leading order correction to the trial state defined through Eq.(2.61) is of first order. The ground state trial wave function for $\tilde{H}$ and for the constraint that the total momentum $\tilde{\vec{\mathsf{P}}}$ be conserved, then becomes extended to

$$\Psi_{\mathrm{g}} \rightarrow \tilde{\Psi}_{\mathrm{g}} \;=\; c\Psi_{\mathrm{g}} \;+\; \sum_{Q} V_Q \sum_{i} \mid \Psi_i \rangle \frac{\langle\, \Psi_i \mid (e^{-i\vec{Q}\cdot\vec{r}} - s_Q) a_Q^{\dagger} \mid \Psi_{\mathrm{g}} \,\rangle}{\Delta\varepsilon_{i-g}} \;. \qquad (2.71)$$

In the above, c is a constant which serves for normalization, and the index i refers to the intermediate states consisting those of the electron and one-phonon with wave vector $\vec{Q}$. The summation over the intermediate states is a rather difficult task, since now the states themselves and the corresponding energies depend on α and the lattice coordinates in involved manners. Nevertheless, this shortcoming can be eliminated by replacing the energy denominator $\Delta\varepsilon_{i-g}$ by an average quantity

$$g_Q = \left\langle \frac{1}{\Delta\varepsilon_{i-g}} \right\rangle_i \qquad (2.72)$$

which in the calculation will be determined variationally. Using completeness the i–summation in Eq.(2.71) can be projected out to yield[65]

$$\tilde{\Psi}_{\mathrm{g}} \;=\; \{c \;+\; \sum_{Q} V_Q g_Q (e^{-i\vec{Q}\cdot\vec{r}} - s_Q) a_Q^{\dagger}\} \Psi_{\mathrm{g}} \;. \qquad (2.73)$$

The variational parameter g_Q sets up a fractional admixture of the strong and weak coupling counterparts of the coupled electron–phonon system and thus is expected to serve for the theory to interpolate between the extreme limits of the coupling constant.

After a series of tedious but straightforward algebra the functional F can be evaluated. In order to trace out the polaron mass, we have to split $\mathsf{F}(\sigma, \vec{v})$ into its parts, consisting of the ground state energy of the polaron alone and the additional kinetic contribution which shows up after imposing a virtual momentum on the polaron;

$$\mathsf{F}(\sigma, \vec{v}) = E_{\mathrm{g}}(\sigma) - \frac{1}{4} v^2 m_{\mathrm{p}} \;, \qquad (2.74)$$

the explicit forms of which are a bit lengthy to be stated here.[66]

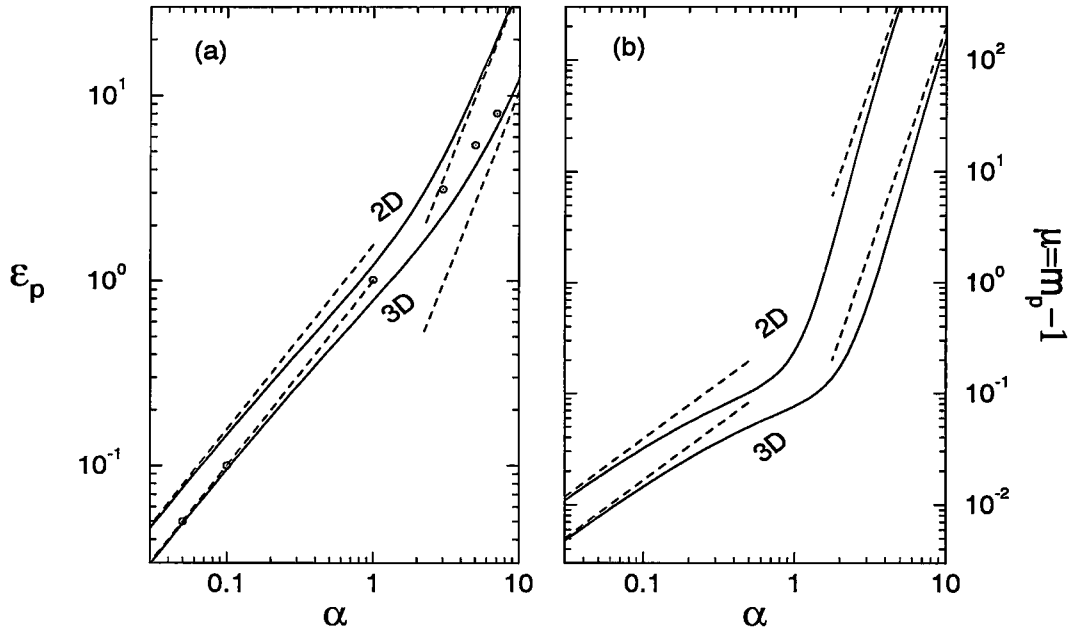

Figure 2.3: 2D and 3D polaron energy and mass
(a) The binding energy and (b) the phonon contribution to the effective mass as a function of α for the 3D and 2D polarons. The broken lines refer to the results of the strong coupling and second-order perturbation theories. The centered dots display the 3D results of the generalized path integral formalism.[75]

In order to provide a general display of our results (beyond those for $\alpha \gg 1$ and $\alpha \ll 1$), we minimize E_g numerically over a reasonably broad range of α, for the 3D and 2D polarons. In Fig.2.3 we plot the binding energy ($\varepsilon_p = \mid E_g \mid$), and the phonon contribution to the effective mass ($\mu = m_p - 1$) as a function of the coupling constant, including also a comparison of the present results with those of the strong-coupling and perturbation theories. An immediate glance at the set of curves on the large α site reveals that the strong coupling theory deviates considerably from the present formalism except in the extreme limit $\alpha \gg 1$. The reason lies in that the pure strong coupling treatment of the problem is totally inadequate to reflect any weak coupling aspect for not too strong α. This shortcoming is however eliminated in the present approach by introducing the first order correction to the trial wave function, through which a detailed interbalance is set up between the strong and weak coupling counterparts of the problem.

A further feature pertaining to the regime of strong phonon coupling is that with growing α, the rate, at which the the strong coupling and present theories approach one another and eventually match, is relatively faster in two dimensions than in three. For $\alpha = 10$, for instance, we find $\varepsilon_{\rm p} = 12.30$ for the 3D-polaron, whereas the corresponding strong-coupling value is $\alpha^2/3\pi = 10.61$, yielding a percentual deviation somewhat close to 14%. The discrepancy for the 2D-polaron, still yet not negligible, is however not more than 3%. This merely is a consequence of the general trend that the electron-phonon interaction is inherently stronger in systems of lower dimensionality.

A complementary remark in concern with the improvement achieved through the perturbative extension in the trial state (2.73) is that the theory gives by far very satisfying results in the strong coupling regime. For the 2D-polaron for example, the bare strong coupling theory (under a Gaussian electron profile) gives $E_{\rm g} = -(\pi/8)\alpha^2 = -0.3927\alpha^2$. The presumably exact upper bound for the ground state energy has been obtained as $-0.4047\alpha^2$ by Xiaoguang, Peeters and Devreese,[81] utilizing what they refer to as the modified Pekar–type ansatz:

$$\Phi_{\rm e} \sim \{1 + br + a(br)^2 + c(br)^3 + d(br)^4\}e^{-br}. \tag{2.75}$$

Even though the usage of such a four parameter form for the electron wavefunction would have been more appropriate, we have chosen to use the approximate Gaussian form to facilitate our calculations which would be very tedious otherwise. Yet, in spite of this simplification, we see that for somewhat large but however finite α, the trial state (2.73) yields far better results compared with those obtained from the expression $-(\pi/8)\alpha^2$. For $\alpha = 10$, for instance, the energy value we attain is -40.43 which is fairly close to the exact upper bound within 0.1%. Clearly, in the limit $\alpha \to \infty$, the present results asymptotically tend to the usual approximate value: $-(\pi/8)\alpha^2$ due to the *a priori* Gaussian type character embedded in our trial wavefunction.

In view of the results we have obtained, we see that the formulation we have considered is quite successful in that the theory, starting from an *a priori* strongly coupled polaron state, and generating fairly well results for large α, extrapolates

towards the opposite extreme and yields the correct perturbation values within first order α. However, unfortunately the coefficient of the second order term of the small expansion of $\varepsilon_{\rm p}(\alpha)$ is negative, which is clearly unacceptable.[29] So we should admit that the theory is only poorly valid to result in a totally dependable characterization of the free polaron in the intermediate coupling regime (cf, Fig.2.3(a)). We feel that the drawback encountered here stems from that in arriving at equation (2.73) the variational parameter g_Q is introduced to replace the energy denominator $\Delta\varepsilon_{i-o}$ as averaged out over the intermediate state index i, thus containing only an average of the detailed content of the Fröhlich interaction interrelated to each of the intermediate states involved in the perturbation sum in equation (2.71).

In summary, we see that the present theory, besides yielding significantly improved energy upper bounds for strong phonon coupling, is as well capable of extrapolating itself towards the weak coupling regime within leading order perturbation calculation.

2.5 Feynman Path-Integral Theory

Feynman's path integral approach has become a unifying formalism in several branches of physics, with such applications in Brownian motion, quantum mechanics, quantum field theory, solid state physics, quantum electro-dynamics, etc. A diverse treatment of the formalism and its applications can be found in the excellent textbook by Feynman and Hibbs,[87] also in some recent publications.[88–90]

In this introductory section we intend to summarize only some basic features of the formalism, required for the treatment of the polaron with path integrals.

2.5.1 Basic Concepts

In quantum mechanics, we deal with the occurrence probabilities of the physical events. The probability of a particle to reach a space-time point $(\vec{r}_b, t_b)$ starting

from a space-time point $(\vec{r}_a, t_a)$ is denoted by

$$P(b,a) = |K(\vec{r}_b, t_b; \vec{r}_a, t_a)|^2 \ . \tag{2.76}$$

Here, $K(\vec{r}_b, t_b; \vec{r}_a, t_a)$ is the probability amplitude (or quantum mechanical propagator) for that event, and it is the sum over the the amplitudes of all possible paths $\vec{r}(t)$ with $\vec{r}(t_a) = \vec{r}_a$ and $\vec{r}(t_b) = \vec{r}_b$. The amplitude associated with each path $\vec{r}(t)$ is proportional to $\exp\{i\mathcal{S}[\vec{r}(t)]/\hbar\}$ where $\mathcal{S}[\vec{r}(t)]$ is the classical action for the trajectory $\vec{r}(t)$:

$$K(\vec{r}_b, t_b; \vec{r}_a, t_a) = \int \mathcal{D}\vec{r}\ e^{i\mathcal{S}[\vec{r}]/\hbar} \tag{2.77}$$

with $\mathcal{D}\vec{r}$ denoting the functional integral over the paths.

If $\Psi(\vec{r}, t) \equiv \langle \vec{r}|\Psi(t)\rangle$ is the wave function of the system in the position representation at time t, the propagator $K(\vec{r}_b, t_b; \vec{r}_a, t_a)$, by definition relates $\Psi(\vec{r}_b, t_b)$ to $\Psi(\vec{r}_a, t_a)$:

$$\Psi(\vec{r}_b, t_b) = \int d\vec{r}_a\, K(\vec{r}_b, t_b; \vec{r}_a, t_a)\Psi(\vec{r}_a, t_a) \tag{2.78}$$

which establishes the relation between path integrals and the operator formulation of quantum mechanics. The path integral in Eq.(2.77) corresponds to a matrix element in position representation of the time-evolution operator in the operator formulation of quantum mechanics. Thus, for a time-independent Hamiltonian,

$$K(\vec{r}_b, t; \vec{r}_a, 0) = \langle \vec{r}_b|e^{-itH/\hbar}|\vec{r}_a\rangle \ . \tag{2.79}$$

With the use of time-independent Schrödinger equation, $H|\Psi_n\rangle = E_n|\Psi_n\rangle$, it is possible to write,

$$\begin{aligned} K(\vec{r}_b, t; \vec{r}_a, 0) &= \sum_n \langle \vec{r}_b|e^{-itH/\hbar}|\Psi_n\rangle\langle\Psi_n|\vec{r}_a\rangle \\ &= \sum_n \langle \vec{r}_b|\Psi_n\rangle\langle\Psi_n|\vec{r}_a\rangle e^{-itE_n/\hbar} \end{aligned} \tag{2.80}$$

i.e. the Fourier expansion of the path integral allows us to determine the eigen energies of a stationary system:

$$K(\vec{r}_b, t; \vec{r}_a, 0) = \sum_n \Psi_n(\vec{r}_b)\Psi_n^*(\vec{r}_a)e^{-itE_n/\hbar} \ . \tag{2.81}$$

Replacing the time variable t by an *imaginary time* variable β, ($t \to -i\hbar\beta$, with β to be interpreted as $1/k_BT$, where T is the temperature and k_B the Boltzmann constant), it is clear that the behavior of the resulting *propagator for imaginary times* is governed by the ground state energy in the asymptotic limit $\beta \to \infty$;

$$K(\vec{r}_b, -i\hbar\beta; \vec{r}_a, 0) \overset{\beta\to\infty}{\longrightarrow} \Psi_0(\vec{r}_b)\Psi_0^*(\vec{r}_a)e^{-\beta E_0} \tag{2.82}$$

whereas for arbitrary β one readily obtains the relation between the propagator and the partition function;

$$\mathcal{Z} \equiv \mathrm{Tr}\, e^{-\beta H} = \int d\vec{r}_0\, K(\vec{r}_0, -i\hbar\beta; \vec{r}_0, 0)\ . \tag{2.83}$$

2.5.2 Elimination of the Phonon Field

The Fröhlich Hamiltonian describes the coupling of the electron to the harmonic phonon modes. Therefore, here, we will state the form of partition function for the system of an electron linearly coupled to a harmonic oscillator. Consider the Hamiltonian

$$H = H_e + \hbar\omega(a^\dagger a + 1/2) + fa + f^\dagger a^\dagger \tag{2.84}$$

where H_e is the part related to the electron and $f, f^\dagger$ sets up the interaction with the oscillator. The partition function can be evaluated by using the ordered operator technique to yield a form independent of the oscillator operators $a, a^\dagger$. In the language of path integrals, the final form of $\mathcal{Z}$ after the elimination of the oscillator, is written as,

$$\mathcal{Z} = \frac{e^{-\beta\hbar\omega/2}}{1 - e^{-\beta\hbar\omega}} \int d\vec{r}_0 \int_{\vec{r}_0}^{\vec{r}_0} \mathcal{D}\vec{r} e^{\mathcal{S}_e + \mathcal{S}'} \tag{2.85}$$

where $\mathcal{S}_e$ is the part of the action corresponding to H_e and

$$\mathcal{S}' = \frac{1}{2}\int_0^\beta d\lambda \int_0^\beta d\lambda'\, G_\omega(|\lambda - \lambda'|) f(\lambda) f(\lambda') \tag{2.86}$$

belongs to the interaction. Here, λ and λ' are the imaginary time variables, and

$$G_\omega(u) = \frac{\cosh((\beta - 2u)\hbar\omega/2)}{\sinh(\beta\hbar\omega/2)} \overset{\beta\to\infty}{\longrightarrow} e^{-\omega u} \tag{2.87}$$

is the Green's function of the harmonic oscillator. Note that the price paid for the elimination of the oscillator is the retarded interaction occurring in $\mathcal{S}'$.

2.5.3 A Variational Principle

When the exact evaluation of the path integrals is not possible or hard to manage, one can use a variational principle, namely Jensen-Feynman inequality for the approximate evaluation of certain type of them.

Suppose we wish to evaluate the free energy F of a system. The partition function can be expressed in the form ($\hbar = 1$)

$$\mathcal{Z} = \int d\vec{r}_0 \int_{\vec{r}_0}^{\vec{r}_0} \mathcal{D}\vec{r} e^{\mathcal{S}} = e^{-\beta F} \ . \tag{2.88}$$

The action $\mathcal{S}$ in the above, is real in ordinary cases without a magnetic field, and the following principle is applicable for real $\mathcal{S}$. (However, recently, the conditions for its validity with imaginary actions have been explored and discussed in detail[88,91]).

To obtain an approximate value of F, one should find another trial action $\mathcal{S}_0$ (with variational parameters) satisfying two conditions. First, $\mathcal{S}_0$ should be simple enough that expressions such as $\int \mathcal{D}\vec{r} e^{\mathcal{S}_0}$ or the weighted averages like $\langle \mathcal{A} \rangle_{\mathcal{S}_0} = (\int \mathcal{D}\vec{r}\, \mathcal{A}\, e^{\mathcal{S}_0})/(\int \mathcal{D}\vec{r} e^{\mathcal{S}_0})$, for simple functionals $\mathcal{A}$ can be evaluated. Second, $\mathcal{S}_0$ should resemble $\mathcal{S}$ as much as possible to be a representative of the general character of it.

Assume that F_0, the free energy associated with $\mathcal{S}_0$, is calculated. That is

$$e^{-\beta F_0} = \int d\vec{r}_0 \int_{\vec{r}_0}^{\vec{r}_0} \mathcal{D}\vec{r} e^{\mathcal{S}_0} \tag{2.89}$$

so that

$$\frac{\int d\vec{r}_0 \int_{\vec{r}_0}^{\vec{r}_0} \mathcal{D}\vec{r} e^{\mathcal{S}}}{\int d\vec{r}_0 \int_{\vec{r}_0}^{\vec{r}_0} \mathcal{D}\vec{r} e^{\mathcal{S}_0}} = e^{-\beta(F-F_0)} \ . \tag{2.90}$$

Then, since $e^{\mathcal{S}} = e^{\mathcal{S}-\mathcal{S}_0} e^{\mathcal{S}_0}$, we can write Eq.(2.90) as

$$\langle e^{\mathcal{S}-\mathcal{S}_0} \rangle_{\mathcal{S}_0} = e^{-\beta(F-F_0)} \ . \tag{2.91}$$

At this point we can make a rigorous approximation. The average value of e^x when x is a random variable, is always larger than or equal to the exponential of

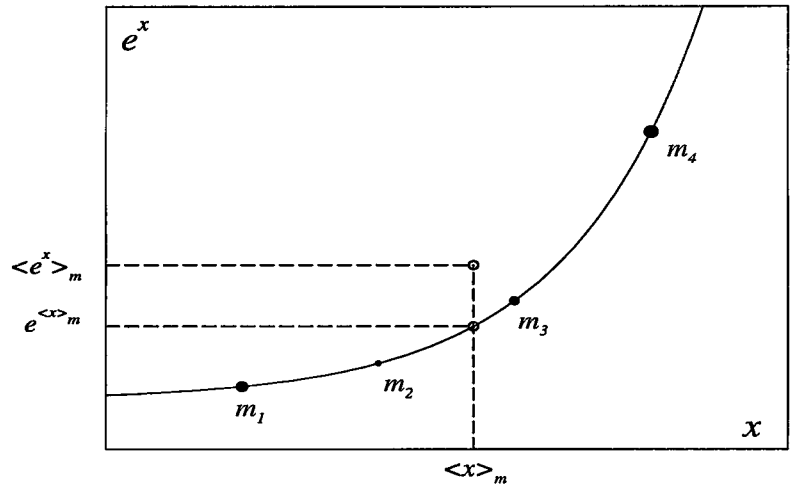

Figure 2.4: Illustration of Jensen's inequality.
The masses m_i have different weights and $\langle\ \rangle_m$ denotes the weighted average.

the average value of x, as long as x is real and the weights used in the averaging process are positive (Jensen's inequality). That is

$$e^{\langle x \rangle} \leq \langle e^x \rangle \tag{2.92}$$

where $\langle x \rangle$ is the weighted average of x. This relation is true for any concave upward function like the exponential function. A pictorial presentation of the relation (2.92) can be clearly seen in Fig.2.4 where a number of masses are placed on the curve e^x.

Changing the left-hand side of Eq.(2.91), we have

$$e^{\langle \mathcal{S}-\mathcal{S}_0 \rangle_{\mathcal{S}_0}} \leq e^{-\beta(F-F_0)} \ . \tag{2.93}$$

This implies that

$$F \leq F_0 - \frac{1}{\beta}\langle \mathcal{S}-\mathcal{S}_0 \rangle_{\mathcal{S}_0} \ . \tag{2.94}$$

The right-hand side of the above equation constitutes an upper bound for the exact free energy F. The closest approximation to F can be determined through the minimization of $F_0 - \frac{1}{\beta}\langle \mathcal{S}-\mathcal{S}_0 \rangle_{\mathcal{S}_0}$ with respect to the variational parameters contained in $\mathcal{S}_0$.

The same variational principle can be used for the ground state energy of the system by simply taking the low temperature limit ($\beta \to \infty$) of Eq.(2.94), since we have $E_g = \lim_{\beta\to\infty} F$.

The important relation given in Eq.(2.94) is referred to as Jensen-Feynman inequality, which we will make use of in the next section on the path integral treatment of confined polaron.

2.5.4 Application: Confined Polaron

Introduction

In this application,[85] we are tempted to formulate the confined polaron problem within the framework of the Feynman path integral theory[7] which proves to be a convenient and powerful technique in the treatment of the Fröhlich interaction over the entire range of the electron-phonon coupling strength and the degree of confinement. A description of the lowest polaron bound state has already been reviewed previously by Yıldırım and Erçelebi[45,61] within a generalized confining potential which can be tuned to all geometric configurations and interesting regimes of the effective dimensionality. However, the relevant discussions therein have been restricted separately to either the strong- or the weak-coupling limit. In what follows we refer to the same model used in these papers and present a means of formulating the problem somewhat differently by utilizing the Feynman path integral technique, thus enabling us to provide a wider comprehensive insight into polaron properties in confined media with arbitrary electron-phonon coupling strength.

In the foregoing theory we consider a low dimensionally confined electron assuming a simple situation, namely an anisotropic potential box with adjustable parabolic barriers. The composite assembly will then be visualized as immersed in a bosonic reservoir where the electron couples to the LO-branch of the bulk phonon spectrum. Under the bulk-phonon approximation, we provide a broad interpolating overview to the one-polaron problem consisting of an electron confined within a deformable box which can be conformed from one geometric configuration to another.

Using units appropriate to a polaron calculation ($m^{\star} = \hbar = \omega_{LO} = 1$), the

Hamiltonian describing the confined electron coupled to LO-phonons is given by

$$H = H_{\rm e} + \sum_Q a_Q^\dagger a_Q + H_{\rm e-ph} \tag{2.95}$$

where

$$H_{\rm e} = \frac{1}{2}p^2 + V_{\rm conf}(\varrho, z) \tag{2.96}$$

is the electron part with $V_{\rm conf}(\varrho, z)$ denoting the confining potential, and

$$H_{\rm e-ph} = \sum_Q V_Q(a_Q e^{i\vec{Q}\cdot\vec{r}} + {\rm hc}) \tag{2.97}$$

is the Fröhlich interaction. In the above, $\vec{r} = (\vec{\varrho}, z)$ denotes the electron position in cylindrical coordinates. The interaction amplitude is related to the electron-phonon coupling constant α and the phonon wave vector $\vec{Q} = (\vec{q}, q_z)$ through $V_Q = (2\sqrt{2}\pi\alpha)^{1/2}/Q$ (note that we take $m^\star = 1$ this time).

For the confining potential we adopt a three dimensional box with adjustable barrier slopes, i.e., we set

$$V_{\rm conf}(\varrho, z) = \frac{1}{2}(\Omega_1^2\varrho^2 + \Omega_2^2 z^2) \tag{2.98}$$

in which the dimensionless frequencies $\Omega_i\,(i = 1, 2)$ serve for the measures of the potential barrier strengths and the degree of confinement of the electron in the respective lateral (ϱ) and $\pm z$ directions. The rationale behind imposing quadratic potential profiles is that such a form for the confining barriers, besides facilitating the calculations, is further compatible with the harmonic charge density fluctuations of the electron due to random scattering in the phonon field.

Ground State Energy

In the Feynman path integral representation of the polaron the phonon variables can be projected out exactly to yield the partition function of the polaron in the form

$$\mathcal{Z}_{\rm pol} = {\rm Tr}\, e^{-\beta H} = \mathcal{Z}_{\rm ph}\,\mathcal{Z} \tag{2.99}$$

where

$$\mathcal{Z}_{\rm ph} = \prod_Q \left[1 - e^{-\beta}\right]^{-1} \tag{2.100}$$

is the phonon part, and

$$\mathcal{Z} = \int d\vec{r}_0 \int_{\vec{r}_0}^{\vec{r}_0} \mathcal{D}\vec{r}\; e^{\mathcal{S}} \tag{2.101}$$

is the path integral in which the action $\mathcal{S}$ consists of two parts, one pertaining to the electron part of the Hamiltonian and the other to the electron-phonon interaction. In imaginary time variables ($t \to -i\lambda$), we express

$$\mathcal{S} = \mathcal{S}_{\rm e} + \frac{1}{2}\sum_Q V_Q^2 \int_0^\beta d\lambda \int_0^\beta d\lambda'\; e^{i\vec{Q}\cdot[\vec{r}(\lambda)-\vec{r}(\lambda')]}\, G_{(\omega_{\rm LO}=1)}(|\lambda-\lambda'|) \tag{2.102}$$

and

$$\mathcal{S}_{\rm e} = -\frac{1}{2}\int_0^\beta d\lambda \left\{\dot{\vec{r}}^2(\lambda) + \Omega_1^2\varrho^2(\lambda) + \Omega_2^2 z^2(\lambda)\right\} \tag{2.103}$$

in which the dimensionless parameter β stands for the inverse temperature, and the memory function G_ω is the Green's function of a harmonic oscillator with frequency ω, as given in Eq.(2.87). In principle, in the low temperature limit, we have $\mathcal{Z}_{\rm pol} = \mathcal{Z}$, and the polaron ground state energy, $E_{\rm g} = -\lim_{\beta\to\infty}\beta^{-1}\log\mathcal{Z}$, can be calculated exactly provided the path integral (2.101) can be evaluated. Since this is not possible due to the analytic complexity of the integral expressions in the action $\mathcal{S}$, Eqs.(2.102) and (2.103), we choose to proceed with the solvable trial action

$$\mathcal{S}_0 = \mathcal{S}_{\rm e} - \frac{{\rm w}(\nu^2-{\rm w}^2)}{8}\int_0^\beta d\lambda \int_0^\beta d\lambda'\,[\vec{r}(\lambda)-\vec{r}(\lambda')]^2\, G_{\rm w}(|\lambda-\lambda'|) \tag{2.104}$$

which provides us with a convenient variational upper bound led by the Jensen-Feynman inequality

$$E_{\rm g} \le E_0 - \lim_{\beta\to\infty}\frac{1}{\beta}\langle\mathcal{S}-\mathcal{S}_0\rangle_{\mathcal{S}_0} \tag{2.105}$$

where the notation $\langle\ \rangle_{\mathcal{S}_0}$ denotes a path-integral average with density function $e^{\mathcal{S}_0}$, and E_0 is the trial ground state energy corresponding to $\mathcal{S}_0$. In Eq.(2.104) w and ν are the variational parameters introduced within the same context as in the original paper by Feynman.[7] The problem then reduces to the evaluation of three quantities, E_0, A and B such that

$$E_{\rm g} = E_0 - B - A \tag{2.106}$$

is an upper bound, where the last two terms are given by

$$A = \lim_{\beta\to\infty} \frac{1}{2\beta} \sum_{Q} V_Q^2 \int_0^\beta d\lambda \int_0^\beta d\lambda' \left\langle e^{i\vec{Q}\cdot[\vec{r}(\lambda)-\vec{r}(\lambda')]} \right\rangle_{\mathcal{S}_0} G_{(\omega_{\rm LO}=1)}(|\lambda-\lambda'|), \tag{2.107}$$

$$B = \lim_{\beta\to\infty} \frac{1}{\beta} \frac{\mathrm{w}(\nu^2-\mathrm{w}^2)}{8} \int_0^\beta d\lambda \int_0^\beta d\lambda' \left\langle [\vec{r}(\lambda)-\vec{r}(\lambda')]^2 \right\rangle_{\mathcal{S}_0} G_{\mathrm{w}}(|\lambda-\lambda'|). \tag{2.108}$$

Since the trial action and the path-integral averages involved in A and B are all separable in the Cartesian coordinates, the calculations can be performed all in identical manners for each spatial direction. Denoting the Cartesian components of the electron position and momentum in any chosen direction by x and p_x, the corresponding Hamiltonian

$$H_0 = \frac{p_x^2}{2} + \frac{p_\phi^2}{2m_\phi} + \frac{1}{2}\Omega^2 x^2 + \frac{1}{2} m_\phi \mathrm{w}^2 (x-\phi)^2 \tag{2.109}$$

(in which Ω stands for either Ω_1 or Ω_2) can be related to the one dimensional analogue, $\mathcal{S}_0^{(1\mathrm{D})}$, of the trial action. Eliminating the harmonic oscillator variables ϕ and p_ϕ, one readily obtains

$$\mathcal{Z}_0 = \int dx_0 \int_{x_0}^{x_0} \mathcal{D}x \, \exp\left[\mathcal{S}_0^{(1\mathrm{D})}\right] = 2\sinh(\frac{1}{2}\beta\mathrm{w}) \, \mathrm{Tr}\, e^{-\beta H_0} \tag{2.110}$$

so that

$$E_0^{(1\mathrm{D})} = \lim_{\beta\to\infty} -\frac{1}{\beta} \log \mathcal{Z}_0. \tag{2.111}$$

The Hamiltonian H_0, in which the term $\frac{1}{2}\Omega^2 x^2$ is the relevant part of the confining potential (2.98) along the chosen coordinate, describes the coupling of the harmonically confined electron to a fictitious particle of mass $m_\phi = (\nu^2 - \mathrm{w}^2)/\mathrm{w}^2$ which, in turn, gives the overall effect of the interaction of the electron with the phonon field (cf. Fig.2.5). Under a suitable coordinate transformation

$$\begin{pmatrix} x \\ \phi \end{pmatrix} \to \begin{pmatrix} X \\ \Phi \end{pmatrix},$$

H_0 can be diagonalized in the normal coordinates X and Φ yielding the eigen frequencies

$$\begin{Bmatrix} \xi_1(\Omega) \\ \xi_2(\Omega) \end{Bmatrix} = \left\{ \frac{\Omega^2+\nu^2}{2} \mp \sqrt{(\frac{\Omega^2+\nu^2}{2})^2 - \Omega^2\mathrm{w}^2} \right\}^{\frac{1}{2}} \tag{2.112}$$

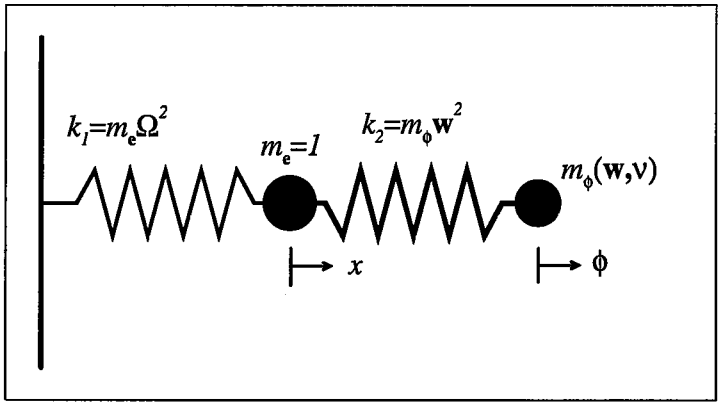

Figure 2.5: The model of confined polaron.
The coordinates and configuration of the coupled particles corresponding to $\mathcal{S}_0^{(1D)}$.

in terms of which H_0 conforms to the canonical form

$$H_0 = \frac{p_X^2}{2M} + \frac{p_\Phi^2}{2\mu} + \frac{1}{2}M\xi_1^2 X^2 + \frac{1}{2}\mu\xi_2^2\Phi^2 \tag{2.113}$$

where $M = \nu^2/w^2$ is sum of the mass of the electron and that of the fictitious particle. Using Eqs.(2.110) and (2.111), the part of the ground state energy contributing from the particular coordinate relevant to $\mathcal{S}_0^{(1D)}$ is obtained simply as

$$E_0^{(1D)} = \frac{1}{2}[\xi_1(\Omega) + \xi_2(\Omega) - w]. \tag{2.114}$$

Noting that the confinement potential $V_{conf}(\varrho, z)$ is characterized by only two parameters, Ω_1 and Ω_2, the former governing the degree of localization of the electron in the lateral directions isotropically and the latter relevant to the z axis, the expression for $E_0^{(1D)}$ can be extended to account for each of the Cartesian coordinates all at once to yield

$$E_0 = \sum_{n=1}^{2} \frac{1}{n}[\,\xi_1(\Omega_n) + \xi_2(\Omega_n) - w\,]\,. \tag{2.115}$$

Expanding the path-integral average in the integrand in Eq.(2.107) up to order Q^2, i.e.,

$$\left\langle e^{i\vec{Q}\cdot[\vec{r}(\lambda)-\vec{r}(\lambda')]}\right\rangle_{\mathcal{S}_0} \approx 1 + i\vec{Q}\cdot\langle[\vec{r}(\lambda) - \vec{r}(\lambda')]\rangle_{\mathcal{S}_0} - \frac{1}{2}Q^2\left\langle[\vec{r}(\lambda) - \vec{r}(\lambda')]^2\right\rangle_{\mathcal{S}_0}, \tag{2.116}$$

and using the integral transform

$$\int_0^\beta d\lambda \int_0^\beta d\lambda' F(|\lambda - \lambda'|) = \beta \int_0^\beta d\eta F(\eta/2), \qquad [F(\beta - \eta) = F(\eta)] \tag{2.117}$$

the quantities A and B can be cast into more convenient forms. We obtain

$$\begin{aligned} A &= \int_0^\infty d\eta\, e^{-\eta} \sum_Q V_Q^2 \, \exp\left[-\frac{1}{2}\left(\frac{q^2}{\sigma_1(\eta)} + \frac{q_z^2}{\sigma_2(\eta)}\right)\eta\right] \\ &= \frac{\alpha}{\sqrt{\pi}} \int_0^\infty d\eta\, e^{-\eta} \sqrt{\frac{\sigma_2(\eta)}{\eta}} \frac{\arctan\gamma}{\gamma} \end{aligned} \tag{2.118}$$

where

$$\gamma = \left\{\frac{\sigma_2(\eta)}{\sigma_1(\eta)} - 1\right\}^{1/2}, \tag{2.119}$$

and

$$\begin{aligned} B &= \frac{\mathrm{w}(\nu^2 - \mathrm{w}^2)}{4} \int_0^\infty d\eta\, \eta\, e^{-\mathrm{w}\eta} \left(\frac{2}{\sigma_1(\eta)} + \frac{1}{\sigma_2(\eta)}\right) \\ &= \sum_{n=1}^{2} \frac{1}{2n} \left[\, b_1(\Omega_n) + b_2(\Omega_n) \,\right]. \end{aligned} \tag{2.120}$$

In the above, the parameters $\sigma_n(\eta)$ and $b_i(\Omega_n)$, $(n = 1, 2$ and $i = 1, 2)$, are given by the following expressions

$$\sigma_n(\eta) = \eta \left\{\sum_{i=1}^{2} \frac{d_i(\Omega_n)}{\xi_i(\Omega_n)} [1 - e^{-\xi_i(\Omega_n)\eta}]\right\}^{-1} \tag{2.121}$$

with

$$d_i(\Omega_n) = \left\{1 + \frac{\mathrm{w}^2(\nu^2 - \mathrm{w}^2)}{[\,\mathrm{w}^2 - \xi_i^2(\Omega_n)\,]^2}\right\}^{-1} \tag{2.122}$$

and

$$b_i(\Omega_n) = \frac{1}{\mathrm{w} + \xi_i(\Omega_n)} \left\{\frac{1}{\nu^2 - \mathrm{w}^2} + \frac{\mathrm{w}^2}{[\,\mathrm{w}^2 - \xi_i^2(\Omega_n)\,]^2}\right\}^{-1}. \tag{2.123}$$

Effective Mass

The variational model used in this work can be extended to yield the effective polaronic mass in various limits of the confinement geometry. When the system

is set in virtual motion with a small velocity $\vec{u} = (\vec{u}_\varrho, u_z)$, the total energy attains an additional kinetic contribution of the form

$$\delta K = \frac{1}{2}\left(m_{\rm p}^{(\varrho)} u_\varrho^2 + m_{\rm p}^{(z)} u_z^2\right),$$

in which, $m_{\rm p}^{(\varrho)}$ and $m_{\rm p}^{(z)}$ are to be identified as the respective masses in the $\hat{\varrho}$ and $\hat{z}$ directions. Imposing a virtual velocity in the theory is straightforward.[7] In Eq.(2.101), the partition function $\mathcal{Z}$ has been written for all the paths with initial coordinate $\vec{r} = \vec{r}_0$ at zero time and final coordinate $\vec{r} = \vec{r}_0$ at the imaginary time β. With the virtual velocity $\vec{u}$ turned on, the final coordinate should now be $\vec{r}(\beta) = \vec{r}_0 + \beta\vec{u}$; and it is through this coordinate that one keeps trace of the composite translational inertia of the coupled electron+phonon complex. We are thus tempted to reformulate all the terms in Eq.(2.106), where each of E_0, A and B now becomes extended to consist of a part of the binding energy of the polaron alone and a part of the kinetic contribution which shows up having imposed a virtual displacement to the polaron.

The additional kinetic extension involved in E_0 can be written readily as $\frac{1}{2}Mu^2$, where M is the total mass (that of the electron and the fictitious particle), i.e., E_0 scales as

$$E_0 \to E_0 + \frac{1}{2}\frac{\nu^2}{\mathrm{w}^2}(u_\varrho^2 + u_z^2). \tag{2.124}$$

For the remaining two quantities, A and B, we have the following modifications:

$$A \to \int_0^\infty d\eta\, e^{-\eta} \sum_Q V_Q^2 \exp\left\{-\frac{1}{2}\left(\frac{q^2}{\sigma_1(\eta)} + \frac{q_z^2}{\sigma_2(\eta)}\right)\eta + i(\vec{q}\cdot\vec{u}_\varrho + q_z u_z)\eta\right\} \tag{2.125}$$

and

$$\begin{aligned} B \;&\to\; \frac{\mathrm{w}(\nu^2 - \mathrm{w}^2)}{4}\int_0^\infty d\eta\, e^{-\mathrm{w}\eta}\left[\left(\frac{2}{\sigma_1(\eta)} + \frac{1}{\sigma_2(\eta)}\right) + (u_\varrho^2 + u_z^2)\eta^2\right] \\ &=\; B + \frac{1}{2}\frac{\nu^2 - \mathrm{w}^2}{\mathrm{w}^2}(u_\varrho^2 + u_z^2)\,. \end{aligned} \tag{2.126}$$

Expanding Eq.(2.125) up to second order in u_ϱ and u_z (the first order terms in $\vec{u}$ vanish after having projected out the $\vec{Q}$-summation), and arranging the relevant

terms in Eq.(2.106) to yield the form $E_g \rightarrow E_g + \delta K$, we obtain the following expressions for the effective mass

$$\left\{ \begin{array}{c} m_p^{(\varrho)} \\ m_p^{(z)} \end{array} \right\} = 1 + \frac{\alpha}{2\sqrt{\pi}} \int_0^\infty d\eta \, \frac{\sqrt{\eta \sigma_2^3(\eta)}}{\gamma^2} \, e^{-\eta} \left\{ \begin{array}{l} \gamma^{-1} \arctan\gamma - (1+\gamma^2)^{-1} \\ 2[1 - \gamma^{-1} \arctan\gamma] \end{array} \right\} \tag{2.127}$$

in which the variational parameters w and ν have to be assigned their optimal-fit values which minimize the ground state energy with $\vec{u}$ set equal to zero.

Results and Conclusions

When $\Omega_i^{-1/2}$, (i=1 and/or 2), is reduced to values comparable with the polaron size, the boundary effects start to become significant and the system enters the regime of reduced dimensionality. Setting $\Omega_1 = 0$ and varying Ω_2 from zero to infinity, one can trace the bulk polaron properties go over to those of a strictly 2D-polaron. On the other hand, deleting the confining potential along the z-axis ($\Omega_2 = 0$) and fixing Ω_1 at non-zero finite values, the theory reflects the Q1D-description in a QWW-like tubular structure. Hereafter, we will consider the polaron binding energy relative to the subband level as $\mathcal{E}_p = \Omega_1 + \frac{1}{2}\Omega_2 - E_g$, and use Ω to mean $\Omega_1(\Omega_2)$ when $\Omega_2(\Omega_1) = 0$. In the spherically symmetric box-type configuration we simply set $\Omega_1 = \Omega_2 = \Omega$. Similarly, we shall use $\sigma(\eta)$ to mean $\sigma_1(\eta)$ and/or $\sigma_2(\eta)$.

Since analytical minimization of E_g (2.106) is not possible, the determination of the optimal fits to w and ν and the polaron quantities of interest, requires treatment on a computer. Before we present our numerical results over a broad range of the confining parameters and the coupling constant, we find it useful to make correspondence with a few extreme cases which have already been treated and well understood in the literature.

Integer Dimensional Space Limits

Setting $\Omega_1 = 0$ and $\Omega_2 = 0$ or ∞, we attain the bulk (3D) and strict two dimensional (2D) limits where the general expressions (2.115, 2.118, 2.120 and

2.127) for the ground state energy and mass conform to more tractable and simple forms. For $\Omega_1 = \Omega_2 = 0$ the theory duplicates the results of the original paper by Feynman.[7] In this limit the eigen frequencies (2.112) reduce to $\xi_1(0) = 0$ and $\xi_2(0) = \nu$, and we obtain

$$\sigma(\eta) = \left\{ \frac{\mathrm{w}^2}{\nu^2} + \left(1 - \frac{\mathrm{w}^2}{\nu^2}\right) \frac{1 - e^{-\nu\eta}}{\nu\eta} \right\}^{-1}, \tag{2.128}$$

$$E_0 = \frac{3}{2}(\nu - \mathrm{w}), \tag{2.129}$$

$$B = \frac{3}{4}(\nu^2 - \mathrm{w}^2)/\nu \tag{2.130}$$

yielding the binding energy

$$\mathcal{E}_\mathrm{p} = -E_\mathrm{g} = A - \frac{3(\nu - \mathrm{w})^2}{4\nu}, \tag{2.131}$$

where

$$A = \frac{\alpha}{\sqrt{\pi}} \int_0^\infty d\eta\, e^{-\eta} \sqrt{\frac{\sigma(\eta)}{\eta}}. \tag{2.132}$$

Furthermore, from Eq.(2.127) we obtain the 3D-(isotropic) mass to be given by

$$m_\mathrm{p} = 1 + \frac{\alpha}{3\sqrt{\pi}} \int_0^\infty d\eta\, e^{-\eta} \sqrt{\eta \sigma^3(\eta)}\ . \tag{2.133}$$

Going over to the strict 2D characterization of the polaron we have

$$\lim_{\Omega_2 \to \infty} \left\{ \begin{array}{c} \xi_1(\Omega_2) \\ \xi_2(\Omega_2) \end{array} \right\} = \left\{ \begin{array}{c} \mathrm{w} \\ \infty \end{array} \right\}, \tag{2.134}$$

and consequently, $\sigma_1(\eta) = \sigma(\eta)$ as given in Eq.(2.128), and $\sigma_2(\eta) \to \infty$. For the 2D binding energy we then obtain[81]

$$\mathcal{E}_\mathrm{p} = -\left(E_\mathrm{g} - \frac{1}{2}\Omega_2\right) = A - \frac{(\nu - \mathrm{w})^2}{2\nu}, \tag{2.135}$$

in which A is provided by the same expression (2.132) given for the bulk case except that the coefficient multiplying the η-integral is now $(\sqrt{\pi}/2)\alpha$. Similarly, the 2D - polaronic mass, $m_\mathrm{p}^{(\varrho)}$, is given by Eq.(2.133) where the corresponding factor multiplying the η–integral scales to $(\sqrt{\pi}/4)\alpha$.

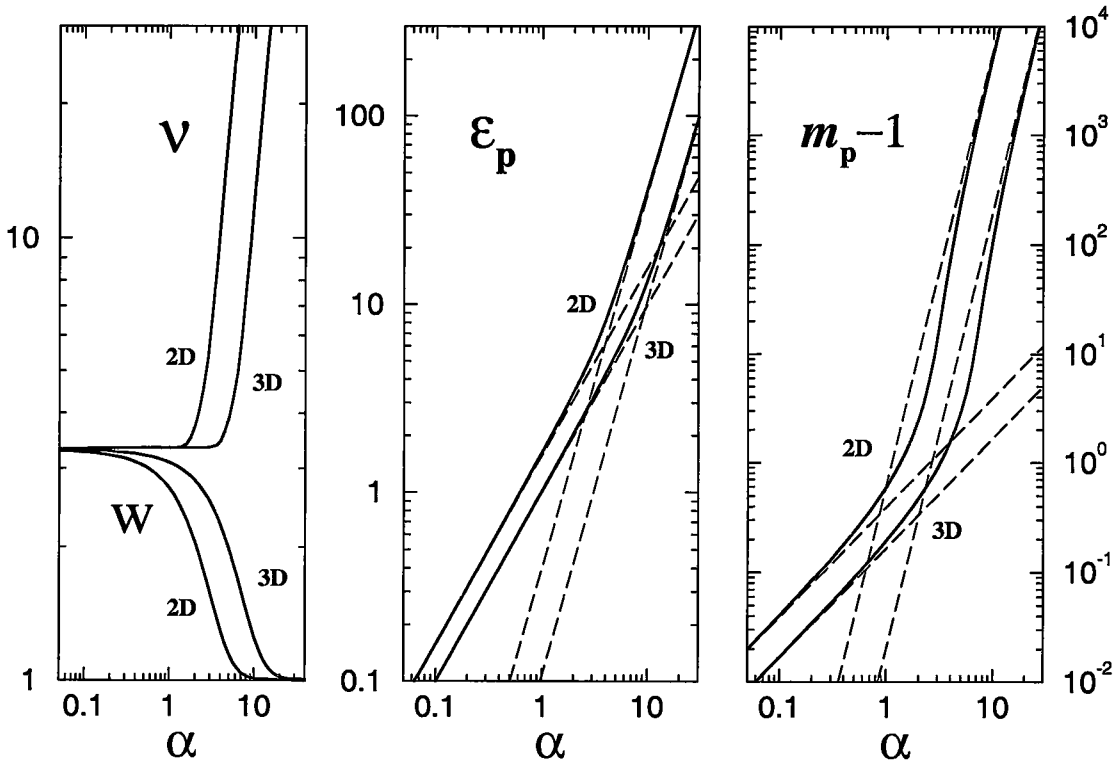

Figure 2.6: Polaron properties in three- and two-dimensions.
The variational parameters w and ν, the binding energy and mass for three and two dimensional polarons as functions of the coupling constant. The dashed lines refer to the perturbation and strong coupling theories.

For an extensive treatment of the polaron problem in (integer) N dimensions the reader is referred to [83]. Here (cf. Fig.2.6), we shall be content by only presenting the numerical displays of the variational parameters w and ν, the binding energy and the polaron mass for $N = 3$ and $N = 2$ over a wide range of the coupling constant interpolating between the weak and strong coupling extremes.

Weak Coupling Limit

Since in the most commonly studied compound semiconductors the electron phonon coupling is rather weak, we would like to devote particular emphasis to the weak coupling regime. A discussion of the present model within the perturbation approach[45] has already been provided in section 2.1 with which we wish to make

some correspondence here.

At weak coupling the parameters w and ν tend asymptotically to the same constant value (≈ 3.3) with the preservation of the intrinsic relation: $\nu > \mathrm{w}$ (cf. Fig.2.6 and [7]), and in the limit $\alpha \to 0$, one has $\nu - \mathrm{w} = \mathcal{O}(\alpha)$ regardless of the degree of confinement. Hence setting $\nu \approx \mathrm{w}$, we have

$$\left\{ \begin{array}{c} \xi_1(\Omega) \\ \xi_2(\Omega) \end{array} \right\} \approx \left\{ \frac{\Omega^2 + \mathrm{w}^2}{2} \mp \frac{|\Omega^2 - \mathrm{w}^2|}{2} \right\}^{\frac{1}{2}} \tag{2.136}$$

yielding the simplifications $E_0 = \Omega_1 + \frac{1}{2}\Omega_2$ and $B = 0$. In the weak – α regime, we thus readily obtain the binding energy to be given solely by A, Eq.(2.118), wherein $\sigma_{n=1,2}$ (2.121) reduces to exactly the same expression derived previously within the framework of second order perturbation theory,[45] i.e.,

$$\sigma_n(\eta) = \frac{\Omega_n \eta}{1 - e^{-\Omega_n \eta}} , \qquad n = 1, 2 . \tag{2.137}$$

An elaborate study of the weak–coupling polaron quantities as a function of Ω_1 and Ω_2 can be found in [45]. We, therefore, do not repeat the relevant results here, and readdress only to the three and two dimensional limits. In approaching the bulk case we assume a spherically symmetric isotropic confinement: $\Omega_1 = \Omega_2 = \Omega \ll 1$, and for the 2D limit we set $\Omega_1 = 0$ and let $\Omega_2 = \Omega \gg 1$. From Eqs.(2.106) and (2.127) we derive the binding energy and the polaron mass to lowest order contribution from Ω as

$$\mathcal{E}_{\mathrm{p}} = \left\{ \begin{array}{ll} \lim_{\Omega \to 0} \alpha(1 + \frac{\Omega}{8}) & 3\mathrm{D} \\ \lim_{\Omega \to \infty} \frac{\pi}{2}\alpha(1 - \frac{4}{\sqrt{\Omega}}) & 2\mathrm{D} \end{array} \right. \tag{2.138}$$

$$m_{\mathrm{p}} = \left\{ \begin{array}{ll} \lim_{\Omega \to 0} 1 + \frac{1}{6}\alpha(1 + \frac{9}{8}\Omega) & 3\mathrm{D} \\ \lim_{\Omega \to \infty} 1 + \frac{\pi}{8}\alpha(1 - \frac{4}{\sqrt{\pi^3 \Omega}}) & 2\mathrm{D} \end{array} \right. \tag{2.139}$$

Arbitrary Dimensionality

For a total description interpolating between all possible extremes of the effective dimensionality and the coupling constant we refer back to the set of equations (2.115), (2.118) and (2.120), and minimize numerically the ground state energy

(2.106) with respect to the variational parameters w and ν. We calculate the polaron binding energy over a reasonably broad range of Ω_1 and Ω_2 covering all interesting regimes of the effective dimensionality. Starting from the bulk case and increasing the value of Ω_2, one arrives at the two dimensional characterization of the polaron. Varying the value of Ω_1, however, $\mathcal{E}_p$ is seen to increase steadily at a much faster rate and rapidly become much larger than in the Q2D configuration, which follows essentially from the fact that in the wire geometry the polaron becomes highly localized towards the wire axis due to confinement coming from all transverse directions. For instance, with α set equal to 0.4, for the Q2D confinement with $\Omega = 10$ we obtain $\mathcal{E}_p$ to be 1.16 times its bulk value, $\mathcal{E}_p^{(3D)}$. For the case of a wire with the same parameter value the binding becomes stronger by a greater factor of about 1.45 over the 3D-energy. Lowering the dimensionality one further step down to the spherically symmetric QW-box – type localization of the polaron, the effective electron-phonon coupling is observed to be even much stronger ($\mathcal{E}_p/\mathcal{E}_p^{(3D)} = 2.02$), since now the polaron becomes radially squeezed in all directions. The corresponding values when Ω is set to 10^2, are 1.34, 2.27 and 5.70.

For completeness, we extend our considerations to the regime of strong phonon coupling and in Fig.2.7, with the confining parameter held fixed ($\Omega = 10^2$), we plot profiles of the polaronic binding as a function of growing α for the quasi-two, -one and -zero dimensional configurations; thus providing a comparison of the binding energy values in a succession of the effective dimensionalities pertaining to the slab, wire and box type geometries. The inset in the figure gives a complementary display of $\mathcal{E}_p$ as a function of Ω where the coupling constant has been selected arbitrarily as 4. The general trend that the electron phonon coupling is inherently stronger in reduced dimensionalities is seen to reflect in the plots which we have generated insofar.

It should be mentioned that, the parameters α and Ω $\{= \Omega_1$ or $\Omega_2\}$ characterizing the model do not enter the problem in an independent way but together take part in a related manner in the binding, dominating the effect of one another, and yet acting collaboratively in favor of stronger binding. Thus,

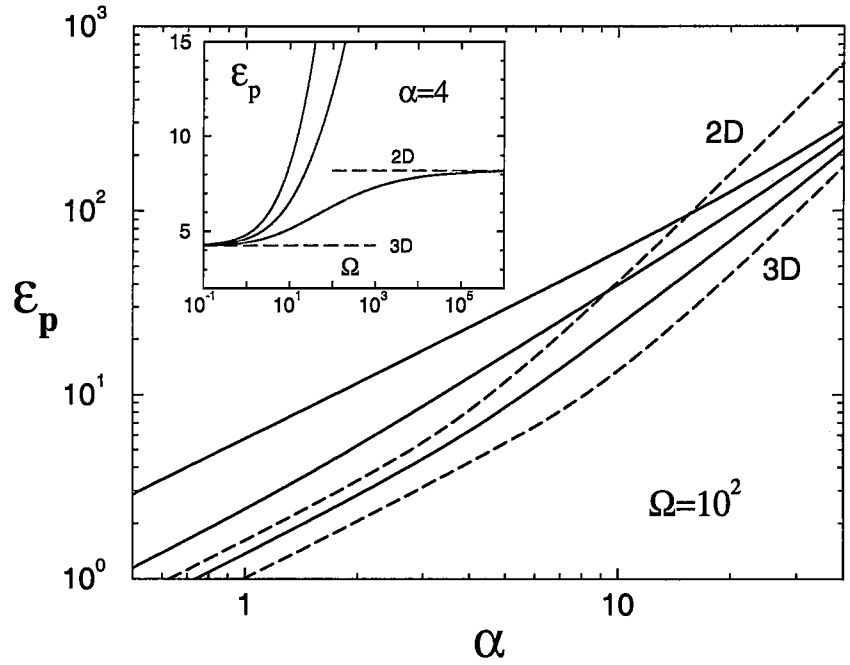

Figure 2.7: Comparison of different confinement geometries.
The binding energy as a function of the coupling constant with $\Omega\,(=\Omega_1$ and/or $\Omega_2)$ held fixed. The solid curves from bottom to top are respectively for the quasi-two, -one and -zero dimensional configurations, and the dashed curves give the bulk and strict-2D polaron energies. The inset provides an alternative view of the binding energy as a function of Ω in the strong coupling regime.

a high degree of localization in reduced dimensionality is expected to lead to a pseudo–enhancement in the effective electron–phonon coupling. Even at weak coupling ($\alpha \ll 1$), when the polaron is in a delocalized state with a large spread, the influence of the geometric confinement on the polaron becomes immediate as Ω is turned on, and to first order in small Ω, the coupling constant is observed to scale as $\alpha \to \alpha[1 + \mathcal{O}(\Omega)]$ (cf. Eqs.(2.138) and (2.139), for instance).

For $\alpha \gg 1$, however, the situation is somewhat different. In this extreme the polaron is already in a highly localized state and a small sized polaron is not expected to feel the effect of the confining boundary except for too large Ω. This peculiar aspect can be seen clearly if the energy and mass of the confined polaron are displayed relative to their corresponding bulk values, $\mathcal{E}_{\rm p}^{(3D)}$ and $m_{\rm p}^{(3D)}$. On this purpose, we choose to refer to the slab - configuration and portray (cf. Fig.2.8) the variations of the binding energy and the mass (along the relevant free direction)

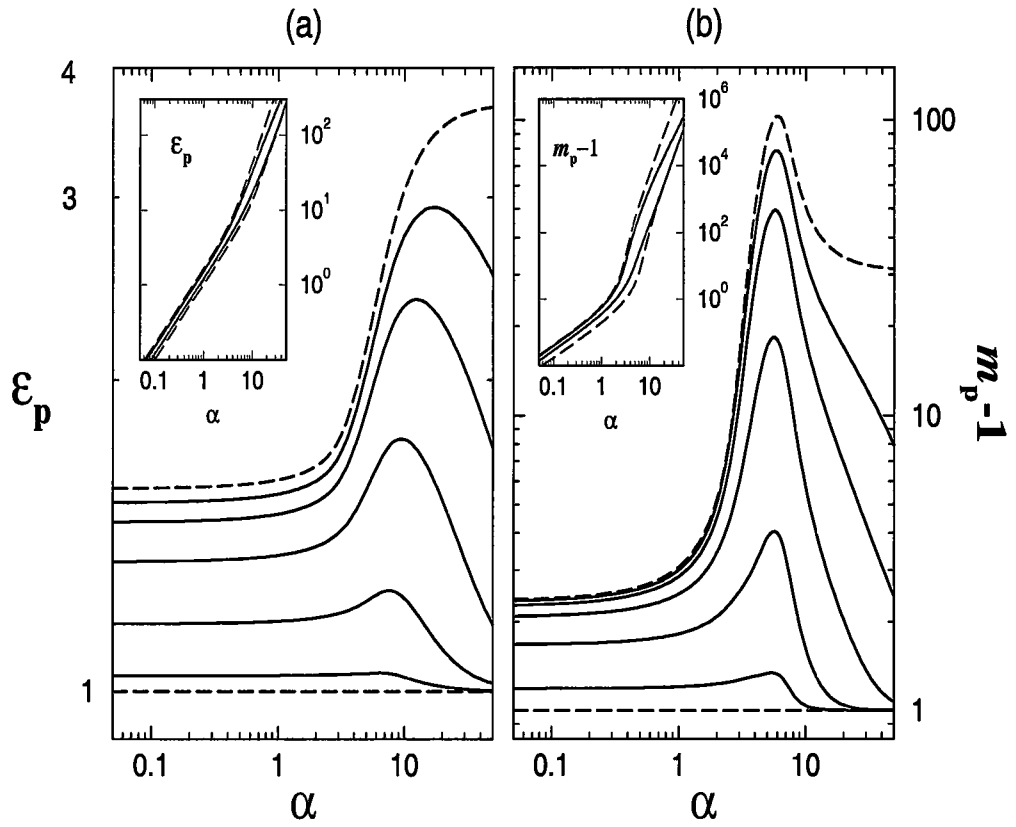

Figure 2.8: The scaling of polaron properties, in Q2D confinement. (a) The binding energy, $\mathcal{E}_p$, and (b) the polaron mass, $m_p - 1$, as functions of the coupling constant in the quasi-two dimensional configuration. All energy and mass values (except those in the insets) are scaled relative to the corresponding bulk values. The solid curves (from bottom to top) constrained by the lower (–3D) and upper (–2D) dashed curves are respectively for $\Omega \equiv \Omega_2 = 1$, 10, 10^2, 10^3 and 10^4. Similarly, the solid curves in the insets are for $\Omega = 10$ and 10^3.

as a function of the electron phonon coupling strength for a succession of different Ω values. In view of our results plotted in the figure we see that, starting from the weak-coupling extreme, the growth rates (with respect to α) of the binding energy and mass in low dimensional configurations ($\Omega > 0$) is not significantly different from that for the bulk polaron. However, as α is tuned to greater values the polaron goes into a more deeply bound state, and under the additional spatial constraint confining it, the binding becomes even much deeper since now the intrinsic collaborative role which the geometric confinement plays on the effective phonon coupling becomes much more efficient and prominent. In the meantime,

contrary to this trend, with growing α the polaron gets substantially localized and becomes unaffected by the boundary potential except for large values of Ω; thus, leading to a partial reduction in the confinement – counterpart of the polaron binding. Clearly, in the extreme limit of an artificially large α dominating over the external confinement the problem should be characterized essentially by its bulk description. This salient feature is depicted in the plots for finite Ω by that the energy and mass profiles, after having displayed a maximum, start to fall off and eventually match with their bulk values as α is made stronger. A complementary remark in this regard is that for a large Ω one requires correspondingly a large α for the polaron to conform to its bulk characterization, and in particular, in the strict 2D-limit ($\Omega \to \infty$) of the slab-like confinement one should correspondingly have $\alpha \to \infty$. This feature can readily be seen from that the upper dashed curves in the figure tend to the two dimensional limiting values, $3\pi^2/8$ and $81\pi^4/256$, for the energy and mass, respectively.

In this section, we have retrieved the fundamental aspects of the polaron problem in a confined medium within a unifying scheme interpolating between the bulk and all low dimensional geometric configurations of general interest. The Feynman path integral theory suited to the "deformable potential box" - model allows us to achieve a simple and yet comprehensive review of the ground state polaron properties in structures with reduced dimensionality.

2.6 Weak– and Strong–Coupling Domains

As we saw in the previous sections, perturbation and strong-coupling theories have limited domains of applicability, being reasonable for small and large values of α, respectively. However, the effect of external confinement strongly alters these domains. The additional localization of the electron due to the external potential causes the adiabaticity condition to be met at smaller values of α and thus broadens the applicability range of strong coupling theory. For example, there is a widely accepted rough criteria that $\alpha >\sim 10$ in bulk and $\alpha >\sim 4$ in strict-2D geometries for the strong-coupling approximation to yield reasonable

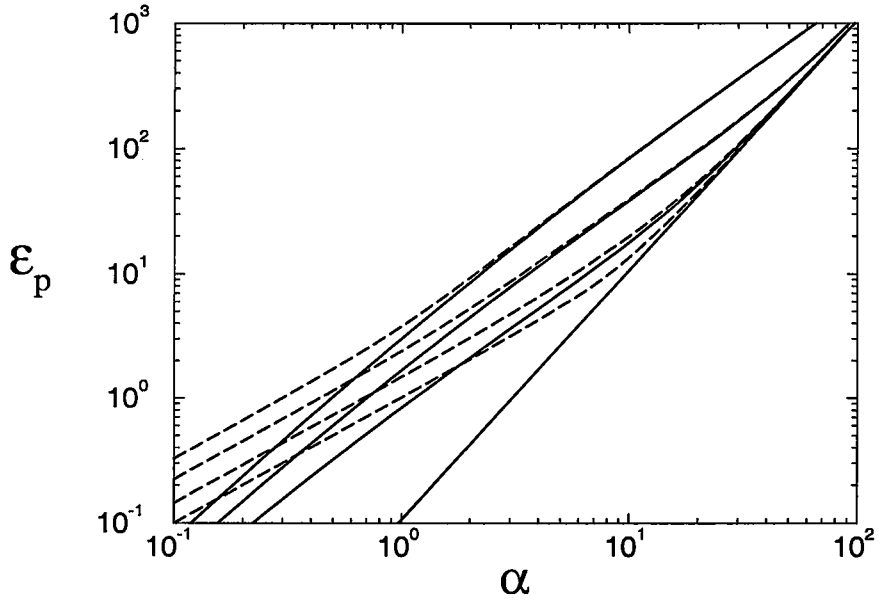

Figure 2.9: The extended domain of validity of strong coupling theory in highly confined systems.
The polaron binding energy as a function of coupling constant, in the parabolic boundary wire configuration. The solid and dashed curves are respectively the results of strong coupling[61] and path integral[85] theories. For each set of curves, from bottom to top, $\Omega = 0$, 10, 10^2, 10^3.

values of polaronic properties. To give a quantitative display of this trend, we would like to compare the ground state energy values of harmonically confined single-polarons, as calculated with perturbation[45] and strong-coupling[61] theories to that with the path-integral theory.[85] Although it is not exact, Feynman path-integral approximation is the most powerful technique for polaron calculations which is known to be valid for all values of the electron-phonon coupling strength.

Consider the comparison of strong-coupling and path-integral results for Q1D polarons in Fig.2.9. An immediate glance at the figure reveals that the strong coupling theory is totally inadequate for small values of α, giving binding energies far below the path integral results, but when the strength of the coupling is increased to larger values, the results of the two theories tend to approach each other, and eventually match, becoming almost identical in the large α limit. It is also seen that the point where the two theories start to be equivalent, shifts down to smaller values of α, with the increased degree of localization. For $\Omega = 10^3$ (the

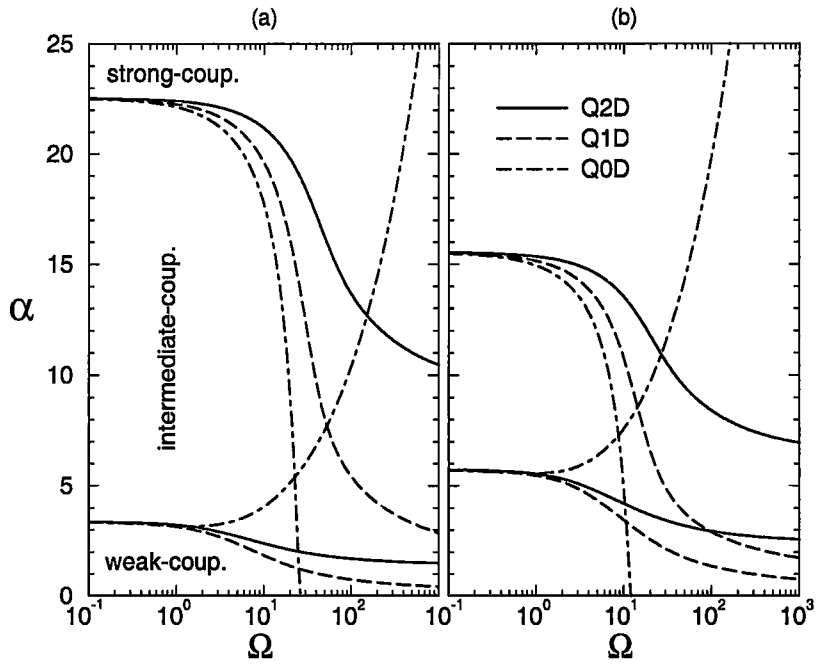

Figure 2.10: Domain of validity of perturbation and adiabatic strong coupling theories

The curves show the boundaries of the domains in which the one-polaron ground state energies as obtained using either strong coupling[61] or perturbation theory[45] deviate from the corresponding path-integral values by less than a certain percentage. The deviation tolerance is arbitrarily set to (a) 5%, (b) 10%.

topmost curves), which corresponds to a rather thin wire, strong coupling theory remains successful down to the intermediate values of $\alpha \sim 2$.

To be more specific, let us define the percentual discrepancy of perturbation (P) and strong-coupling (SC) theory results for the polaron binding energy as compared to path-integral (PI) ones, for particular values of α and Ω;

$$\Delta_{\mathrm{P,SC}}(\alpha,\Omega) = \frac{\mathcal{E}_{\mathrm{PI}}(\alpha,\Omega) - \mathcal{E}_{\mathrm{P,SC}}(\alpha,\Omega)}{\mathcal{E}_{\mathrm{PI}}(\alpha,\Omega)}$$

The curves in Fig.2.10(a) are generated by assigning a constant value of 5% to Δ_{P} and Δ_{SC} in the three basic types of confinement geometries. That is, in the regions below (above) the couple of curves of a particular type of geometry, the discrepancy of the perturbation (strong-coupling) theory results are less than 5%. For the region between the curves (intermediate coupling), the both approximations fail to provide satisfactory results within the chosen tolerance,

and one requires more precise methods for dependable results.

In the figure, we should point out an interesting outcome regarding the application of perturbation theory in Q0D (spherical box) confinement. Contrary to the cases of Q2D and Q1D confinement, with increasing Ω the domain of perturbation theory extends towards larger values of α. In the mean time the strong coupling theory becomes available for smaller and smaller α. Eventually, for small quantum-dots ($\Omega > 10$) the three approximation methods yield same energy values within at most 5% discrepancy.

Chapter 3

BIPOLARON

3.1 Introduction

The effective interaction of electrons in the presence of a phonon field is modified in a non-trivial manner. The effect of a dielectric medium is not limited to screening of electric charge, but also as a quantum mechanical aspect, the electron-phonon interaction results in attractive forces between the electrons. If this phonon mediated attractive interaction can overcome the mutual Coulomb repulsion, then a pair of electrons can form a bound state. Such a quasiparticle is referred to as a bipolaron. The bipolaronic pairing mechanism is in real space, unlike the Cooper pairs which exist in reciprocal space.

Apart from its connection to bipolaronic superconductivity theories of high T_c materials, the investigation of conditions for the formation and stability of a bipolaron is an interesting problem of its own. Therefore, in the present work, we will study the stability region of *one* bipolaron, not the many particle aspects of the bipolaron gas. Our considerations will also be limited to large bipolarons which are characterized by the Fröhlich Hamiltonian.

Among the numerous amount of papers published within the context of two-polaron systems, we at first cite the pioneering work of Haken[92] who studied the problem of the interaction between an electron and a hole via the coupling to the LO-branch of the phonon spectrum in polar semiconductors. Using a variational

method he showed that the polaron corrections to the effective interaction at large distances decrease exponentially, reflecting the exponentially decreasing overlap between the clouds of bound charges around the polarons. The same problem was further considered by Mahanti and Varma[93] and by Sak[94] where they included the corrections to the electron-hole potential coming from the dynamic polarization of the lattice, and showed how deviations from the Coulomb form could occur. The intrinsic effect of electron (hole) phonon interactions on the nature of forces acting between the particles was reconsidered by Kuleshov, Matveev and Smondyrev,[95] and the same work was revised later.[96] Basing their calculations on Feynman path-integral formalism, they developed a scheme for obtaining expressions for the particle interaction potentials and the ground state energy in both the strong- and weak-coupling approximations. A similar problem in the same area was considered by Bishop and Overhauser[14] to investigate the phonon-mediated interaction between two electrons where they showed that for ionic crystals the effective electron-electron potential may lead to an attractive deep potential well with a minimum occurring for particle separations as small as a few tens of Angstrom units. There are many other studies[97–105] which deal with the bipolaron problem, and have direct relevance to the present work.

For the problem of confined bipolaron, the Fröhlich Hamiltonian is generalized to the case of two electrons as

$$\mathsf{H} = H_e + \sum_Q a_Q^\dagger a_Q + \sum_Q V_Q \left[a_Q \left\{ \exp(i\vec{Q}\cdot\vec{r}_1) + \exp(i\vec{Q}\cdot\vec{r}_2) \right\} + \mathrm{hc} \right] \qquad (3.1)$$

where

$$H_e = \frac{1}{2} \sum_{i=1,2} \left(p_i^2 + \Omega_1^2 \varrho_i^2 + \Omega_2^2 z_i^2 \right) + \frac{U}{|\vec{r}_1 - \vec{r}_2|} \qquad (3.2)$$

We take $\hbar = \omega_{LO} = m^\star = 1$ for notational convenience. In the above, a_Q ($a_Q^\dagger$) is the phonon annihilation (creation) operator and $\vec{r}_i = (\vec{\rho}_i, z_i)$, $(i = 1, 2)$, are the positions of the electrons in cylindrical coordinates. p_1 and p_2 denote the momenta of the electrons. The interaction amplitude is related to the electron-phonon coupling constant α and the phonon wavevector $\vec{Q} = (\vec{q}, q_z)$ through $V_Q = (2\sqrt{2}\pi\alpha)^{1/2}/Q$. The coupling constant is given, in terms of the high frequency

and static dielectric constants of the material, by

$$\alpha = \frac{e^2}{\sqrt{2}}\left(\frac{1}{\epsilon_\infty} - \frac{1}{\epsilon_0}\right)$$

in terms of which the unscreened Coulomb repulsive amplitude is

$$U = \frac{e^2}{\epsilon_\infty} = \frac{\alpha\sqrt{2}}{1-\eta}, \qquad \eta = \epsilon_\infty/\epsilon_0 < 1\ . \tag{3.3}$$

Over its long history, the bipolaron properties have been extensively studied and fairly well understood in the literature. Determination of bipolaron stability regions require finding the critical values of the two independent material parameters α and η. From these studies it is known that the bipolarons can only exist above rather high critical values, α_c, of the electron-phonon coupling constant. For example Adamovski[21] found $\alpha_c = 7.3$, and Verbist, Peeters and Devreese[23] obtained $\alpha_c = 6.9$ for the bulk bipolarons. Consequently, the strong coupling theory seems to be a valid first approximation for the bipolaron problem which we will consider now.

3.2 Strong Coupling Theory

The formulation of the problem is simplified in the center of mass and relative coordinates:

$$\vec{R} = \frac{1}{2}(\vec{r}_1 + \vec{r}_2)\,, \qquad \vec{r} = \vec{r}_1 - \vec{r}_2\,, \tag{3.4}$$

with corresponding momenta $\vec{P} = \vec{p}_1 + \vec{p}_2$ and $\vec{p} = \frac{1}{2}(\vec{p}_1 - \vec{p}_2)$. The Hamiltonian (3.1),(3.2) can be rewritten as

$$\mathsf{H} = H_e + \sum_Q a_Q^\dagger a_Q + 2\sum_Q V_Q \cos\left(\frac{1}{2}\vec{Q}\cdot\vec{r}\right)\left[a_Q e^{i\vec{Q}\cdot\vec{R}} + \mathrm{hc}\right] \tag{3.5}$$

where

$$H_e = \frac{1}{4}P^2 + p^2 + \Omega_1^2\left(R_\varrho^2 + \frac{1}{4}r_\varrho^2\right) + \Omega_2^2\left(R_z^2 + \frac{1}{4}r_z^2\right) + \frac{U}{r} \tag{3.6}$$

in which $\vec{R}_\varrho$ and R_z stand for the lateral and z components of the center of mass position vector. The components $\vec{r}_\varrho$ and r_z have similar meanings for the relative position vector $\vec{r}$.

In the variational approximation that we follow here, we use the conventional trial ansatz of the adiabatic polaron theory consisting of a part relevant to the phonon variables and a part which contains the particle coordinates only, i.e.,

$$\Psi_{\rm bipol} = \Phi(\vec{r}_1, \vec{r}_2)\,|0\rangle \tag{3.7}$$

where $|0\rangle$ denotes the phonon vacuum state. The bipolaron state, $\Psi_{\rm bipol}$, thus constructed, is to be used in concert with the optimal displaced–oscillator transformation

$$\mathsf{H} \to \mathcal{H} = \exp(-\mathcal{S})\,\mathsf{H}\,\exp(\mathcal{S})\,, \qquad \mathcal{S} = \sum_Q V_Q s_Q\,(a_Q - a_Q^\dagger) \tag{3.8}$$

in which

$$s_Q = \langle\Phi(\vec{r}_1, \vec{r}_2)|\left(e^{\pm i\vec{Q}\cdot\vec{r}_1} + e^{\pm i\vec{Q}\cdot\vec{r}_2}\right)|\Phi(\vec{r}_1, \vec{r}_2)\rangle\ . \tag{3.9}$$

A further optimization of

$$E_{\rm g} \equiv \langle\Psi_{\rm bipol}|\mathcal{H}|\Psi_{\rm bipol}\rangle \tag{3.10}$$

with respect to the variational parameters contained in $\Phi(\vec{r}_1, \vec{r}_2)$ corresponds to the self-trapping description of the polarons where the charge density distribution of the electrons and the lattice polarization influence each other in such a way that a stable relaxed state of the "two-electron + phonon" complex is eventually attained.

To reach this goal we need to use an appropriate form for $\Phi(\vec{r}_1, \vec{r}_2)$ that suits to reflect a reasonable description of the bipolaron state in a wide range of the confining parameters extending from the bulk to all low dimensional geometries. As a sensible approximation, we set

$$\Phi(\vec{r}_1, \vec{r}_2) \propto G(\vec{r}_1)\,G(\vec{r}_2)\,g(r_1, r_2, |\vec{r}_1 - \vec{r}_2|) \tag{3.11}$$

where $G(\vec{r}_i)\,(i = 1, 2)$ are the one-electron Gaussian wavefunctions, and g is the Coulomb correlation function of Jastrow type. Compatible with the anisotropy imposed by the confining potential, we write

$$G(\vec{r}_i) = \exp\left(-a_1^2\varrho_i^2 - a_2^2 z_i^2\right) \tag{3.12}$$

and

$$g(\vec{r}_1, \vec{r}_2, |\vec{r}_1 - \vec{r}_2|) = \sqrt{r_\varrho^2 + r_z^2}\, \exp\left(b_1^2 r_\varrho^2 + b_2^2 r_z^2\right) \tag{3.13}$$

in which, the factor $r = \sqrt{r_\varrho^2 + r_z^2}$ multiplying the exponential ensures that $\Phi(\vec{r} = 0) = 0$, so that the electrons are repulsively kept separated.

Under the coordinate transformations (3.4), it is possible to conform Φ into a product form $\Phi(\vec{R}, \vec{r}) = \phi(\vec{R}) \times \varphi(\vec{r})$, where each of ϕ and φ assumes an oscillator-type waveform, given by

$$\phi(\vec{R}) = N_R \exp\left\{-\frac{1}{2}\kappa_1^2(R_\varrho^2 + \mu_1^2 R_z^2)\right\} \tag{3.14}$$

$$\varphi(\vec{r}) = N_r\, r \exp\left\{-\frac{1}{2}\kappa_2^2(r_\varrho^2 + \mu_2^2 r_z^2)\right\} \tag{3.15}$$

where the coefficients N_R and N_r serve for normalization, and $\{\kappa_i, \mu_i\}$, $(i = 1, 2)$ is the set of new variational parameters linked to those given in Eqs.(3.12),(3.13) through

$$\begin{aligned} a_1 &= \frac{1}{2}\kappa_1, & a_2 &= \frac{1}{2}\kappa_1\mu_1, \\ b_1^2 &= \frac{1}{8}\kappa_1^2 - \frac{1}{2}\kappa_2^2, & b_2^2 &= \frac{1}{8}\kappa_1^2\mu_1^2 - \frac{1}{2}\kappa_2^2\mu_2^2 \end{aligned} \tag{3.16}$$

It should be noted that during obtaining the optimal fits to κ_i and μ_i, the variational theory is expected to set up a detailed fractional admixture of all the contributions coming from each single parameter (U, α, Ω_1 and Ω_2) characterizing the system.

We should remark that the oscillator-oscillator type waveform (3.14), (3.15) for $\phi(\vec{R}) \times \varphi(\vec{r})$ has proved to be the most efficient approximation yielding the largest lower bound on η_c among the possible sets of different combinations of Pekar, Coulomb and oscillator type trial-wavefunctions tackled earlier by Verbist *et al*[25] for the three and two dimensional bipolarons. We hope that the results derived here will provide us a revision of the phase stability of bipolarons within a broader context beyond the already existing literature concerning the bulk and strict 2D cases. We shall set up a total description of the problem uncovering the quasi-two, -one and -zero dimensional configurations as a function of the degree of confinement, and devote our concern mainly to the basic qualitative aspects of the

confined bipolaron in the large α limit. We shall not concern ourselves seriously with the numerals in absolute sense since it has been found that the value of η_c lays out a considerable amount of digression depending on the different types of wavefunctions used for the center of mass and relative motions (cf., Table 1 in Ref.25). We therefore disregard all the other possible forms for $\Phi(\vec{R},\vec{r})$, and adopt plainly the oscillator-oscillator wavefunction as the most feasible approximation which, on the other hand, lends a great amount of computational simplification due to its compatibility with the quadratic barriers of the confining potential.

In complete form, the ground state energy (3.10) of the composite system of two polarons is evaluated as

$$E_{\rm g} = \lambda_R + \lambda_r + \Omega_1^2\lambda_\varrho + \Omega_2^2\lambda_z + \lambda_{\rm c} - \lambda_{\rm ph} \tag{3.17}$$

In the above, λ_R and λ_r stand for the kinetic terms $\langle\frac{1}{4}P^2\rangle$ and $\langle p^2\rangle$, respectively; λ_ϱ and λ_z are the energies relevant to the confining potential; $\lambda_{\rm c}$ is the Coulomb energy and $\lambda_{\rm ph}$ refers to the contribution coming from the lattice. We obtain the following explicit expressions for each of these terms:

$$\lambda_R = \langle -\frac{1}{4}\nabla_R^2\rangle_\phi = \frac{1}{8}\kappa_1^2(2+\mu_1^2) \tag{3.18}$$

$$\lambda_r = \langle -\nabla_r^2\rangle_\varphi = \kappa_2^2\left[\frac{2+3\mu_2^2+2\mu_2^4}{2+4\mu_2^2}\right] \tag{3.19}$$

$$\lambda_\varrho = \langle R_\varrho^2\rangle_\phi + \langle\frac{1}{4}r_\varrho^2\rangle_\varphi = \frac{1}{\kappa_1^2} + \frac{1+4\mu_2^2}{4\kappa_2^2(1+2\mu_2^2)} \tag{3.20}$$

$$\lambda_z = \langle R_z^2\rangle_\phi + \langle\frac{1}{4}r_z^2\rangle_\varphi = \frac{1}{2\kappa_1^2\mu_1^2} + \frac{3+2\mu_2^2}{8\kappa_2^2\mu_2^2(1+2\mu_2^2)} \tag{3.21}$$

Defining, for notational convenience,

$$F_n(t) \equiv \int_0^\infty dx\, x^n\, e^{(1-t)x^2}\mathrm{erfc}(x) \tag{3.22}$$

with erfc denoting the complementary error function, we write

$$\lambda_{\rm c} = \langle Ur^{-1}\rangle_\varphi = 2U\frac{\mu_2\kappa_2}{1+2\mu_2^2}\left\{\frac{1}{\sqrt{\pi}} + \mu_2 F_0(\mu_2^2)\right\} \tag{3.23}$$

Also, calculating s_Q (3.9); and using Eq.(3.22), we derive

$$\begin{aligned}\lambda_{\rm ph} &= \sum_Q V_Q^2 s_Q^2 = \frac{\alpha\sqrt{2}}{\pi}\int_0^\infty dq\, q \int_0^\infty dq_z \frac{s_Q^2}{q^2+q_z^2} \\ &= 2\sqrt{2}\alpha b\left\{F_0(\xi) + \delta\left(\frac{b}{2}\right)^2 F_2(\xi) + \frac{\delta^2}{2}\left(\frac{b}{2}\right)^4 F_4(\xi)\right\} \\ &- \frac{\alpha\, a^2 b\,\delta}{2\sqrt{2\pi}(1-\mu_2^4)}\left\{1 + \frac{a^2\delta}{2^4(1-\mu_2^4)}\left[1 - \frac{1}{2}\xi - 2\mu_2^4\right]\right\} \qquad (3.24)\end{aligned}$$

in which

$$a = \left\{\frac{8\kappa_1^2\kappa_2^2}{\kappa_1^2+4\kappa_2^2}\right\}^{1/2}, \qquad b = \left\{\frac{8\kappa_1^2\kappa_2^2\mu_1^2\mu_2^2}{\mu_1^2\kappa_1^2+4\mu_2^2\kappa_2^2}\right\}^{1/2} \qquad (3.25)$$

and

$$\xi = \frac{b^2}{a^2}, \qquad \delta = \frac{\mu_2^{-2}-\mu_2^2}{\kappa_2^2(1+2\mu_2^2)} \qquad (3.26)$$

3.2.1 Results

Since analytical minimization of $E_{\rm g}$ (3.17) is not possible, the determination of the optimal fits to the variational parameters $\{\kappa_i, \mu_i\}$, $(i = 1, 2)$, requires treatment on a computer. In the foregoing discussions we shall be content with the limited information the strong coupling approximation can impart to the understanding of the problem, and devote our concern mainly to the qualitative aspects of the model uncovering different geometries and dimensionalities other than those for the 3D- and 2D-analogs which have already been investigated extensively[23–25,28,29] within the framework of the same approximate adiabatic theory.

The fundamental condition under which a bipolaron can exist is that the repulsive Coulomb interaction should not be too strong to dominate over and hence break up the phonon-mediated binding which holds the particles together. It has been found that for a bipolaron state to be stable, one should have the ratio U/α be smaller than a critical value. For instance, in three dimensions, adopting the strong coupling theory and using oscillator-type wavefunctions (3.14), (3.15) for $\phi(\vec{R})$ and $\varphi(\vec{r})$, one obtains the bipolaron phase when $U/\alpha < 1.627$. The corresponding critical bound in two dimensions is inevitably larger ($U/\alpha < 1.679$) due to the pronounced effective phonon coupling.

The criterion for which a stable bipolaronic state takes place can be derived by demanding that the energy of the system of two interacting polarons be lower than twice that of a single polaron. Stating alternatively, for the bipolaron formation to be favorable, one requires

$$E_g - 2E_g^{(1)} = \varepsilon < 0 \tag{3.27}$$

where $E_g^{(1)}$ refers to the one-polaron ground state energy, calculated within the identical framework as for the bipolaron system and under the identical numerical precision. The corresponding one polaron energy results can readily be recovered from Ref.61. For completeness, we have reviewed a brief content of this reference in a previous section (cf., Eq.(2.46)), where the single electron wavefunction is provided by the same oscillator form as given by Eq.(3.14).

In conformity with the inequality $\varepsilon < 0$, the condition which favors the bipolaron phase is that parameter η (3.3) must be smaller than the critical value $\eta_c = \eta|_{\varepsilon=0}$ (i.e., the value at which E_g and $2E_g^{(1)}$ cross over). Clearly, the approximate η_c thus determined may lie either below or above its actual value depending on respectively whether the discrepancy between the variational and true energies for the bipolaron is larger or smaller than the corresponding discrepancy for two separated polarons. Although, at this point, we do not have a solid ground to judge or differentiate between the two possibilities, we are inclined to suppose that the variational error should be somewhat smaller for the one-polaron case. The underlying reason in that is the complexity of the situation for the bipolaron state where the intricate and opposing roles which the Coulomb and phonon parameters (U, α) play in the problem limits our skills in selecting an appropriate trial wavefunction that suits to give the least possible energy upper bound. Apparently, the additional parameters Ω_1 and Ω_2 add more to the complexity by greatly influencing the Coulomb and phonon counterparts of the problem and their percentual involvements in the binding (or dissociation). In view of this reasoning we feel that the variational estimate of η_c is probably smaller, rather than being larger, than its true value. Thus, adopting the assumption that $\eta_c < \eta_c^{\text{exact}}$, we think it would be somewhat more consistent

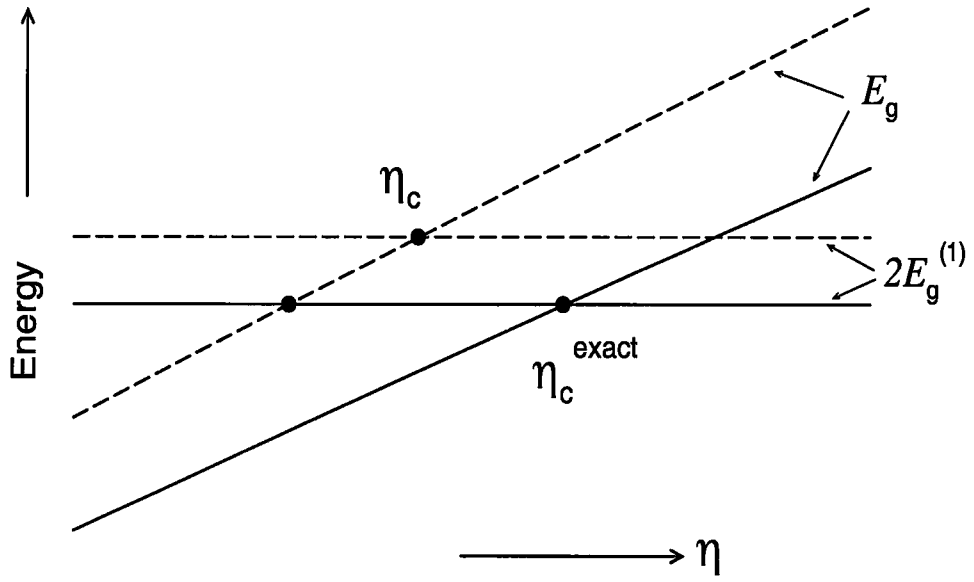

Figure 3.1: How to determine η_c ?
E_g and $2E_g^{(1)}$ versus η. The full curves are the *supposed* exact energies, the dashed curves represent the corresponding variational upper bounds. The crossover point at which the full curves meet yield the presumably-exact value of η_c. Similarly, the point at which the dashed lines cross gives the variationally computed η_c. The crossover point on the very left refers to the critical η determined by comparing the variational bipolaron energy with the exact single polaron energy.

to rely on the approach where both E_g and $E_g^{(1)}$ are calculated variationally under similar approximations, rather than to have η_c determined by comparing the variational bipolaron energy with the exact single polaron energy derived from a superior formalism or any possible reference (see, for instance, Miyake,[57] and Wu and Peeters[81] for the 3D and 2D cases). We provide a graphic summary of the content of our arguments in Fig. 3.1 illustrating the pure-variational η_c to lie closer to the true value than the one calculated using the exact one-polaron results.

In regard with the strong coupling expansion to leading order in α, i.e., $\mathcal{O}(\alpha^2)$, we would like to draw attention to that, if in Eqs.(3.1),(3.2) the energies are scaled by α^2 and lengths by α, i.e., $E \to E\alpha^2$ and $L \to L\alpha$, the only modification in the Hamiltonian would be to replace the confining parameter Ω by Ω/α^2 and the

Ω/α^2	$2\Delta E_g^{(1)}/\alpha^2$	$\Delta E_g/\alpha^2$						
		$\eta = 0.01$	$\eta = 0.10$	$\eta = 0.12$	$\eta = 0.13$	$\eta = 0.14$	$\eta = 0.15$	$\eta = 0.16$
0	0.2122	**0.2558**	**0.2241**	**0.2166**	**0.2127**	0.2089	0.2050	0.2010
10^{-2}	0.2219	**0.2654**	**0.2337**	**0.2262**	**0.2223**	0.2184	0.2145	0.2105
10^{-1}	0.2830	**0.3270**	**0.2924**	**0.2841**	0.2799	0.2756	0.2713	0.2669
1	0.4362	**0.4905**	**0.4426**	0.4311	0.4252	0.4193	0.4133	0.4072
10	0.6018	**0.6840**	**0.6202**	**0.6049**	0.5971	0.5891	0.5811	0.5729
10^2	0.7100	**0.8248**	**0.7489**	**0.7307**	**0.7213**	**0.7119**	0.7022	0.6924
10^3	0.7589	**0.8939**	**0.8118**	**0.7919**	**0.7818**	**0.7715**	**0.7611**	0.7505
∞	0.7854	**0.9333**	**0.8473**	**0.8266**	**0.8160**	**0.8052**	**0.7943**	0.7832

Table 3.1: The polaron and bipolaron ground state energies
The ground state energy of the two-polaron complex compared with twice that of a single polaron in the quasi-2D configuration. The energy values are given in positive terms where the corresponding lowest subband energies have been subtracted out, i.e., $\Delta E_g = \Omega - E_g$ and $\Delta E_g^{(1)} = \frac{1}{2}\Omega - E_g^{(1)}$. Those entries typed in boldface correspond to the set of parameter values, α, η and Ω, for which bipolaron formation is favorable.

Coulomb coefficient U by U/α. Thus, in a representation where the critical value of parameter η is plotted against Ω/α^2, rather than Ω, we find that, irrespective of the value of α, one can display the phase boundary on a single universal curve for each individual geometry. In every case, whatever the geometric configuration is, the ground state energy is seen to be proportional to the square of the coupling constant, i.e., $E_g = -\mathcal{C}\alpha^2$, where the corresponding coefficient of proportionality bears a functional relation solely to Ω/α^2 for both the single-polaron and two-polaron systems. Therefore, in the foregoing particular plots for which the abscissae are expressed in units of the ratio Ω/α^2, one can conveniently assign α any arbitrary large value with no loss in generality.

In Table 3.1 we give an explicit numerical discourse of the binding energy values of the "two-polaron" system compared with that of infinitely separated noninteracting polarons. We shall be content by tabulating a sample of our numerical results pertaining to only the slab-like configuration where we set $\Omega_1 = 0$ and select a succession of Ω_2 values ranging between infinity and zero, thus encompassing the integer dimensional space limits which are of immediate relevance to the three and two dimensional one- and two-polaron models studied

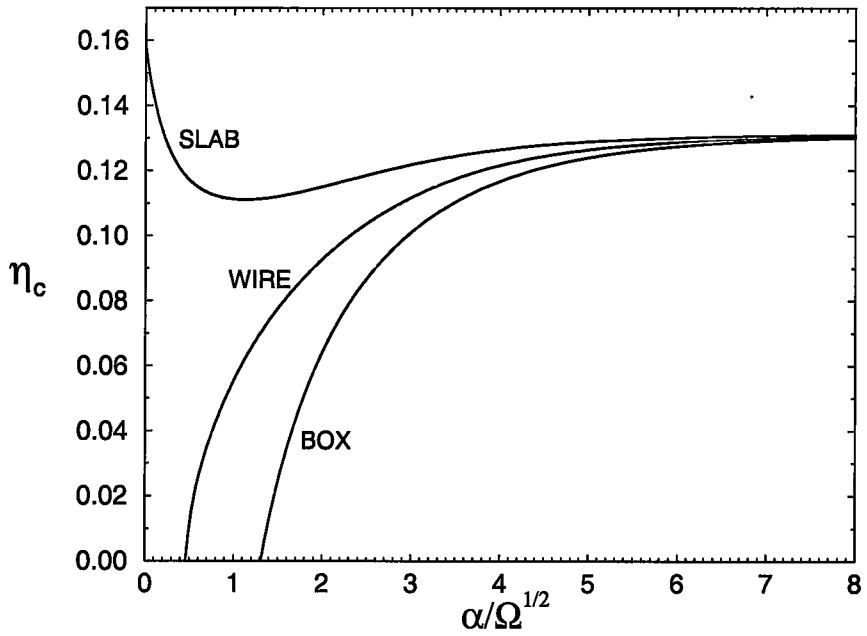

Figure 3.2: Critical η for different confinement types.
The critical ratio η_c as a function of $\alpha/\sqrt{\Omega}$ for the quasi-two, -one and -zero dimensional configurations.

in the literature in so far. We should recall that for the case of a free single polaron the binding energy calculated by the oscillator-type wavefunction is given by

$$-\frac{E_g^{(1)}}{\alpha^2} \equiv C\left(\frac{\Omega}{\alpha^2}\right) = \begin{cases} (3\pi)^{-1} & \text{for } \Omega = 0 \\ \pi/8 & \text{for } \Omega \to \infty \end{cases}$$

The more general values of the coefficient $C(\Omega/\alpha^2)$, extended to non-integer dimensionality $(0 \leq \Omega < \infty)$, are displayed in a succession of columns in the table for the one- and two-polaron cases with a series of distinctive Coulomb repulsion strengths; thus yielding an explicit tracking of the condition, Eq.(103), for which a bipolaronic bound state is favorable.

In Fig. 3.2 we plot three simultaneous curves describing the effect of confinement on the critical value of η in the quasi-two, -one and -zero dimensional configurations. Holding α fixed at any desired value and following the variations in η_c as Ω is turned on, we first note that for each type of confinement the critical η, starting from the common 3D-value, $\eta_c^{(3D)} = 0.131$, displays in common a decreasing trend where the respective decay rates are observed to become faster

as the effective dimensionality is reduced from two to one, and to zero. Thus, in the wire– and box–type configurations the critical Coulomb strength below which a bipolaron forms lies deviated considerably below the corresponding value in the slab-type geometry. The essential feature portrayed by the strong coupling theory is therefore that, the lower the dimensionality is, the more unlikely is to realize the bipolaron state to form; and in particular, in the box-type confinement, even a small value of η may turn out to be sufficient enough to lead the Coulomb force to oppose and dominate over the phonon - coupling - induced localization of the composite assembly of the two nearby electrons. The same feature has also been depicted explicitly in an earlier paper by Mukhopadhyay and Chatterjee[32] for bipolarons in quantum dots. As an immediate reasoning to understand such a characteristic of low-dimensional bipolarons treated within the adiabatic theory we are tempted to argue that, with increasing degree of confinement (i.e., with growing Ω_1 and/or Ω_2), the Coulomb repulsion is steadily strengthened due to that the particles are squeezed to get closer; and the rate at which this happens should be most prominent in the Q0D-configuration where the electrons are pushed towards one another from all radially inward directions. In the Q1D- and Q2D-configurations, however, the electrons are free to expand and relax themselves respectively in either one or two directions; thus resulting with comparatively weaker Coulomb repulsion and weaker dominating strength over the lattice polarization field holding the particles together.

In contrast with the outcomes of the present work and those of Ref. [32], we should mention two parallel contravening papers by Wan *et al*[106] and by Pokatilov *et al*,[33] both treating the Q0D-bipolaron problem within the framework of the path-integral formulation and leading to the common finding that, unlike to the strong-coupling results, the confinement effects act in favor of bipolaronic stability in the zero-dimensional configuration. Moreover, it has been argued that, even at weak coupling, bipolarons can form in quantum dots under strong confinement.[106] Since the path-integral formalism is highly superior over the strong-coupling approximation, we think that the counter-view laid out in Fig. 3.2 regarding the box-geometry is rather suspect and should be accounted for as an artifact

of the adiabatic theory. Thus, having pointed out this particular conflicting digression between the two theories, we continue with our discussions within the present context to lay out a complete and self-consistent characterization of strong-coupling bipolarons in confined media uncovering a broad variety of the basic features induced by the adiabatic theory.

We should note that in confined systems it is not only the Coulomb repulsion strength which gets pronounced, but in the meantime the phonon-coupling becomes pseudo-enhanced leading to a more effective and deeper polaronic binding to oppose and counterbalance the repulsive forces. The competitive interrelation between these aspects of the problem determines the phase boundary and moreover may even pose a salient feature stemming from a cross-overing of this competition as the confining parameters are varied. In particular, in the Q2D slab-geometry where this feature shows up with extreme prominence, we observe that the critical η does not display a monotonically increasing behavior interpolating between the 3D- and 2D-limits, but instead reaches its two dimensional value[25] ($\eta_c^{(2D)} = 0.158$) after having passed through a minimum; thus reflecting an explicit image of the dominating effect of either the Coulomb repulsion or the phonon mediated attraction over the other.

On top of these general arguments we should remind that the stability condition for the bipolaron state is determined as compared to the state of two separate polarons. As seen in Table 3.1, the effect of confinement is to lower the ground state energies of the two alternative states of the two-electron system monotonically. However, although the bipolaronic bound state exists beyond the stability regions presented here, it is just not favorable energetically as compared to the state of two polarons.

Peculiar to the slab geometry in Fig. 3.2, we note explicitly that, whatever the value of Ω is, there is always a non-zero critical η below which a stable bipolaronic state can be realized. In the wire- and box-type confinements, however, no matter how weak the Coulomb strength might be set, there is always an upper value for Ω beyond which the bipolaron breaks up into two individual polarons. Increased values of α can only support the bipolaron to conserve its stability

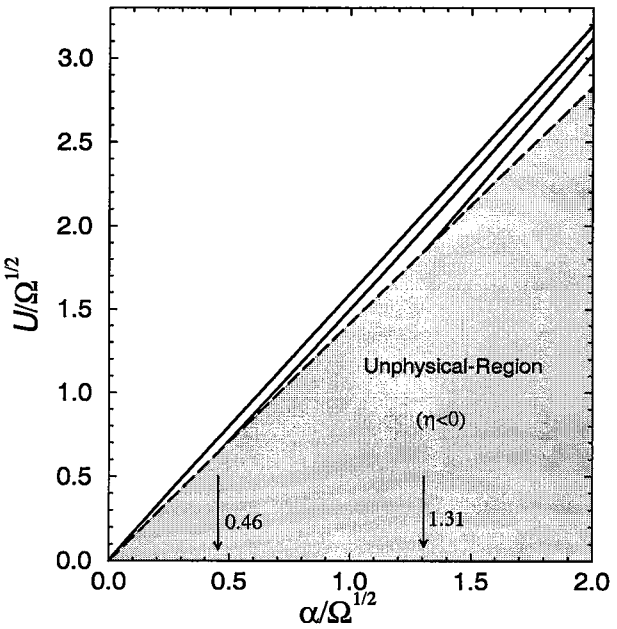

Figure 3.3: Bipolaron phase-diagram, strong coupling approximation
The phase diagram for bipolaron formation as a function of the Coulomb coefficient and electron-phonon coupling constant. The solid lines from top to bottom are respectively, for the quasi-two, -one and -zero dimensional configurations. The dashed line ($\eta_c = 0$) is the boundary of the unphysical region. The arrows refer to the corresponding critical values of α (in units of $\Omega^{1/2}$) in the wire- and box-type confinements.

at correspondingly higher degrees of confinement. A more clear picture of such a trait pertaining to the quasi-two, -one and -zero dimensional geometries is provided by the phase diagrams in Fig. 3.3 where we plot the Coulomb coefficient U against α. Scaling both the abscissa and the ordinate in units of $\Omega^{1/2}$ allows us to display the stability region for any desired Ω-value. In the phase picture the space lying below the dashed line corresponds to $\eta_c < 0$, and is therefore unphysical. The upper space bounded from below by the solid lines plotted for different geometries gives the unstable region where the polarons choose to remain separated. Thus, it is only the narrow triangular area bounded by the dashed and either of the solid lines in which the polarons can be found in a bound state forming a stable bipolaron. The vertex of each triangular region at which the dashed and solid lines join defines an infimum for the coupling constant for a given Ω-value. We observe that the critical α below which the unphysical region is

obtained gets shifted to larger values as the degree of confinement is increased. It should be remarked that in the Q2D-configuration the solid and dashed lines join at the origin; yielding an evidence in favor of bipolaronic stability for any degree of confinement provided the Coulomb coefficient does not exceed its corresponding critical value.

3.3 Path Integral Treatment

3.3.1 Bipolaron Model

In the Feynman path integral representation of the polaron, the phonon variables can be projected out exactly to yield the partition function of the bipolaron system in the form

$$\mathcal{Z}_{\rm BP} = \mathcal{Z}_{\rm ph}\,\mathcal{Z} \tag{3.28}$$

where

$$\mathcal{Z}_{\rm ph} = \prod_{Q}\left(\frac{1}{1-e^{-\beta\hbar\omega_{\rm LO}}}\right)^{3} \tag{3.29}$$

is the phonon part, and

$$\mathcal{Z} = \prod_{i=1,2}\left(\int d\vec{r}_0 \int_{\vec{r}_i(0)=\vec{r}_0}^{\vec{r}_i(\beta)=\vec{r}_0} \mathcal{D}\vec{r}_i(\lambda)\right)\; e^{\mathcal{S}[\vec{r}_1(\lambda),\vec{r}_2(\lambda)]} \tag{3.30}$$

is the path integral in which the action $\mathcal{S}$ consists of two parts, one pertaining to the electron part of the Hamiltonian and the other to the electron-phonon interaction. In imaginary time variables ($t \rightarrow -i\lambda$), we have respectively, the following expressions

$$\mathcal{S}_{\rm e} = -\frac{1}{2}\int_0^\beta d\lambda \sum_{i=1,2}\left(\dot{\vec{r}}_i^{\,2}(\lambda) + \Omega_1^2\varrho_i^2(\lambda) + \Omega_2^2 z_i^2(\lambda)\right) + \mathcal{S}_{\rm c} \tag{3.31}$$

where

$$\mathcal{S}_{\rm c} = -\int_0^\beta d\lambda\,\frac{U}{|\vec{r}_1(\lambda)-\vec{r}_2(\lambda)|} \tag{3.32}$$

is the Coulomb term, and

$$\mathcal{S}_{\rm e-p} = \frac{1}{2}\sum_{i=1,2}\sum_{j=1,2}\sum_{Q} V_Q^2 \int_0^\beta d\lambda \int_0^\beta d\lambda'\, G_{(\omega_{\rm LO}=1)}(\lambda-\lambda')\, e^{i\vec{Q}\cdot[\vec{r}_i(\lambda)-\vec{r}_j(\lambda')]} \tag{3.33}$$

is the part describing the phonon mediated retarded attractive interaction between the electrons. In the above, the dimensionless parameter β stands for the inverse temperature, and the memory function

$$G_\omega(u) = \frac{\cosh((\beta - 2|u|)\omega/2)}{\sinh(\beta\omega/2)} \tag{3.34}$$

is the Green's function of a harmonic oscillator with frequency ω. In principle, at zero temperature, we have $\mathcal{Z}_{\rm BP} = \mathcal{Z}$, and the bipolaron ground state energy,

$$E_{\rm g} = -\lim_{\beta\to\infty} \beta^{-1} \log \mathcal{Z},$$

can be calculated exactly provided the path integral (3.30) can be evaluated. Since this is not possible due to the analytic complexity of the integral expressions in the action $\mathcal{S}$, Eqs. (3.31)-(3.33), we choose to proceed with the introduction of a solvable trial action $\mathcal{S}_0$ intended to provide us with a convenient variational upper bound to the ground state energy, led by the Jensen-Feynman inequality

$$E_{\rm g} \leq E_0 - \lim_{\beta\to\infty} \frac{1}{\beta} \langle \mathcal{S} - \mathcal{S}_0 \rangle_{\mathcal{S}_0} \tag{3.35}$$

where the notation $\langle\ \rangle_{\mathcal{S}_0}$ denotes a path-integral average with density function $e^{\mathcal{S}_0}$, and E_0 is the trial ground state energy corresponding to $\mathcal{S}_0$. The form of the trial action should be simple enough to permit analytical calculations and yet be detailed enough to cover all the basic features of the exact action $\mathcal{S}$.

3.3.2 The Trial Model and its Diagonalization

For the trial action we choose the model which was successfully applied to similar polaron or bipolaron problems[23,7,85] where the electrons are considered to be in quadratic interaction with the fictitious masses. We write

$$\mathcal{S}_0 = \mathcal{S}_{\rm e} + \mathcal{S}_{\rm s} + \mathcal{S}_{\rm m} \tag{3.36}$$

where the part of $\mathcal{S}_{\rm e}$, relevant to the Coulomb interaction, has the form

$$\mathcal{S}_{\rm c} = \frac{1}{2} K \int_0^\beta d\lambda\, [\vec{r}_1(\lambda) - \vec{r}_2(\lambda) - \vec{a}]^2\,. \tag{3.37}$$

$\mathcal{S}_{\rm s}$ and $\mathcal{S}_{\rm m}$ refer to the self and mutual interaction of the electrons with the fictitious masses, each with its own and with that of the other electron, respectively. These terms assume the following path-integral representations

$$\mathcal{S}_{\rm s} = -\frac{c_{\rm s}}{2}\int_0^\beta d\lambda \int_0^\beta d\lambda'\, G_{\rm w}(\lambda-\lambda') \sum_{i=1,2} [\vec{r}_i(\lambda)-\vec{r}_i(\lambda')]^2 \,, \tag{3.38}$$

$$\mathcal{S}_{\rm m} = -2\times\frac{c_{\rm m}}{2}\int_0^\beta d\lambda \int_0^\beta d\lambda'\, G_{\rm w}(\lambda-\lambda') \,[\vec{r}_1(\lambda)-\vec{r}_2(\lambda')-\vec{a}]^2 \,. \tag{3.39}$$

In the above K, $c_{\rm s}$, $c_{\rm m}$ and w are variational parameters introduced within a similar context as in the original paper by Feynman.[7] Vector $\vec{a}$ is a further parameter describing the mean distance between the central positions about which the electrons fluctuate. We should remark that in the extreme limits $\vec{a}=0$ and $|\vec{a}|\to\infty$, the model yields respectively a description of either the bipolaronic state of the two electrons or a pair of two independent polarons.[23]

Since the trial action and the path-integral averages involved in Eqs.(3.35)-(3.39) are all separable in the Cartesian coordinates, the calculations can be performed all in identical manners for each spatial direction. Denoting the Cartesian component of the ith electron in any chosen direction by x_i and that of the ith fictitious mass M by X_i, the part of the model Lagrangian relevant to that coordinate

$$\begin{aligned} L^{(x)}_{\rm mod} &= \frac{1}{2}\sum_{i=1,2}\left(\dot{x}_i^2-\Omega^2 x_i^2+M\dot{X}_i^2\right)+\frac{K}{2}(x_1-x_2-a_x)^2-\frac{\kappa}{2}\sum_{i=1,2}(x_i-X_i)^2 \\ &- \frac{\kappa'}{2}\left\{(x_1-X_2-a_x)^2+(x_2-X_1+a_x)^2\right\} \end{aligned} \tag{3.40}$$

can be related to the following model action,

$$\begin{aligned} \mathcal{S}^{(x)}_{\rm mod} &= -\frac{1}{2}\int_0^\beta d\lambda \sum_{i=1,2}\left(\dot{x}_i^2(\lambda)+\Omega^2 x_i^2(\lambda)+M\dot{X}_i^2(\lambda)\right) \\ &+ \frac{1}{2}\int_0^\beta d\lambda\left\{K\,[x_1(\lambda)-x_2(\lambda)-a_x]^2-\sum_{i=1,2}\kappa\,[x_i(\lambda)-X_i(\lambda)]^2\right\} \\ &- \frac{\kappa'}{2}\int_0^\beta d\lambda\left\{[x_1(\lambda)-X_2(\lambda)-a_x]^2+[x_2(\lambda)-X_1(\lambda)+a_x]^2\right\} \end{aligned} \tag{3.41}$$

Here, it should be understood that $\Omega=\Omega_2$ when one refers to the z-direction, but assumes Ω_1-value for the remaining two directions.

Similar to the elimination of the phonon degrees of freedom, also eliminating the fictitious mass coordinates, X_i, we obtain the relevant trial action, expressed solely in terms of the electron coordinates, in the form as given in Eqs.(3.36)-(3.39). The variational parameters of the trial action can then be identified in terms of the parameters of the model Lagrangian;

$$\mathrm{w} = \sqrt{\frac{\kappa + \kappa'}{M}}, \qquad c_{\mathrm{s}} = \frac{\kappa^2 + \kappa'^2}{4M\mathrm{w}}, \qquad c_{\mathrm{m}} = \frac{\kappa\kappa'}{2M\mathrm{w}} \tag{3.42}$$

In order to calculate the ground state energy of the variational model and the path integral average required in Eq.(111), one needs to diagonalize $L^{(x)}_{\mathrm{mod}}$ (3.40). Introducing $x_{\mathrm{CM}}\,(X_{\mathrm{CM}})$ and $x_{\mathrm{rel}}\,(X_{\mathrm{rel}})$ as the center of mass and relative coordinates for the electrons (fictitious masses) through

$$\left\{ \begin{array}{c} x_1 \\ x_2 \end{array} \right\} = \frac{1}{2}(x_{\mathrm{CM}} \pm x_{\mathrm{rel}}) \pm \frac{a_x}{2}$$

$$\left\{ \begin{array}{c} X_1 \\ X_2 \end{array} \right\} = \frac{1}{2}(X_{\mathrm{CM}} \pm X_{\mathrm{rel}}) \pm \frac{a_x}{2}$$

we rewrite the Lagrangian relevant to the chosen direction as

$$L^{(x)}_{\mathrm{mod}} = L^{(x)}_{\mathrm{CM}} + L^{(x)}_{\mathrm{rel}}$$

where

$$\begin{aligned} L^{(x)}_{\mathrm{CM}} &= \frac{1}{4}\dot{x}^2_{\mathrm{CM}} + \frac{1}{4}M\dot{X}^2_{\mathrm{CM}} - \frac{1}{4}(\Omega^2 + \kappa + \kappa')x^2_{\mathrm{CM}} \\ &- \frac{1}{4}(\kappa + \kappa')X^2_{\mathrm{CM}} + \frac{1}{2}(\kappa + \kappa')x_{\mathrm{CM}}X_{\mathrm{CM}}\,, \end{aligned} \tag{3.43}$$

$$\begin{aligned} L^{(x)}_{\mathrm{rel}} &= \frac{1}{4}\dot{x}^2_{\mathrm{rel}} + \frac{1}{4}M\dot{X}^2_{\mathrm{rel}} - \frac{1}{4}(\Omega^2 + 2K + \kappa + \kappa')x^2_{\mathrm{rel}} \\ &- \frac{1}{4}(\kappa + \kappa')X^2_{\mathrm{rel}} + \frac{1}{4}(\kappa - \kappa')x_{\mathrm{rel}}X_{\mathrm{rel}}\,. \end{aligned} \tag{3.44}$$

Under appropriate coordinate transformations

$$x_{\mathrm{CM}} = \eta_0 + \eta_1$$

$$X_{\rm CM} = \frac{\mathrm{w}^2}{\mathrm{w}^2-\xi_0^2}\eta_0 + \frac{\mathrm{w}^2}{\mathrm{w}^2-\xi_1^2}\eta_1 \tag{3.45}$$

$$\begin{aligned} x_{\rm rel} &= \eta_2+\eta_3 \\ X_{\rm rel} &= \frac{\kappa-\kappa'}{\kappa+\kappa'}\frac{\mathrm{w}^2}{\mathrm{w}^2-\xi_2^2}\eta_2 + \frac{\kappa-\kappa'}{\kappa+\kappa'}\frac{\mathrm{w}^2}{\mathrm{w}^2-\xi_3^2}\eta_3 \end{aligned} \tag{3.46}$$

$L_{\rm CM}^{(x)}$ and $L_{\rm rel}^{(x)}$ can be diagonalized in the respective normal coordinates $\{\eta_0,\eta_1\}$ and $\{\eta_2,\eta_3\}$, yielding the canonical forms

$$L_{\rm CM}^{(x)} = \frac{1}{2}\sum_{i=0,1} m_i(\dot\eta_i^2-\xi_i^2\eta_i^2) \qquad L_{\rm rel}^{(x)} = \frac{1}{2}\sum_{i=2,3} m_i(\dot\eta_i^2-\xi_i^2\eta_i^2) \tag{3.47}$$

where

$$m_0 = \frac{1}{2}\frac{\xi_1^2-\xi_0^2}{\mathrm{w}^2-\xi_0^2}, \qquad m_1 = \frac{1}{2}\frac{\xi_1^2-\xi_0^2}{\xi_1^2-\mathrm{w}^2} \tag{3.48}$$

$$m_2 = \frac{1}{2}\frac{\xi_2^2-\xi_3^2}{\xi_2^2-\mathrm{w}^2}, \qquad m_3 = \frac{1}{2}\frac{\xi_2^2-\xi_3^2}{\mathrm{w}^2-\xi_3^2} \tag{3.49}$$

are the relevant mass values and $\xi_i(\Omega)$ $(i=0,1,2,3)$ refer to the eigenfrequencies, given by

$$\left\{\begin{array}{c}\xi_0\\ \xi_1\end{array}\right\} = \frac{1}{\sqrt{2}}\left\{\Omega^2+\omega_1^2 \mp \sqrt{(\Omega^2+\omega_1^2)^2-4\Omega^2\mathrm{w}^2}\right\}^{1/2} \tag{3.50}$$

$$\left\{\begin{array}{c}\xi_2\\ \xi_3\end{array}\right\} = \frac{1}{\sqrt{2}}\left\{\Omega^2+\omega_2^2+\omega_3^2 \pm \sqrt{(\Omega^2+\omega_2^2+\omega_3^2)^2-4(\Omega^2\mathrm{w}^2+\omega_2^2\omega_3^2)}\right\}^{1/2} \tag{3.51}$$

We note that, in the limit $\Omega \to 0$, the eigenfrequencies ξ_i reduce to

$$\xi_0(0)=0 \quad \text{and} \quad \xi_i(0)=\omega_i \quad (i=1,2,3) \tag{3.52}$$

in which ω_i are the normal mode frequencies calculated previously by Verbist *et al.*[23] for the bulk case, expressed as

$$\begin{aligned} \omega_1 &= \left\{\frac{M+1}{M}(\kappa+\kappa')\right\}^{1/2} \\ \left\{\begin{array}{c}\omega_2\\ \omega_3\end{array}\right\} &= \frac{1}{\sqrt{2}}\left\{\frac{M+1}{M}(\kappa+\kappa')-2K \right. \\ &\qquad \left. \pm\sqrt{\left[\frac{M-1}{M}(\kappa+\kappa')-2K\right]^2+\frac{4}{M}(\kappa-\kappa')^2}\right\}^{1/2}. \end{aligned} \tag{3.53}$$

Here we shall adopt the conventional HO (harmonic oscillator) - operator representation which allows us to calculate all the required path integral averages easily. On this purpose we introduce the lowering and raising operators c_i and $c_i^\dagger$, $(i = 0, 1, 2, 3)$, defined by

$$\eta_i = \lambda_i(c_i^\dagger + c_i), \qquad [c_i, c_i^\dagger] = 1 \tag{3.54}$$

in which

$$\lambda_i = (2m_i\xi_i)^{-1/2} \tag{3.55}$$

The corresponding Hamiltonian relevant to $L_{\rm mod}^{(x)}$ can be expressed in the HO-form

$$H_{\rm mod}^{(x)} = \sum_{i=0}^{3} \xi_i(\Omega) \left(c_i^\dagger c_i + \frac{1}{2} \right)$$

where the summation index i takes values 0 and 1 for the center of mass coordinates, and values 2 and 3 for the relative coordinates. Hence, the part of the ground-state energy contributed by the particular coordinate relevant to $\mathcal{S}_0^{(x)}$ is obtained simply as

$$E_0^{(x)} = -\mathrm{w} + \frac{1}{2} \sum_{i=0}^{3} \xi_i(\Omega) \tag{3.56}$$

wherein the additional term "–w" comes about under eliminating the fictitious mass coordinates to obtain the trial action $\mathcal{S}_0$ from the model action.

The expression for $E_0^{(x)}$ can be extended to account for each of the Cartesian coordinates all at once, yielding

$$E_0 = -3\mathrm{w} + \sum_{i=0}^{3} \left[\xi_i(\Omega_1) + \frac{1}{2}\xi_i(\Omega_2) \right] . \tag{3.57}$$

3.3.3 Path-Integral Averages

In order to reach the upper bound to the bipolaronic ground state energy, one has to evaluate the path integral average involved in Eq.(3.35), where

$$\langle \mathcal{S} - \mathcal{S}_0 \rangle_{\mathcal{S}_0} = -\frac{K}{2} \int_0^\beta d\lambda \left\langle [\vec{r}_1(\lambda) - \vec{r}_2(\lambda) - \vec{a}]^2 \right\rangle_{\mathcal{S}_0}$$

$$
\begin{aligned}
&- U\int_0^\beta d\lambda \sum_Q \frac{4\pi}{Q^2}\left\langle e^{i\vec{Q}\cdot[\vec{r}_1(\lambda)-\vec{r}_2(\lambda)]}\right\rangle_{\mathcal{S}_0} \qquad (3.58)\\
&+ \frac{1}{2}\int_0^\beta d\lambda \int_0^\beta d\lambda'\, G_{\rm w}(\lambda-\lambda')\\
&\quad\times\left\{c_{\rm s}\sum_{i=1,2}\left\langle[\vec{r}_i(\lambda)-\vec{r}_i(\lambda')]^2\right\rangle_{\mathcal{S}_0}+2c_{\rm m}\left\langle[\vec{r}_1(\lambda)-\vec{r}_2(\lambda')-\vec{a}]^2\right\rangle_{\mathcal{S}_0}\right\}\\
&+ \frac{1}{2}\sum_Q V_Q^2\int_0^\beta d\lambda\int_0^\beta d\lambda'\, G_{\omega_{\rm LO}}(\lambda-\lambda')\sum_{i,j=1,2}\left\langle e^{i\vec{Q}\cdot[\vec{r}_i(\lambda)-\vec{r}_j(\lambda')]}\right\rangle_{\mathcal{S}_0}
\end{aligned}
$$

in which, for computational convenience, the Coulomb potential has been written in its Fourier expanded form.

Using the well established identity for a harmonic oscillator with frequency ω and the relevant annihilation and creation operators, c and $c^\dagger$,

$$\left\langle\exp\left\{\int_0^\beta d\lambda[f^*(\lambda)c^\dagger+f(\lambda)c]\right\}\right\rangle_\omega=\exp\left\{\frac{1}{2}\int_0^\beta d\lambda\int_0^\beta d\lambda' G_\omega(\lambda-\lambda')f(\lambda)f^*(\lambda')\right\} \qquad (3.59)$$

we readily write

$$\lim_{\beta\to\infty}\left\langle e^{i\vec{Q}\cdot[\vec{r}_1(\lambda)-\vec{r}_1(\lambda')]}\right\rangle_{\mathcal{S}_0} = e^{-q^2D_{1,1}(\lambda-\lambda',0)}e^{-q_z^2D_{1,1}(\lambda-\lambda',\Omega)} \qquad (3.60)$$

$$\lim_{\beta\to\infty}\left\langle e^{i\vec{Q}\cdot[\vec{r}_1(\lambda)-\vec{r}_2(\lambda')-\vec{a}]}\right\rangle_{\mathcal{S}_0} = e^{-q^2D_{1,2}(\lambda-\lambda',0)}e^{-q_z^2D_{1,2}(\lambda-\lambda',\Omega)} \qquad (3.61)$$

where

$$D_{1,1}(\tau,\Omega) = \frac{1}{4}\sum_{i=0}^{3}\lambda_i^2(\Omega)\left(1-e^{-\xi_i(\Omega)|\tau|}\right) \qquad (3.62)$$

$$D_{1,2}(\tau,\Omega) = \frac{1}{4}\sum_{i=0,1}\lambda_i^2(\Omega)\left(1-e^{-\xi_i(\Omega)|\tau|}\right)+\frac{1}{4}\sum_{i=2,3}\lambda_i^2(\Omega)\left(1+e^{-\xi_i(\Omega)|\tau|}\right). \qquad (3.63)$$

Using the integral transform

$$\int_0^\beta d\lambda\int_0^\beta d\lambda' F(|\lambda-\lambda'|)=2\beta\int_0^{\beta/2}d\tau\, F(\tau), \qquad (3.64)$$

valid for $F(\beta-\tau)=F(\tau)$, we can express the variational upper bound to the ground state energy of the "two-electron + phonon" complex in the following convenient form

$$E_{\rm g} = -3{\rm w}+\sum_{n=1,2}\frac{1}{n}\sum_{i=0}^{3}\xi_i(\Omega_n)+K\sum_{n=1,2}\frac{2}{n}D_{1,2}(0,\Omega_n)$$

$$
\begin{aligned}
&+ U\sum_{Q}\frac{4\pi}{Q^2}e^{i\vec{Q}\cdot\vec{a}}e^{-q^2D_{1,2}(0,\Omega_1)}e^{-q_z^2D_{1,2}(0,\Omega_2)} \\
&- 4\int_0^\infty d\tau e^{-\mathrm{w}\tau}\sum_{n=1,2}\frac{2}{n}\left\{c_{\mathrm{s}}D_{1,1}(\tau,\Omega_n)+c_{\mathrm{m}}D_{1,2}(\tau,\Omega_n)\right\} \\
&- 2\sum_{Q}V_Q^2\int_0^\infty d\tau e^{-\tau}\Big\{e^{-q^2D_{1,1}(\tau,\Omega_1)}e^{-q_z^2D_{1,1}(\tau,\Omega_2)} \\
&\qquad\qquad +e^{i\vec{Q}\cdot\vec{a}}e^{-q^2D_{1,2}(\tau,\Omega_1)}e^{-q_z^2D_{1,2}(\tau,\Omega_2)}\Big\}\,. \qquad (3.65)
\end{aligned}
$$

Using equations (3.42) and (3.53), the variational parameters K, c_{s} and c_{m} can be expressed in terms of w and ω_i $(i=1,2,3)$,

$$
\begin{aligned}
K &= \frac{1}{2}(\omega_1^2-\omega_2^2-\omega_3^2) \\
\left\{\begin{array}{c} c_{\mathrm{s}} \\ c_{\mathrm{m}} \end{array}\right\} &= \frac{1}{8\mathrm{w}}\left\{\mathrm{w}^2(\omega_1^2-\mathrm{w}^2)\pm(\omega_2^2-\mathrm{w}^2)(\mathrm{w}^2-\omega_3^2)\right\}\,. \qquad (3.66)
\end{aligned}
$$

Consequently, one can treat w and $\{\omega_i\}$ as an alternative set of variational parameters satisfying the intrinsic relation

$$0\le\omega_3\le\mathrm{w}\le\omega_2\le\omega_1 \qquad (3.67)$$

When the two electrons are set a large distance apart, i.e., in the limit $|\vec{a}|\to\infty$, the energy expression (3.65) should conform exactly to that of a single polaron multiplied by a factor of two. Indeed, a careful examination reveals that in this extreme, $\omega_3\to 0$, $\omega_1\to\omega_2$, and consequently, the present results reduce to those reported previously by Senger and Erçelebi[85] for the one-polaron problem with an identical framework consisting of the same parabolic confining potential (see below). We should further emphasize that energetically the most favorable bipolaronic state has been found[23] to take over for $\vec{a}=0$. Therefore, in the foregoing numerical calculations and discussions, we shall presume a vanishing mean separation between the electrons.

With the corresponding values of K, c_{s} and c_{m}, Eq.(3.66), substituted in Eq.(3.65) and having projected out the $\vec{Q}$-summations, the variational bipolaron energy can be written as a function of w and ω_i $(i=1,2,3)$, given by

$$
E_{\mathrm{g}} = -3\mathrm{w}+\sum_{n=1,2}\frac{1}{n}\sum_{i=0}^{3}\xi_i(\Omega_n)+\frac{U}{\sqrt{\pi D_{1,2}(0,\Omega_2)}}\mathrm{F}\left(\frac{D_{1,2}(0,\Omega_1)}{D_{1,2}(0,\Omega_2)}\right)
$$

$$
\begin{aligned}
&- \sum_{n=1,2} \frac{1}{2n} \left\{ \frac{\omega_1^2 - \mathrm{w}^2}{\xi_0(\Omega_n) + \xi_1(\Omega_n)} + \frac{\omega_2^2 + \omega_3^2 - \mathrm{w}^2}{\xi_2(\Omega_n) + \xi_3(\Omega_n)} \right. \\
&\qquad \left. + \frac{\omega_2^2 \omega_3^2}{\xi_2(\Omega_n)\xi_3(\Omega_n)[\xi_2(\Omega_n) + \xi_3(\Omega_n)]} \right\} \\
&- \alpha \sqrt{\frac{2}{\pi}} \int_0^\infty d\tau \, e^{-\tau} \left\{ \frac{1}{\sqrt{D_{1,1}(\tau, \Omega_2)}} \mathrm{F}\left(\frac{D_{1,1}(\tau, \Omega_1)}{D_{1,1}(\tau, \Omega_2)} \right) \right. \\
&\qquad \left. + \frac{1}{\sqrt{D_{1,2}(\tau, \Omega_2)}} \mathrm{F}\left(\frac{D_{1,2}(\tau, \Omega_1)}{D_{1,2}(\tau, \Omega_2)} \right) \right\}
\end{aligned} \tag{3.68}
$$

where

$$
\mathrm{F}(x) = \frac{\arctan\left(\sqrt{x-1}\right)}{\sqrt{x-1}}. \tag{3.69}
$$

3.3.4 Integer-dimensional-space limits

Before we present our results at large, we find it useful to investigate the conformity with the extreme limits of the bulk and strict two-dimensional cases which have already been studied extensively in the literature. When Ω_1 and Ω_2 are set equal to zero, the present model readily conforms to that tackled in a previous paper by Verbist *et al*,[23] and duplicates the same results presented therein for the bulk bipolaron. In this limit we get the simplification: $\mathrm{F}(x) = 1$. Using further Eq.(3.52) in Eq.(3.68), the 3D ground state energy can be written in the simple form, given by

$$
\begin{aligned}
E_{\mathrm{g}}^{(3D)} &= -N\mathrm{w} + \frac{N}{2}(\omega_1 + \omega_2 + \omega_3) + C_1 \frac{U}{\sqrt{D_{1,2}(0,0)}} \\
&- \frac{N}{4} \left\{ \frac{\omega_1^2 - \mathrm{w}^2}{\omega_1} + \frac{\omega_2^2 + \omega_2\omega_3 + \omega_3^2 - \mathrm{w}^2}{\omega_2 + \omega_3} \right\} \\
&- \alpha C_2 \int_0^\infty d\tau \, e^{-\tau} \left\{ \frac{1}{\sqrt{D_{1,1}(\tau, 0)}} + \frac{1}{\sqrt{D_{1,2}(\tau, 0)}} \right\}
\end{aligned} \tag{3.70}
$$

in which $N = 3$, $C_1 = \pi^{-1/2}$ and $C_2 = (2/\pi)^{1/2}$.

Going over to the strict 2D characterization of the polarons, we have the set

of eigenfrequencies (3.50),(3.51), relevant to the z-axis, to simplify as

$$\lim_{\Omega_2\to\infty}\xi_i(\Omega_2)=\begin{cases}\mathrm{w} & \text{for } i=0 \text{ and } 3\\ \infty & \text{for } i=1 \text{ and } 2\end{cases} \tag{3.71}$$

Moreover, using Eqs.(3.48),(3.49) and (3.55), we further have the corresponding λ_i, $(i=0,1,2,3)$, all to vanish. It thus follows that the functions $D_{1,1}(\tau,\Omega_2)$ and $D_{1,2}(\tau,\Omega_2)$, Eqs.(3.62),(3.63), both reduce to zero. Hence, evaluating

$$\frac{1}{\sqrt{D_{1,i}(\tau,\Omega_2)}}\mathrm{F}\left(\frac{D_{1,i}(\tau,\Omega_1)}{D_{1,i}(\tau,\Omega_2}\right)\to\frac{\pi}{2\sqrt{D_{1,i}(\tau,\Omega_1)}}, \tag{3.72}$$

we obtain the corresponding ground state energy in two dimensions to have exactly the same form (3.70) as for the bulk case, except that we now have $N=2$, $C_1=\sqrt{\pi}/2$ and $C_2=(\pi/2)^{1/2}$.

3.3.5 One-polaron limit

When the electrons are thought of as infinitely separated, the part of the trial action relevant to the Coulomb and mutual interactions must fall off to zero, and from equations (3.37) and (3.39) it is not very difficult to guess that the variational coefficients K and c_{m} should both tend to zero. From Eq.(3.66), we find that the only way this can happen is to have $\omega_3\to 0$ and $\omega_1-\omega_2\to 0$. Hence, setting $\nu=\omega_1=\omega_2$, we further have the self-energy coefficient to simplify to

$$c_{\mathrm{s}}=\frac{1}{4}\mathrm{w}(\nu^2-\mathrm{w}^2) \tag{3.73}$$

which we identify exactly as the coefficient in the energy term given by Eq.(27) in a previous paper on the confined one-polaron problem by Senger and Erçelebi,[85] which hereafter will be referred to as SE.

A further simplification is that the eigenfrequencies $\xi_i(\Omega)$ (3.50),(3.51) now read as

$$\begin{aligned}\xi_0(\Omega)=\xi_3(\Omega) &\to \xi_1^{(SE)}(\Omega)\\ \xi_1(\Omega)=\xi_2(\Omega) &\to \xi_2^{(SE)}(\Omega)\end{aligned} \tag{3.74}$$

where $\xi_1^{(SE)}(\Omega)$ and $\xi_2^{(SE)}(\Omega)$ are the eigenfrequencies given by Eq.(19) in SE.

We should also remark that in the limit $a \to \infty$, the rapidly oscillating term $e^{i\vec{Q}\cdot\vec{a}}$ involved in Eq.(3.65) yields zero mean value.

In view of all the above simplifications, we rewrite the energy expression (3.65) as

$$\begin{aligned}\lim_{a\to\infty} E_{\rm g} &= \sum_{n=1,2} \frac{2}{n} \left[\xi_0(\Omega_n) + \xi_1(\Omega_n) - {\rm w}\right] \\ &- 4c_{\rm s} \int_0^\infty d\tau\, e^{-{\rm w}\tau} \left[2D_{1,1}(\tau,\Omega_1) + D_{1,1}(\tau,\Omega_2)\right] \\ &- 2\sum_Q V_Q^2 \int_0^\infty d\tau\, e^{-\tau} \exp\left\{-q^2 D_{1,1}(\tau,\Omega_1) - q_z^2 D_{1,1}(\tau,\Omega_2)\right\} \qquad (3.75)\end{aligned}$$

which indeed is a replica of twice the expression for the one-polaron ground state energy given through the series of equations (13,22,25–30) in SE. The correspondence with the notation of SE can be established through

$$D_{1,1}(\tau,\Omega_i) = \frac{\tau}{2\sigma_i(\tau)} \qquad (3.76)$$

where $\sigma_i(\tau)$ is defined by SE–Eq.(28).

3.3.6 Q2D Slab Confinement

For the Q2D confinement we simply set $\Omega_1 = 0$ and $\Omega_2 = \Omega$. Determining the optimal fits to the variational parameters w and $\{\omega_i\}$ $(i = 1, 2, 3)$, in our computations we shall trace the domain of stability $\{\eta < \eta_c,\, \alpha > \alpha_c\}$ of the bipolaron as a function of the confining parameter Ω.

The criterion for which a stable bipolaron state takes place will be derived by demanding that the ground state energy of the pair of composite polarons making up the bipolaron be lower than twice the energy of one single polaron. To provide a consistent comparison of the variational energy minima of the bipolaron system with those of the single polaron case, one needs further to compute the corresponding one-polaron energy values, $E_{\rm g}^{(1)}$, derived within an identical framework of the present model and formalism, and under the same numerical precision. On this purpose, one may either carry out a parallel variational

computation of Eq.(3.65) in the limit $a \to \infty$, or alternatively, refer directly to the series of equations (13,22,25–30) given in SE.

In exploiting the variational bipolaron energy one faces an entangled admixture of a series of competitive aspects introduced by the parameters α, η and Ω which characterize the system. It should be evident that these parameters do not enter the problem in an independent way but all together take part in the binding in connected and somewhat involved manners, opposing the effect of one against the other. Distinguished from the case of a three or two dimensional bipolaron, the extra parameter Ω adds more to the complexity in the delicate balance between the Coulomb and phonon counterparts of the problem and their percentual involvements in the binding. Clearly, in a confined volume where Ω is tuned from zero to large values, i.e., when the particles are squeezed to get closer, one expects their kinetic energy to increase and the Coulomb repulsion between them to become stronger. In the meantime, due to the rapid charge density fluctuations of the pair of electrons, the phonon-coupling becomes pseudo-enhanced leading to a more effective and deeper "phonon-mediated" interaction between the particles to oppose and counterbalance the kinetic and Coulomb repulsions. Thus, the overall role of the confinement on the phonon-coupling induced localization of the electron-electron pair and the withstanding repulsion is to make these competing counter aspects stronger. What is more peculiar to the present context is that during when Ω is varied, the phonon-coupling and the Coulomb strengths may not in general grow or decrease monotonically in concert at the same rate and consequently, the relative dominating strength of either the Coulomb potential or the electron-phonon interaction over the other may become altered as a function of the degree of confinement. Yet, a further aspect of the problem intruded by the confining potential is that, in the Q2D geometry, the electrons are confined along only one spatial coordinate, but are free to expand and relax themselves in the transverse directions normal to the confining barriers; thus, in the overall, resulting in a comparatively increased inter-particle separation and a relatively weakened repulsive interaction against the lattice polarization field which holds the particles together. It is therefore the

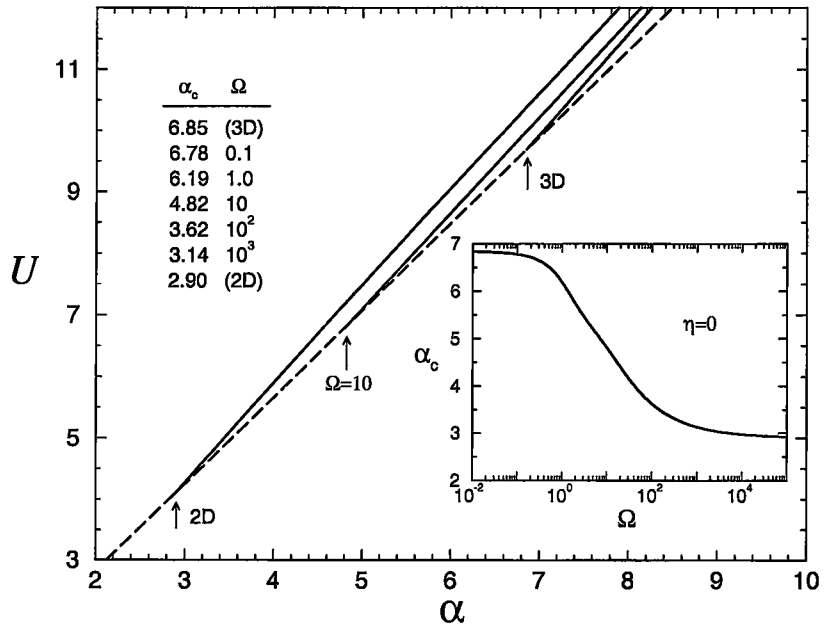

Figure 3.4: Q2D bipolaron phase diagram

The phase diagram for bipolaron formation in the space of the Coulomb coefficient and the electron-phonon coupling constant. The solid lines from top to bottom are respectively, for the two, quasi-two ($\Omega = 10$) and three dimensional configurations, and the arrows refer to the corresponding critical values of α. The dashed line ($\eta = 0$) is the boundary of the unphysical region. The insets display the variation of α_c as a function of the confining parameter.

mutual competition between such aforementioned aspects of the problem and the interrelated roles which the parameters U, α and Ω play all together that lead to the formation (or dissociation) of a bipolaron.

The common theoretical prediction led by the relevant works in the literature is that bipolaron formation is more favorable in 2D than it is in bulk. For instance, with parameter η set equal to zero, i.e., when the Coulomb repulsion is thought of as tuned down to its hypothetical minimum strength ($U = \sqrt{2}\alpha$), the critical value of the coupling constant over which the bipolaron state can form is found to be $\alpha_c^{(3D)}|_{\eta=0} = 6.85$ and $\alpha_c^{(2D)}|_{\eta=0} = 2.90$ in three and two dimensions, respectively.[23] For actual material parameters of interest where $\eta > 0$, the corresponding critical coupling constants scale inevitably to larger values so as to compete with the stronger Coulomb repulsion, and yet, regardless

of η, one always has $\alpha_c^{(2D)}$ to lie considerably deviated below $\alpha_c^{(3D)}$ due to that the electrons interact more effectively with the phonons in two dimensions, and consequently, a pseudo-enhanced effective electron-phonon interaction leads to a relatively smaller numerical value of the coupling constant. Such a conspicuous feature met in switching the dimensionality from three to two should naturally lead one to await that, in the quasi-two dimensional (Q2D) configuration where Ω is tuned from zero to large values, an increased degree of confinement should play a constructive role in favor of bipolaronic stability; hence, the larger the value of Ω is, the less is the need for strong α. A clear description of this trait is provided by the phase diagrams in Fig. 3.4 where we plot the Coulomb coefficient U against α. In the phase picture the space lying below the dashed line corresponds to $\eta < 0$, and is therefore unphysical. The upper space bounded from below by the solid lines plotted for three distinctive degrees of confinement ($\Omega = 0$, $\Omega = 10$ and $\Omega \to \infty$) gives the unstable region where the polarons choose to remain separated. Thus, it is only the narrow triangular area bounded by the dashed and either of the solid lines in which the polarons can be found in a bound state forming a stable bipolaron. The vertex of each triangular region at which the dashed and solid lines join defines an infimum for the coupling constant in the 3D, Q2D ($\Omega = 10$) and 2D configurations. Coupling constants larger than these critical vertex values serve for supporting the bipolaron to conserve its stability at correspondingly stronger Coulomb repulsions. The relevant numerical data of α_c for a few sample values of Ω is tabulated in the upper left inset of the figure. A more tractable display of α_c is given in the lower right inset where we plot its variation continuously as a function of Ω encompassing the bulk- and the 2D-limits. The overall conclusion led by the content of Fig. 3.4 is that the critical α below which a bipolaron state is unfavorable gets shifted to smaller values as the degree of confinement is increased. Also, for a given fixed value of α, the lower the dimensionality is, the more favorably the bipolaron state can be sustained. In numerical terms, setting $\alpha = 8$ for instance, we evaluate the critical upper bound for the Coulomb coefficient beyond which the bipolaron dissociates into two individual polarons as $U_c = 11.59$, 11.79, and 12.17, respectively, for the 3D,

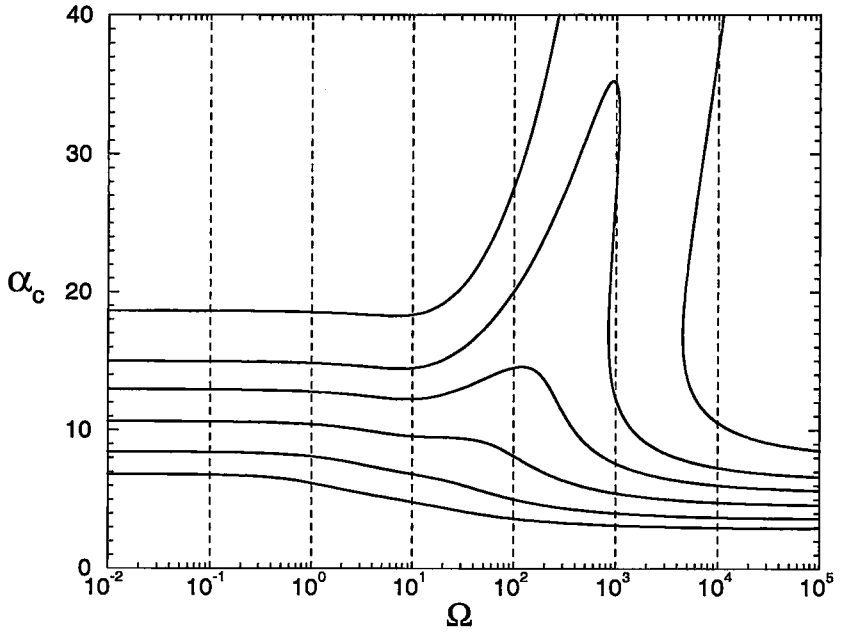

Figure 3.5: Critical α for Q2D bipolaron
The variation of α_c as a function of confinement for different values of η. The curves are for $\eta = 0$, 0.03, 0.05, 0.06, 0.065, 0.07 from bottom to top, respectively.

Q2D ($\Omega = 10$) and 2D cases.

When defining α_c, usually the Coulomb coefficient U is taken at its hypothetical minimum value (equivalently $\eta = 0$), which is in fact a mathematical idealization, because for real physical materials the ratio of dielectric constants can never be zero. To visualize the effect of non-zero η, on the degree-of-confinement dependence of α_c, consider Fig.3.5. The bottom most curve is for $\eta = 0$ which is also presented in the inset of Fig.3.4. It is a monotonically decreasing curve interpolating between the bulk and strict-2D limit values of α_c as Ω is varied. Interestingly, for non-zero values of η, we see the formation of a rapidly growing pattern which forbids the existence of stable bipolarons for certain degrees of confinement. Such a high sensitivity of α_c to η for intermediate values of Ω, is another consequence of the delicate balance formed by the parameters of the system.

In the next paragraph we review the content of Fig. 3.4 from an alternative viewpoint where we give an explicit and broader picture of U_c against Ω over a

succession of distinctive α values extended towards the strong-coupling limit.

Setting α fixed at any desired value, Eq.(3.3) allows us to trace the critical condition on the Coulomb strength as a function of the degree of confinement, displayed equivalently in terms of the alternative related parameter η. In Fig. 3.6 we plot a series of curves describing the effect of confinement on the critical value of η for different coupling constants ranging in between 4 and 30. In the same figure, for the purpose of comparison, we also include a supplementary layout of η_c versus Ω derived within the framework of the strong-coupling adiabatic polaron theory. Over the scale of the abscissa we choose to express Ω in units α^2, mainly for two reasons; one is that the ratio Ω/α^2 (rather than bare Ω) proves to be a more sensible measure of the degree of confinement, and the other stems from that, in the strong coupling expansion to leading order in α, the ground state energy is seen to be proportional to the square of the coupling constant, i.e., $E_g = -c\alpha^2$, where the corresponding coefficient of proportionality bears a functional relation solely to Ω/α^2 for both the single-polaron and two-polaron systems.[107] We should note that the polarons can feel the boundary potential and enter a regime of reduced dimensionality only when the effective well width ($\sim 1/\sqrt{\Omega}$) is smaller than, or at least comparable with the mean (bi)polaron size ($\sim 1/\alpha$), and consequently, even a large Ω would not mean anything, but bulk medium, unless $\alpha < \sqrt{\Omega}$. It is therefore due to this reasoning that we are tempted to accept the ratio Ω/α^2 as a convenient measure of confinement. Thus, at "strong coupling", if η_c is plotted against Ω/α^2, rather than Ω, we find that one can display the phase boundary on one universal curve with no loss in generality for all large α.

A plain implication led by the plots in Fig. 3.6 is that, the stronger the phonon coupling, or the larger the degree of confinement is, the more easily the bipolaron state can form and be supported against the repulsive Coulomb potential. We should remark that any plot of η_c pertaining to $\alpha < 6.85$ intersects the abscissa at a nonzero value of Ω; hence, for not strong enough α, a bipolaron can form only beyond a critical degree of confinement, and the larger the coupling constant is, the smaller is the corresponding critical Ω. Clearly, for $\alpha \geq 6.85$ one has

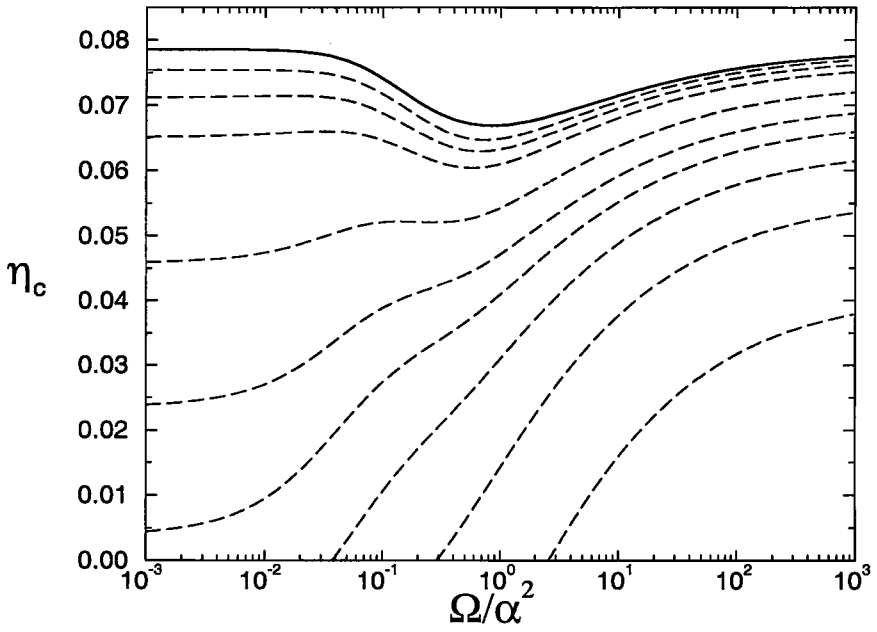

Figure 3.6: The critical ratio η_c for Q2D bipolaron
The critical ratio η_c as a function of degree of confinement for a succession of different α values. The dashed curves from bottom to top give the path-integral results obtained for $\alpha = 4, 5, 6, 7, 8, 10, 15, 20, 30$. The topmost solid curve is universal for all large α and has been obtained within the framework of the strong-coupling polaron theory.

$\Omega_c = 0$, where in this case bipolaron formation is favorable even in bulk, and the sole effect of the confinement is to take over in favor of enhancing the already established stability of the bipolaron.

A careful look at the series of curves from bottom to top reveals that as α is made indefinitely large, a peculiar feature starts to build up, and contrary to our anticipations, we observe that the critical η does no more display a steady increasing behavior interpolating between the 3D- and 2D-limits, but instead attains its corresponding 2D-value after having gone through a minimum located at some place about $\Omega/\alpha^2 \simeq 1$. We feel that this salient characteristic is an implicit consequence of the dominating effect of either the Coulomb repulsion or the phonon mediated attraction over the other, and the cross-overing of the competition between these counter aspects as the confining parameter is varied. In regard with the strong-coupling limit, we should add the note that, as α is

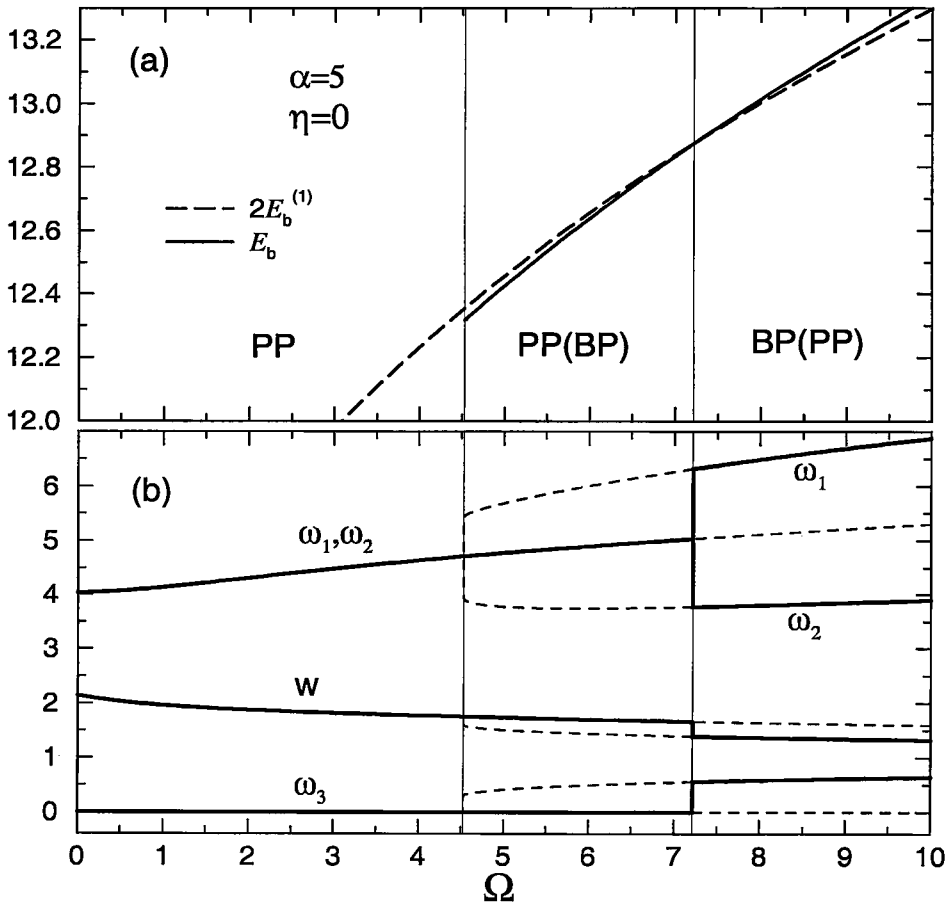

Figure 3.7: Binding energy and variational parameters of the bipolaron state (a) Bipolaron and two single-polaron binding energies, and (b) the variational parameters, as functions of the degree of confinement.

adjusted to larger and larger values, the sequence of dashed (path-integral) curves converge towards the topmost solid curve which we have obtained independently adopting the adiabatic approximation. In the extreme strong-coupling limit we obtain $\eta_c = 0.079$ in both three and two dimensions, as reported earlier in Ref.25.

Before we close our discussions we would like to shed some insight into polaron-polaron versus bipolaron bound state energies and display the profiles of the corresponding variational parameters w and $\{\omega_i\}$ against the degree of confinement. To provide an explicit track of the evolution of the "polaron-polaron" complex as a function of the effective dimensionality, we refer back to

the simple case for which we artificially set $\eta = 0$, and choose $\alpha = 5$ as a sample value being somewhat smaller than the corresponding bulk critical minimum, $\alpha_c^{(3D)}|_{\eta=0} = 6.85$. In Figure 3.7(a) we plot the possible bipolaronic binding energy

$$E_b = \Omega - E_g$$

accompanied by twice the binding energy of the corresponding single polaron over the range $0 \leq \Omega \leq 10$. To give a complementary understanding of the polaron-polaron (PP) and bipolaron (BP) phases and the transition from one phase to the other, we also display the variational parameters as a function of Ω (cf., Fig.3.7(b)). We at first note that for $\Omega > 7.21$, i.e., in the region "BP (PP)", the bipolaronic phase is energetically more likely to show up compared to the PP-phase of two individual polarons, and yet, increasing the degree of confinement enhances the stability of the BP-phase. For $\Omega < 7.21$, however, the state of two individual polarons is favored. In the region "PP (BP)" $(4.53 < \Omega < 7.21)$ the bipolaronic phase is seen to persist rather recessively where, with decreasing Ω, the corresponding local minimum in its ground state energy starts to lose its depth and eventually diminishes for $\Omega = 4.53$. When Ω is made even smaller, i.e., as the bulk limit is approached, one achieves solely the PP-phase with whatsoever no relevance to any possible bipolaronic characterization of the two-polaron system. In Fig.3.7(b) the variational parameters pertaining to the energetically favorable phase are plotted in boldface curves and those which correspond to the metastable state of either phase are given in dashed lines. It should be noted that if the bipolaronic phase should indeed be realized either as a metastable state or otherwise, the corresponding variational parameters all achieve non-zero and distinctive values. The phase of two independent polarons, however, is characterized by that ω_1 and ω_2 coalesce into one single curve, and $\omega_3 = 0$ regardless of Ω. Consequently, one has w and $\nu\,(= \omega_1 = \omega_2)$ to be recognized as the well established Feynman variational parameters of the usual one-polaron problem.[7,85]

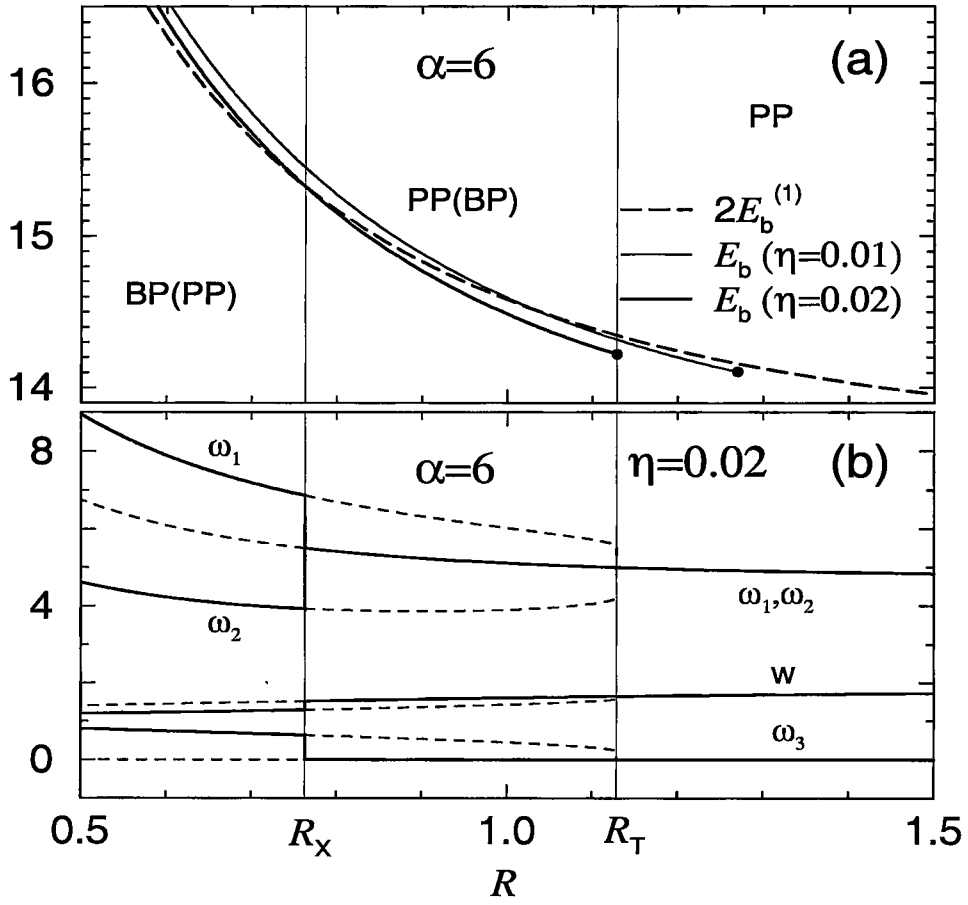

Figure 3.8: Energy and variational parameters
(a) Bipolaron and two single-polaron binding energies, and (b) the variational parameters, as functions of $R = \Omega^{-1/2}$. The sample parameter values are: $\alpha = 6$ and $\eta = 0.01, 0.02$. The crossover and cut-off radii (R_X and R_T) and the vertical lines separating the phases are relevant to only $\eta = 0.02$.

3.3.7 Q1D Wire Confinement

For the wire-type confinement we simply set $\Omega_1 = \Omega$ and $\Omega_2 = 0$.

To provide an understanding of the influence of Q1D confinement on the evolution of the complex of two polarons in favor of a bipolaron bound state, we undertake two illustrative cases for which the Coulomb repulsion is considered to be not too strong, and the phonon mediated binding somewhat deep enough to overcome that repulsion. Setting $\alpha = 6$ and $\eta = 0.01, 0.02$ as sample values,

we display (cf., Fig. 3.8(a)) a graphical comparison of the corresponding binding energies in the polaron-polaron ("PP") and bipolaron ("BP") phases as a function of $R = \Omega^{-1/2}$ which we hereafter refer to as simply the radius. A glance at the plots in Fig. 3.8(a) reveals that there are three major regions in the overall domain of R. For $R < R_{\rm X}$, i.e., in the region "BP (PP)", the bipolaronic phase is energetically more favorable than the PP-phase of two individual polarons, and yet, decreasing the wire radius enhances the stability of the BP-phase. In going toward the opposite extreme and relaxing the degree of confinement, the BP-state can no more be sustained, and beyond the crossover radius, $R_{\rm X}$, the bipolaronic phase is seen to persist recessively as a metastable state and eventually terminate at a cut-off radius $R_{\rm T}$ (shown in the figure by a dark dot). For $R \geq R_{\rm T}$ one achieves solely the PP-phase with whatsoever no relevance to any possible bipolaronic characterization of the two-polaron system. An additional remark led by the content of the Fig. 3.8(a) is that, for a given fixed α, the stronger the Coulomb repulsion is, the more is the requirement for a thinner wire to favor and sustain the bipolaron state. In this regard, for $\alpha = 6$, we have calculated $R_{\rm X} = 1.03\,(0.76)$ and $R_{\rm T} = 1.27\,(1.13)$ for $\eta = 0.01\,(0.02)$. For completeness, we also display complementary plots of the variational parameters as a function of the transition from one phase to the other (cf., Fig. 3.8(b)). The parameters pertaining to the energetically favorable phase are plotted in boldface curves and those which correspond to the metastable state of either phase are given in dashed lines.

In Fig. 3.9 we plot a phase diagram in the "$U-\alpha$" plane, picturing the domain of stability of the bipolaron state at different degrees of confinement. In the diagram the space lying below the dashed line corresponds to $\eta < 0$, and is therefore irrelevant. The upper space bounded from below by the solid lines plotted for three distinctive radii ($R = 0.3$, $R = 1.0$ and $R \gg 1$) gives the unstable region. It is therefore only the narrow triangular area bounded by the dashed and either of the solid lines in which the polarons can be found in a stable bound state forming a bipolaron. The vertex of each triangular region at which the dashed and solid lines join defines a critical minimum for the coupling constant

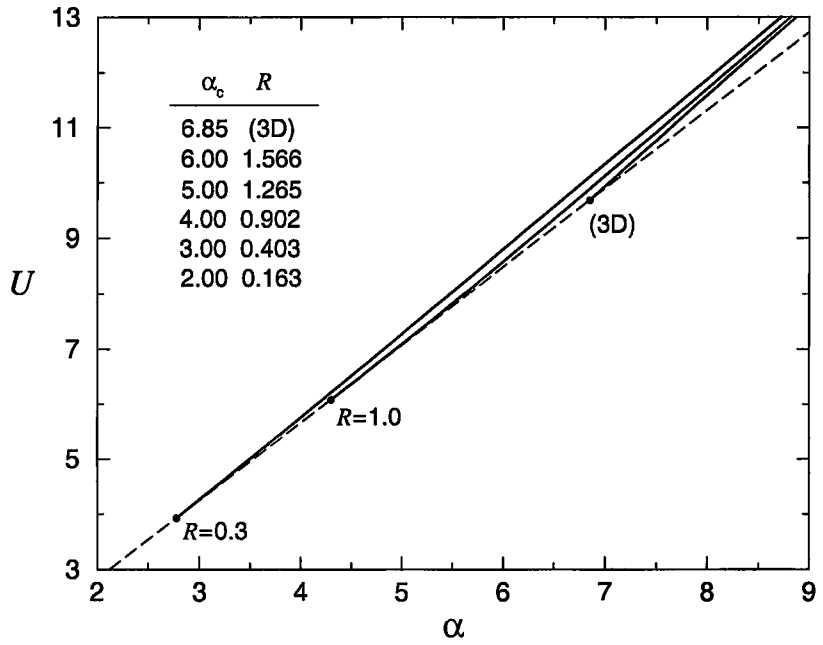

Figure 3.9: Phase diagram for Q1D bipolaron
The phase diagram for bipolaron formation in the space of the Coulomb coefficient and the electron-phonon coupling constant. The solid lines from top to bottom are respectively, for $R = 0.3$, 1.0 and $R \to \infty$. The dashed line ($\eta = 0$) is the boundary of the unphysical region. The inset tabulates the corresponding radii for a few sample values of α_c.

in the bulk and Q1D ($R = 1.0$, and 0.3) configurations. Coupling constants larger than these critical vertex values serve for supporting the bipolaron to maintain its stability at correspondingly stronger Coulomb repulsions. In numerical terms, setting $\alpha = 8$ for instance, we evaluate the critical upper bound for the Coulomb coefficient beyond which the bipolaron dissociates into two individual polarons as $U_c = 11.59$, 11.70, and 11.88, respectively, for the cases $R =$ bulk, 1.0, and 0.3.

A more complete trace of the critical condition on the Coulomb strength as a function of the degree of confinement is given in Fig. 3.10 where we provide a layout of the alternative related parameter η against R plotted for a sequence of coupling constants ranging from 4 to 10. An immediate glance at the series of plots in Fig. 3.10 reveals that, starting from the bulk limit, η_c displays in general an increasing trend with decreasing R, yielding an explicit evidence in favor of a pronounced effective phonon coupling with the increase in the

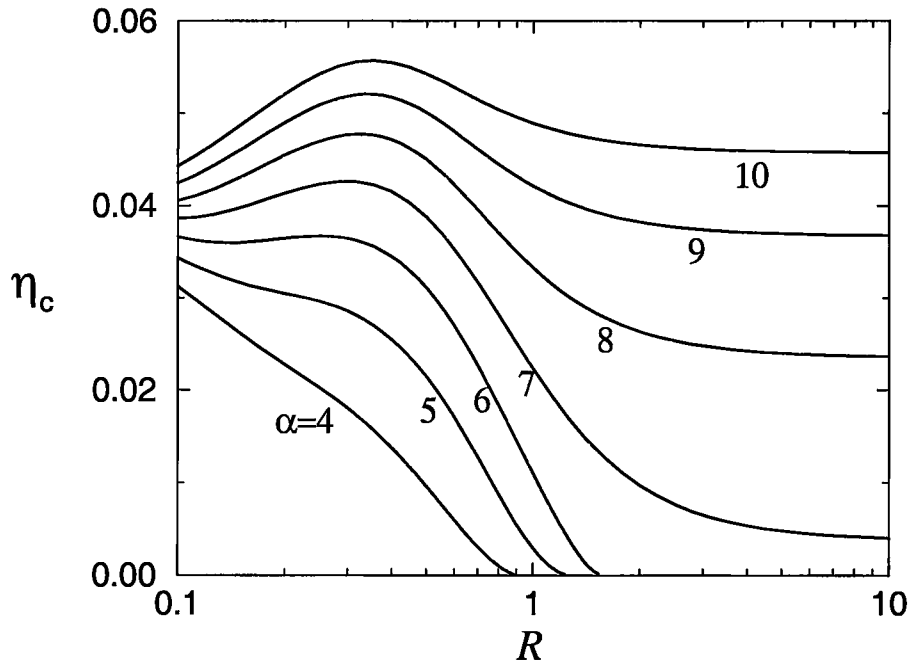

Figure 3.10: The critical ratio η_c for Q1D bipolaron
The critical ratio η_c as a function of $R = \Omega^{-1/2}$.

degree of confinement, which correspondingly results in an enhancement in the phonon mediated interaction between the electrons to serve for opposing and counterbalancing even more stronger Coulomb repulsions. Examining the low lying plots in the figure, we note that for $\eta = 0$, i.e., for the Coulomb coefficient taken as assuming its hypothetical minimum value ($U = \sqrt{2}\alpha$), the critical coupling constant over which the bipolaron phase is realized is found to be $\alpha_c^{(3D)} = 6.85$ for the bulk case.[23] Correspondingly, we note that our plots of η_c for $\alpha = 4$, 5, 6 all intersect the abscissa at finite values of R; hence, for not strong enough α, a bipolaron can form only beyond a critical degree of confinement; and the smaller the coupling constant is, the smaller is the corresponding critical radius. Clearly, for $\alpha > 6.85$ one has $R_c \to \infty$, where in this case bipolaron formation is favorable even in bulk, and the additional effect of the confinement is to take over in favor of enhancing the already established stability of the bipolaron.

We would like to draw attention to that, for comparatively large α, the critical η exhibits a peculiar variation as the wire radius is decreased; compatible with

our anticipations, it first increases, and after having gone through a maximum, displays a decreasing trend. We feel that this salient feature is an implicit consequence of the fact that the parameters α, η and Ω which characterize the system do not enter the problem in an independent way but, all together take part in the binding in related manners through an entangled admixture of the competing effects of the Coulomb repulsion and the phonon mediated attraction over the other and the cross-overing between these counter aspects as the confining parameter is varied. Clearly, in a confined volume where Ω is tuned from zero to large values, it is not only the phonon coupling which gets pronounced, but in the meantime the kinetic energy of the electrons increases and the Coulomb repulsion becomes steadily strengthened due to that the particles are squeezed to get closer. Thus, the overall role of the confinement on the phonon-coupling induced localization of the electron-electron pair and the withstanding kinetic and Coulomb repulsions is to make these competing counter aspects stronger. What is more peculiar to the present context is that during when Ω is varied, the phonon-coupling and the Coulomb strengths may not in general grow or decrease monotonically in concert at the same rate and consequently, the relative dominating strength of either the Coulomb potential or the electron-phonon interaction over the other may become altered as a function of the degree of confinement. In the particular Q1D configuration, with contracting wire radius, the electrons experience an increasingly large restriction toward the wire axis and therefore, below a certain wire size, the phonon-mediated attraction starts to lose its overwhelming strength against the rapidly increasing Coulomb and kinetic repulsions; thus leading to a decreasing profile of η_c as R is made even smaller. This feature however is seen to diminish as α is tuned to smaller values. For comparatively weak α, where the electrons are not too tightly bound by the lattice, we think that, with shrinking wire size, the charge density of the electrons acquire a spatial extent expanded to relax itself in the longitudinal ($\pm z$) directions along the wire axis, resulting in the overall a weaker repulsion between the particles; thus enabling the phonon-mediated attraction to maintain its capability in supporting the bipolaron state against larger values of the Coulomb coefficient,

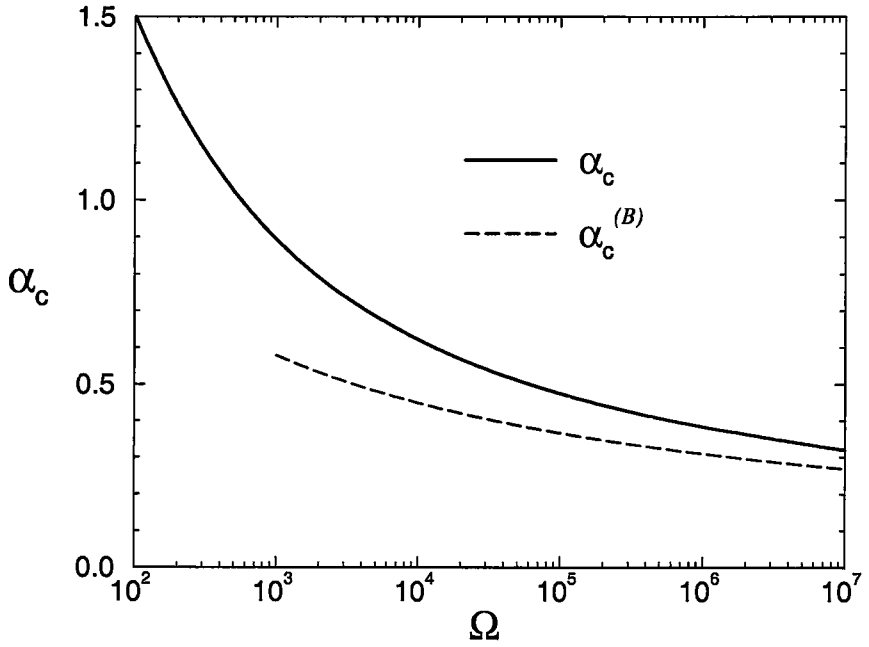

Figure 3.11: The critical coupling constant α_c for Q1D bipolaron
The critical coupling constant α_c as a function of Ω in the extreme high confinement limit. The solid curve reflects the results of the present model. The dashed curve is the asymptotic 1D relation: $\alpha_c^{(B)} = 4.6/\ln B$ derived by Smondyrev *et al*[108] for the 3D magneto-bipolaron in the strong magnetic field limit. For compatibility, we have set $B = 2\sqrt{2}\Omega$.

and correspondingly, larger values of η_c.

As a final complementary remark we would like to add the note that the confined bipolaron model adopted here reproduces almost similar qualitative features as for the alternative case of a 3D bipolaron in a magnetic field. In both cases it is seen that the common fundamental effect of either the cylindrical parabolic potential or the external magnetic field is to enlarge the region of bipolaron formation so that the critical coupling constant required to sustain the bipolaron phase assumes smaller values as the parabolic potential or the magnetic field are made stronger. The similarity between the two problems become more closer in the high magnetic field limit ($B \rightarrow \infty$), since it is only then the dominant contribution to the magneto-bipolaron energy comes from the ground Landau level and the essential digression originating from the angular momentum term in the vector-potential part of the Hamiltonian gets

removed. It has already been shown by Smondyrev and his co-workers[108] that the 3D magneto-bipolaron maps onto a 1D bipolaron for strong fields and that the effective critical coupling constant scales to smaller values with proportionality to the reciprocal of $\ln B$. Numerical treatment of the present calculation tackled in the *unrealistic* extreme high confinement limit ($\Omega \rightarrow \infty$) reproduces somewhat the same nature in an asymptotic manner, where we observe that the critical coupling constant seems to bear a linkage to the confining parameter through an analogous relation: $\alpha_c \simeq 1/\ln\Omega$ (cf., Fig.3.11).

Chapter 4

CONCLUSIONS

In this report we have studied the possibility and criteria in achieving stable bipolarons in low dimensionally confined media. The "deformable potential box" – model adopted in this work allows us to attain a simple and yet comprehensive review of the two-polaron problem within a unifying scheme interpolating between the bulk and all low dimensional geometric configurations of general interest. In the limit of strong coupling, it has been illustrated that in structures with reduced dimensionality, the phase description displays an explicit relevance to the phonon-coupling parameter α, distinguished from that reported earlier for the strongly coupled bipolaron in three and two dimensions. It has been shown further that in conforming the potential box to a thin quantum well, the critical ratio of the dielectric constants may undergo an interesting variation, exhibiting a decrease first, then ascending and eventually going over to its topmost two dimensional value.

Since strong coupling theory provides a limited information about the bipolaron properties, we have obtained more dependable results through path integral formalism. The overall implication led by the numerical outcomes of this work is that, in general the stronger the phonon coupling and/or the larger the degree of confinement is, the more favorably the bipolaron state can form and be supported against the repulsive Coulomb potential. However, there are minor exceptions of this general trend, such that in Q2D geometry, increased degree of

confinement for non-zero values of η leads to extremely high values of α_c in going to the strict-2D limit. We further conclude that it is the mutual and interrelated roles which the Coulomb and phonon coupling parameters play together with the confinement that lead to the formation (or dissociation) of a bipolaron.

Bibliography

[1] L.D. Landau, *Phys. Zeitschrift Sowjetunion* **3**, 664 (1933)

[2] H. Fröhlich, "Theory of electrical breakdown in ionic crystals", *Proc. Roy. Soc.* A **160**, 230 (1937)

[3] S.I. Pekar, *Zh. Eksp. Teor. Fiz.* **16**, 341 (1946)

[4] S.I. Pekar, *Zh. Eksp. Teor. Fiz.* **18**, 105 (1948)

[5] L.D. Landau and S.I. Pekar, *Zh. Eksp. Teor. Fiz.* **18**, 419 (1948)

[6] H. Fröhlich, H. Pelzer and S. Zienau, "Properties of slow electrons in polar materials", *Philos. Mag.* **41**, 221 (1950)

[7] R.P. Feynman, "Slow electrons in polar crystals", *Phys. Rev.* **97**, 660 (1955)

[8] S.I. Pekar, *Untersuchungen über die Elektronentheorie der Kristalle*, (Berlin, Akademie, 1954)

[9] H. Fröhlich, *Adv. Phys.* **3**, 325 (1954)

[10] S.V. Tjablikov, *Zh. Eksp. Teor. Fiz.* **23**, 381 (1952)

[11] T. Holstein, *Ann. Phys.* **8**, 325 (1959)

[12] A.S. Alexandrov and N.F. Mott, "Bipolarons", *Rep. Prog. Phys.* **57**, 1197 (1994)

[13] V.L. Vinetskii and M.S. Gitterman, *Zh. Eksp. Teor. Fiz.* **33**, 730 (1957)

[14] M.F. Bishop and A.W. Overhauser, "Phonon-mediated electron-electron interaction in real space", *Phys. Rev. B* **23**, 3627 (1981)

[15] P.W. Anderson, "Model for the electronic structure of amorphous semiconductors", *Phys. Rev. Lett.* **34**, 953 (1975)

[16] S. Lakkis, C. Schlenker, B.K. Chakraverty, R. Budder and M. Marizio, "Metal-insulator transitions in Ti_4O_7 single crystals: Crystal characterization, specific heat, and electron paramagnetic resonance", *Phys. Rev. B* **14**, 1429 (1976)

[17] A. Alexandrov and J. Ranninger, "Theory of bipolarons and bipolaronic bands", *Phys. Rev. B* **23**, 1796 (1981)

[18] B.K. Chakraverty, D. Feinberg, H. Zhengand, and M. Avignin, "Squeezed bipolaronic states and high temperature superconductivity in BaLaCuO systems", *Solid State Commun.* **64**, 1147 (1987)

[19] D. Emin, "Formation, motion, and high-temperature superconductivity of large bipolarons", *Phys. Rev. Lett.* **62**, 1544 (1989)

[20] M.H. Cohen, E.N. Economou, and C.M. Soukoulis, "Small-bipolaron formation", *Phys. Rev. B* **29**, 4496 (1984)

[21] J. Adamovski, "Formation of Fröhlich bipolarons", *Phys. Rev. B* **39**, 3649 (1989)

[22] F. Bassani, M. Geddo, G. Iadonisi, and D. Ninno, "Variational calculations of bipolaron binding energies", *Phys. Rev. B* **43**, 5296 (1991)

[23] G. Verbist, F.M. Peeters, and J.T. Devreese, "Large bipolarons in two and three dimensions", *Phys. Rev. B* **43**, 2712 (1991)

[24] S. Sil, A.K. Giri, and A. Chatterjee, "Stability of the Fröhlich bipolaron in two and three dimensions", *Phys. Rev. B* **43**, 12642 (1991)

[25] G. Verbist, M.A. Smondyrev, F.M. Peeters, and J.T. Devreese, "Strong-coupling analysis of large bipolarons in two and three dimensions", *Phys. Rev. B* **45**, 5262 (1992)

[26] J. Adamovski and S. Bednarek, "Stability of large bipolarons", *J. Phys.: Condens. Matter* **4**, 2845 (1992)

[27] P. Vansant, M.A. Smondyrev, F.M. Peeters, and J.T. Devreese, "Exact equations for bipolarons in the strong-coupling limit", *J. Phys. A: Math. Gen.* **27**, 7925 (1994)

[28] C. Qinghu, W. Kelin, and W. Shaolong, "Variational calculation for large bipolarons in the strong-coupling limit", *Phys. Rev. B* **50**, 164 (1994)

[29] F. Luczak, F. Brosens, and J.T. Devreese, "Formation of large bipolarons", *Phys. Rev. B* **52**, 12743 (1995)

[30] M.A. Smondyrev, J.T. Devreese, and F.M. Peeters, "Asymptotic expansions in the path-integral approach to the bipolaron problem", *Phys. Rev. B* **51**, 15008 (1995)

[31] S. Sahoo, "The regular perturbation theory on the stability of the strong-coupling bipolaron", *J. Phys.: Condens. Matter* **7**, 4457 (1995)

[32] S. Mukhopadhyay and A. Chatterjee, "Formation and stability of a singlet optical bipolaron in a parabolic quantum dot", *J. Phys.: Condens. Matter* **8**, 4017 (1996)

[33] E.P. Pokatilov, V.M. Fomin, J.T. Devreese, S.N. Balaban, and S.N. Klimin, "A bipolaron in a spherical quantum dot with parabolic confinement", *J. Phys.: Condens. Matter* **11**, 9033 (1999)

[34] R.T. Senger and A. Erçelebi, "Quasi-two-dimensional Feynman bipolarons", *Phys. Rev. B* **60**, 10070 (1999)

[35] R.T. Senger and A. Erçelebi, "Path-integral approximation on the stability of large bipolarons in quasi-one-dimensional confinement", *Phys. Rev. B* **61**, 6063 (2000)

[36] W.B. da Costa and F.M. Peeters, "The polaron-bipolaron transition for acoustical three-dimensional polarons", *J. Phys.: Condens. Matter* **8**, 2173 (1996)

[37] G.A. Farias, W.B. da Costa, and F.M. Peeters, "Acoustical polarons and bipolarons in two dimensions", *Phys. Rev. B* **54**, 12835 (1996)

[38] D.M. Larsen, in *Proc. 17th Int. Conf. on the Physics of Semiconductors*, edited by J.D. Chadi and W. Harrison (Berlin: Springer, 1985) p.421

[39] S.N. Klimin, E.P. Pokatilov, and V.M. Fomin, "Bulk and interface polarons in quantum wires and dots", *Phys. Stat. Sol. (b)* **184**, 373 (1994)

[40] *Polarons and Excitons*, edited by C.G. Kuper and G.D. Whitfield, (Oliver and Boyd, Edinburgh and London, 1963)

[41] H. Haken, *Quantum Field Theory of Solids*, (North-Holland, Amsterdam, 1983)

[42] E. Kartheuser, in *Polarons in Ionic Crystals and Polar Semiconductors*, edited by J.T. Devreese, (North-Holland, Amsterdam, 1972) p.717

[43] D.M. Larsen, "Polaron ground-state energy in two-dimensions", *Phys. Rev. B* **35**, 4435 (1987)

[44] B.E. Sernelius, "Polaron in n dimensions", *Phys. Rev. B* **36**, 9059 (1987)

[45] T. Yıldırım and A. Erçelebi, "Weak-coupling optical polaron in QW-confined media", *J. Phys.: Condens. Matter* **3**, 4357 (1991)

[46] T.D. Lee, F.E. Low, and D. Pines, "The motion of slow electrons in a polar crystal", *Phys. Rev.* **90**, 297 (1953)

[47] E.P. Gross, "Small oscillation theory of the interaction of a particle and scaler field", *Phys. Rev.* **100**, 1571 (1955)

[48] D. Pines, "Intermediate-coupling polaron theory",
in *Polarons and Excitons*, edited by C.G. Kuper and G.D. Whitfield,
(Oliver and Boyd, Edinburgh and London, 1963)

[49] D.M. Larsen, "Upper and lower bounds for the intermediate-coupling polaron ground-state energy", *Phys. Rev.* **172**, 967 (1968)

[50] W.J. Huybrechts, "Internal excited state of the optical polaron",
J. Phys. C **10**, 3761 (1977)

[51] N. Tokuda, "A variational approach to the polaron problem",
J. Phys. C **13**, L851 (1980)

[52] R.T. Senger and A. Erçelebi, "Q1D polarons in rigid boundary cylindrical wires: Mixed–coupling approximation", *Tr. J. Physics* **22**, 169 (1998)

[53] N.N. Bogolubov, "On a new form of the adiabatic perturbation theory in the problem of interaction of a particle with a quantum field",
Ukr. Mat. Zh. **2**, 3 (1950)

[54] S.V. Tjablikov, "To a theory of interaction of a particle with a quantum field", *Zh. Eksper. Teor. Fiz.* **21**, 377 (1951)

[55] G.R. Allcock, "On the polaron rest energy and effective mass",
Adv. Phys. **5**, 412 (1956)

[56] G. Whitfield and P.M. Platzman, "Simultaneous strong and weak coupling in the piezoelectric polaron", *Phys. Rev. B* **6**, 3987 (1972)

[57] S.J. Miyake, "Strong-coupling limit of the polaron ground state",
J. Phys. Soc. Jpn. **38**, 181 (1975)

[58] E.P. Gross, "Strong coupling polaron theory and translational invariance",
Ann. Phys. **99**, 1 (1976)

[59] J. Adamovski, B. Gerlach, and H. Leschke, "Strong-coupling limit of polaron energy, revisited", *Phys. Lett. A* **79**, 249 (1980)

[60] A. Erçelebi, "The two-dimensional magneto-polaron in the strong-coupling regime", *J. Phys.: Condens. Matter* **1**, 2321 (1989)

[61] T. Yıldırım and A. Erçelebi, "The ground-state description of the optical polaron versus the effective dimensionality in quantum-well-type systems", *J. Phys.: Condens. Matter* **3**, 1271 (1991)

[62] C.Y. Chen, D.L. Lin, and R. Chen, "Strong-coupling theory of quasi-two-dimensional polarons", *Phys. Rev. B* **49**, 13680 (1994)

[63] A. Erçelebi and R.T. Senger, "Strong-coupling characterization of quasi-1D polarons in cylindrical QW-wires", *Solid State Commun.* **97**, 509 (1996)

[64] F.M. Peeters and J.T. Devreese, "Scaling relations between the two- and three-dimensional polarons for static and dynamical properties", *Phys. Rev. B* **36**, 4442 (1987)

[65] J.T. Devreese, R. Evrard, E. Kartheuser, and F. Brosens, "Energy levels of bound polarons", *Solid State Commun.* **44**, 1435 (1982)

[66] A. Erçelebi and R.T. Senger, "Energy and mass of 3D and 2D polarons in the overall range of the electron-phonon coupling strength", *J. Phys.: Condens. Matter* **6**, 5455 (1994)

[67] A. Erçelebi and R.T. Senger, "Ground-state description of quasi-one-dimensional polarons with arbitrary electron-phonon coupling strength", *Phys. Rev. B* **53**, 11008 (1996)

[68] A. Erçelebi and R.T. Senger, "A variational study of the ground Landau level of the 2D Fröhlich polaron in a magnetic field", *J. Phys.: Condens. Matter* **7**, 9989 (1995)

[69] T.D. Schultz, "Slow electrons in polar crystals: self-energy, mass and mobility", *Phys. Rev.* **116**, 526 (1959)

[70] Y. Osaka, "Polaron state at finite temperature", *Prog. Theor. Phys.* **22**, 437 (1959)

[71] P.M. Platzman, "Ground-state energy of bound polarons", *Phys. Rev.* **125**, 1961 (1962)

[72] J.T. Marshall and M.S. Chawla, "Feynman path integral calculation of the polaron effective mass", *Phys. Rev. B* **2**, 4283 (1970)

[73] D. Matz and B.C. Burkey, "Dynamical theory of the large polaron: Fock approximation", *Phys. Rev. B* **3**, 3487 (1971)

[74] R. Abe and K. Okamoto, "An improvement of the Feynman action in the theory of polaron", *J. Phys. Soc. Jpn.* **33**, 343 (1972)

[75] J.M. Luttinger and Ch.Y. Lu, "Generalized path-integral formalism of the polaron problem, and its second-order semi-invariant correction to the ground-state energy", *Phys. Rev. B* **21**, 4251 (1980)

[76] E.A. Kochetov and M.A. Smondyrev, "Temperature effects in the polaron model", *Sov. Phys. - Theor. Math. Phys.* **47**, 375 (1981)

[77] H. Shoji and N. Tokuda, "Phase-transition-like behavior in the problems of different types of polaron", *J. Phys. C: Solid State Phys.* **14**, 1231 (1981)

[78] V.K. Fedyanin and K. Rodriguez, "Path-integral approach to polaron mass and radius at finite temperatures", *Physica A* **112**, 615 (1982)

[79] A.L. Koledenko and K.F. Freed, "Direct path integral treatment of the polaron problem", *Phys. Rev. B* **27**, 4586 (1983)

[80] Y. Lépine, "On the phase transitions for the large polaron in a magnetic field", *J. Phys. C: Solid State Phys.* **18**, 1817 (1985)

[81] Wu Xiaoguang, F.M. Peeters, and J.T. Devreese, "Exact and approximate results for the ground-state energy of a Fröhlich polaron in two dimensions", *Phys. Rev. B* **31**, 3420 (1985)

[82] B.A. Mason and S. Das Sarma, "Path-integral study of localization in the generalized polaron problem", *Phys. Rev. B* **33**, 1412 (1986)

[83] F.M. Peeters, X. Wu, and J.T. Devreese, "Ground-state energy of a polaron in n dimensions", *Phys. Rev. B* **33**, 3926 (1986)

[84] B. Gerlach and H. Löwen, "Absence of phonon-induced localization for the free optical polaron and the corresponding Wannier exciton-phonon systems", *Phys. Rev. B* **37**, 8042 (1988)

[85] R.T. Senger and A. Erçelebi, "Path integral description of low-dimensional polarons in parabolic confinement potentials"
J. Phys.: Condens. Matter **9**, 5067 (1997)

[86] R. Parker, G.D. Whitfield, and M. Rona, "Strong coupling theory of the moving piezoelectric polaron", *Phys. Rev. B* **10**, 698 (1974)

[87] R.P. Feynman and A.R. Hibbs, *Quantum Mechanics and Path Integrals*, (McGraw-Hill, New York, 1965)

[88] *Lectures on Path Integration (Trieste 1991)*,
edited by H.A. Cerdeira, S. Lundqvist, D. Mugnai, A. Ranfagni, V. Sayakanit, and L.S. Schulman, (World Scientific, Singapore, 1993)

[89] L.S. Schulman, *Techniques and Applications of Path Integration*,
(J. Wiley and Sons Inc., New York, 1981)

[90] *Path Integrals and their Applications in Quantum, Statistical and Solid State Physics*, edited by G.J. Papadopoulos and J.T. Devreese,
(Plenum, New York, 1978)

[91] J.T. Devreese and F. Brosens, "Extension of the Feynman inequality for path integrals to a non-zero magnetic field",
Solid State Commun. **79**, 819 (1991)

[92] H. Haken, in *Polarons and Excitons* edited by C.G. Kuper and G.D. Whitfield (New York: Plenum, 1963)

[93] S.D. Mahanti and C.M. Varma, "Effective electron-hole interactions in polar semiconductors", *Phys. Rev. B* **6**, 2209 (1972)

[94] J. Sak, "Effective electron-hole interaction in polar semiconductors", *Phys. Rev. B* **6**, 2226 (1972)

[95] S.P. Kuleshov, V.A. Matveev, and M.A. Smondyrev,
Preprint JINR E2-9116, Dubna (1975)

[96] E.A. Kochetov, S.P. Kuleshov, V.A. Matveev, and M.A. Smondyrev, "Strong and weak coupling approximations in the teo-polaron problem", *Theor. Math. Phys.* **30**, 117 (1977)

[97] Y. Takada, "Large bipolaron in one- and two-dimensional systems", *Phys. Rev. B* **26**, 1223 (1982)

[98] H. Hiramoto and Y. Toyozawa, "Inter-polaron interaction and bipolaron formation I", *J. Phys. Soc. Jpn.* **54**, 245 (1985)

[99] T.K. Mitra, "On the stability of a Fröhlich bipolaron",
Phys. Lett. A **142**, 398 (1989)

[100] A. Chatterjee and S. Sil, "Stability of all-coupling large optical singlet bipolarons", *Int. J. Mod. Phys. B* **7**, 4763 (1993)

[101] G. Verbist, F.M. Peeters, and J.T. Devreese, "The stability region of bipolaron formation in two and three dimensions in relation to high-T_c superconductivity", *Solid State Commun.* **76**, 1005 (1990)

[102] V. Cataudella, G. Iadonisi, and D. Ninno, "Binding-energies, effective masses and screening effects of Fröhlich bipolarons", *Physica Scripta* **T39**, 71 (1991)

[103] V.M. Fomin and M.A. Smondyrev, "Bipolaron confinement in two-dimensional layers", *Phys. Rev. B* **49**, 12748 (1994)

[104] M.A. Smondyrev and J.T. Devreese, "Comment on adiabatic theory for the bipolaron", *Phys. Rev. B* **53**, 11878 (1996)

[105] F. Brosens and J.T. Devreese, "Stability of bipolarons in the presence of a magnetic field", *Phys. Rev. B* **54**, 9792 (1996)

[106] Y. Wan, G. Ortiz, and P. Phillips, "Origin of pair-tunneling states in semiconductor quantum dots", *Phys. Rev. B* **55**, 5313 (1997)

[107] R.T. Senger and A. Erçelebi, "Stability of low-dimentionally-confined bipolarons", *Eur. Phys. J. B* **16**, 439 (2000)

[108] M.A. Smondyrev, E.A. Kochetov, G. Verbist, F.M. Peeters, and J.T. Devreese, "Equivalence of 3D bipolarons in a strong magnetic field to 1D bipolarons", *Europhys. Lett.* **19**, 519 (1992)